Process optimization under uncertainty: stochastic integer programming approaches

Zur Erlangung des akademischen Grades eines

Dr.-Ing.

von der Fakultät Bio- und Chemieingenieurwesen
der Technischen Universität Dortmund
genehmigte Dissertation

vorgelegt von

Dipl.-Ing. Egidio Leo

aus

Matera, Italien

Tag der mündlichen Prüfung: 25.09.2023

1. Gutachter: Prof. Dr.-Ing. Sebastian Engell
2. Gutachter: Prof. Dr.-Ing. Ignacio Grossmann

Dortmund, 2023

Thesis outcome

Financial support is gratefully acknowledged from the Marie Skłodowska Curie Horizon 2020 EID-ITN project "PROcess NeTwork Optimization for efficient and sustainable operation of Europe's process industries taking machinery condition and process performance into account – PRONTO", Grant agreement No 675215.
The thesis has led to the following journal and conference publications:

Journal articles

1. Leo E. and Engell S., *Integrated day-ahead energy procurement and production scheduling*, Automatisierungtechnik 2019
2. Leo E., Dalle Ave G., Harjunkoski I. and Engell S., *Stochastic short-term integrated electricity procurement and production scheduling for a large consumer*, Computers & Chemical Engineering, Volume 145, February 2021
3. Leo E. and Engell S., *Condition-based maintenance optimization via stochastic programming with endogenous uncertainty*, Computers & Chemical Engineering, Volume 156, January 2022
4. Leo E. and Engell S., *Handling Type-I and Type-II endogenous uncertainties in simultaneous production planning and condition-based maintenance optimization in continuous production*, Computers & Chemical Engineering, volume 174, June 2023
5. Rahimi-Adli K., Leo E., Beisheim B. and Engell S., *Optimization of the operation of an industrial power plant under steam demand uncertainty*, Energies 2021
6. Azadi P., Winz J., Leo E., Klock R. and Engell S., *A transient hybrid model for prediction of molten iron and slag quality indices in a large-scale blast furnace process*, Computers & Chemical Engineering, Volume 156, January 2022

Proceedings papers

7. Leo E. and Engell S., *A novel multi-stage stochastic formulation with decision-dependent probabilities for condition-based maintenance optimization*, European Symposium on Computer-Aided Process Engineering 2020 (ESCAPE-30), Volume 48, 1795-1800.
8. Leo E., Rahimi-Adli K., Beisheim B., Gesthuisen R. and Engell S., *Applying Stochastic Optimization to Demand-Side Management of a Combined Heat and Power Plant*, ECCE12 The 12th European Congress of Chemical Engineering Florence 15-19 September 2019.
9. Leo E. and Engell S., *A two-stage stochastic programming approach to integrated short-term electricity procurement and production scheduling*, European Symposium on Computer-Aided Process Engineering 2018 (ESCAPE-28)
10. Leo E. and Engell S., *Multi-stage integrated electricity procurement and production scheduling*, International Symposium on Process Systems Engineering (PSE), San Diego, California, USA, July 1-5, 2018.

11. Leo E. and Engell S., *Condition-based operational optimization of industrial combined heat and power plants under time-sensitive electricity prices*, European Symposium on Computer-Aided Process Engineering (ESCAPE-27), Volume 40, pages 1261-1266, Barcelona, Spain, Oct 1-5, 2017.

Abstract

The ability of a production plant to be flexible by adjusting the operating conditions to changing demands, prices of the products and the raw materials is crucial to maintain a profitable operation. In this respect, the application of mathematical optimization techniques is unanimously recognized to be successful to improve the decision-making process. Typical examples are production planning, scheduling, real-time optimization and advanced process control. The more information are available to the optimization approach, the more "optimal" are the resulting decisions: the "optimal" production strategy cannot reduce the inventory costs if no supply-chain model is integrated into the production planning optimization. This thesis lies in the context of Enterprise-wide optimization with the goal of integrating decision layers and functions while accounting for uncertain information. A stochastic programming approach is adopted to integrate production scheduling with energy management and production planning with predictive maintenance. The approaches are analysed from a formulation perspective and from a computational point of view, which is necessary to deal with one of the challenges of the presented methods consisting in the size of the resulting optimization problems.

To reduce the electricity cost that is generated by the uncertain peaks of the day-ahead price, a two-stage risk-averse optimization is proposed to simultaneously define the optimal bidding curves for the day-ahead market and the optimal production schedule. The large-scale MILP problem is solved with a scenario-based decomposition technique, the progressive hedging algorithm. Heuristic procedures are applied to speed up the solution phase and to avoid the oscillatory behaviour due to the integer variables. Since large electricity consumers rely on Time-Of-Use power contracts to handle the volatility of the day-ahead price, the two-stage formulation is expanded into a multi-stage optimization to optimally purchase electricity from different sources and to generate electric power with a power plant. The unpractical size of the resulting problem is handled by approximating the multi-stage tree with a series of two-stage scenario-trees within a rolling horizon procedure. A mixed time grid handles the multi-scale nature of the problem by making short-term decisions with a detailed model and catching their effect on the long-term future with an aggregated model.

While the electricity prices introduce exogenous uncertain information into the optimization problem, the predictive maintenance optimization carries endogenous uncertain sources into the production planning problem. Endogenous uncertainties, contrary to the exogenous ones, are uncertain information that can be modified (in the probability or in the timing of the realization) by the decision maker. The prognosis technique of the Cox model is embedded into a multi-stage stochastic program to consider an uncertain Remaining Useful Life of the equipment when the optimal operating conditions of the plant are defined. Two modelling approaches (based on superstructure-scenario trees and on conditional non-anticipativity constraints) are proposed to formulate the optimization problem with endogenous uncertainties. Two Benders-like decomposition techniques and several branching priority schemes are applied to handle the high complexity of the resulting optimization problems.

Contents

List of Figures

List of Tables

List of Abbreviations

AOD	Argon oxygen de-carburization
BD	Benders decomposition
CC	Continuous Caster
CBM	Condition-based maintenance
CVaR	Conditional Value at Risk
DA	Day-ahead electricity market
EAF	Electric Arc Furnace
ECRM	Expected conditional risk measure
EE	Expected Excess
E-CVaR	Expected Conditional Value at Risk
GBD	Generalized Benders decomposition
GOP	Global Optimization algorithm
GDP	Generalized disjunctive programming
(i)DSR	(Industrial) Demand-side Response
LP	linear program
MIP	Mixed integer programming
MILP	Mixed integer linear programming
MIQP	Mixed integer quadratic programming
MINLP	Mixed integer non-linear programming
MSP	Multi-stage program
PHA	Progressive hedging algorithm
RTN	Resource task network
SD	Semi-deviation
SIP	Stochastic integer programming
SP	Stochastic programming
TOU	Time-Of-Use
VaR	Value at Risk
VSS	Value of the stochastic solution
2SSP	Two-stage stochastic program

Part I

Motivation

From a process engineering point of view, the purpose of automatic feedback control is not primarily to keep the controlled variables at their set-points as well as possible or to nicely track dynamic set-point changes, but to operate the plant such that the net return is maximized

---

Sebastian Engell

Chapter 1

Enterprise Wide Optimization

1.1 The challenges of Enterprise Wide Optimization

Enterprise-wide optimization (EWO) is a new and promising approach emerging in the process industry with the goal of maintaining profitability in the global market by making more efficient decisions (Shapiro, 2001, Grossmann, 2005). The key idea of EWO is to integrate different decision layers and functions of the decision-making process to exploit synergies and couplings and avoid possible conflicting decisions. From the operation perspective, EWO involves planning, scheduling, real-time optimization and process control. A typical example is the integration of production planning and scheduling (Maravelias and Sung, 2009). A sequential approach consists of the planning level making long-term strategic decisions that represent the set-points of the scheduling level that defines short-term production sequences. Due to the interconnections and the trade-offs, to achieve a solution that is globally optimal the synergies between the two levels must be taken into account to avoid contradictory strategies. However, this leads to much more complicated optimization problems not only because of the natural increase of the problem size but also because of the need of accounting for uncertain information. In fact, different decision layers make decisions at different points in time when some information might be incomplete or not known. According to (Grossmann, 2005), there are four major challenges to be addressed to fully exploit the concept of EWO:

- the modelling challenge
- the uncertainty challenge
- the multi-scale challenge
- the algorithmic and computational challenge

The modelling challenge is the hardest challenge to face (and to define) and somehow it is coupled to all the others. In fact, it does not only pose questions related to the most suitable mathematical formulations (e.g. continuous time *vs* discrete time formulations or precedence-based models *vs* Resource Task Network (RTN)) but also, and more interestingly, to the necessary level of detail of the modelling phase to fully exploit concept of EWO. A typical question is whether non-linearities should be introduced in an EWO problem. In fact, if on one hand the introduction of non-linear terms would increase the model accuracy, on the other hand it drastically complicates the solution, forcing, most likely, the decision maker to accept a local optimum without an estimation of the potential optimality gap. A judicious balance

between model accuracy and model complexity must be found.

The multi-scale challenge arises inevitably with the integration of different levels of the decision-making process (e.g. planning and scheduling, scheduling and control) since decisions across different time-scales (e.g. long-term strategic decisions and short-term production decisions) must be made simultaneously. The obvious strategy of extending short-term decisions to the long-term horizon typical of the strategic layer (e.g. one month) with a fine discretization (e.g. minute or hour) gives rise to large-scale intractable problems.

Handling uncertainty in the optimization is recognized as a crucial and open challenge to address. The choice of the optimization approach to edge against uncertainty is already a difficult step. Common choices rely on stochastic programming (SP) (Birge and Louveaux, 2011), robust optimization (RO) and chance programming (CP) (Li, Garcia, and Gunter, 2008) (that however can be reformulated in terms of the previous two methods). Regardless the preferred optimization approach, handling uncertainty means increasing the complexity of the optimization problem in terms of computational time and global optimality of the solution.

Solving large-scale optimization problems is a key point to exploit the concept of EWO. Many large-scale real-world problems cannot be solved by using off-the-shelf tools. Therefore, efficient solution methods have to be developed in order to improve the computational performance and to guarantee global optimality of large scale Mixed-integer linear Programming (MILP), Non-linear Programming (NLP) and Mixed-Integer Non-linear Programming (MINLP) problems.

As highlighted in the course of the thesis, the challenges of EWO are interconnected and coupled to each other and, therefore, multiple challenges have to be faced simultaneously to efficiently solve EWO problems. For instance, accounting for uncertain information not only poses the challenge of formulating an optimization program that suitably describes the lack of knowledge but also requires a solution tool that is able to solve the stochastic formulation in a reasonable amount of time according to the specific application (e.g. from minutes for control problems to hours for planning problems).

This thesis identifies and addresses an additional challenge of EWO, i.e. the online nature of these problems. In fact, the environment and the information of EWO problems change continuously and, therefore, the need of reacting to changing situations becomes crucial to fully exploit this approach. This challenge is connected to the four challenges that were previously discussed. In fact, a computational method that enables the online solution of the problem by adjusting the decisions to new information is essential to address the online challenge. Moreover, due to their nature, online optimization problems are characterized by incomplete or uncertain information. The connection with the uncertainty challenge would enable robust decisions that allow to anticipate and optimally react to uncertain information. The interconnection between the online challenge and the modelling and multi-scale challenges must also be taken into account to represent the problem. In fact, the online nature of these problems can influence the level of detail that is needed to provide value. For example, in an environment that continuously changes, a very detailed model of the remote future might provide low added value increasing, on the other hand, the complexity of the problem.

Outline

Part I places the thesis in the context of EWO, which is already introduced in Chapter 1, for the process industry. Sections 1.2 and 1.3 apply the general concept of EWO to industrial Demand-Side Management (iDSM) and Condition-Based Maintenance (CBM), respectively. These topics represent two key approaches to increase the profitability of the process industry by integrating decision functions and levels. The scope of this work is to provide mathematical formulations and solution methods that enable the integration of different levels of the decision-making process taking into account their synergies in order to avoid myopic decisions.

Since this thesis focuses on the uncertainty challenge (and the tightly coupled computational challenge), **Part II** presents the theoretical foundations of optimization under uncertainty on which the rest of the thesis is based. The framework of stochastic programming is presented from a modelling point of view in Chapter 2.1 covering the topic of risk-averse optimization in Section 2.1.2 and endogenous uncertainty in Chapter 2.2. From a solution algorithm perspective, Chapter 2.3 introduces the mathematical programming decomposition methods that have been adopted in this thesis. Section 2.3.1 describes the Progressive Hedging Algorithm (PHA) that has been adopted to solve a large-scale two-stage MILP problem via a scenario-based approach. Sections 2.3.2 and 2.3.3 describe the primal Benders decomposition and its generalized version to handle convex MINLP problems. A Benders-like decomposition that is able to handle non-convex bi-linear NLPs, the Global Optimization (GOP) algorithm, is introduced in Section 2.3.4. Section 2.3.5 reviews methods and algorithms that were used in literature to solve stochastic problems with endogenous uncertainty.

Part III reports the contributions and the applications of the proposed approaches and algorithms to real-world industrial case studies. Chapter 3 studies the day-ahead electricity procurement problem from a consumer point of view considering an uncertain day-ahead electricity price. A bidding process is introduced to model the day-ahead market. The two-stage MILP program is efficiently solved by adopting the Progressive Hedging Algorithm. Section 3.2 extends the electricity procurement options to power contracts covering a medium-term horizon for a real-world industrial combined heat and power plant. Some judicious approximations are proposed to balance computational time and accuracy of the problem. Chapter 4 proposes two novel formulations with endogenous uncertainties to integrate production planning, prognosis and condition-based maintenance. Section 4.1 introduces a stochastic problem with decision-dependent probabilities to simultaneously optimize the production level of a single production campaign and the timing of the maintenance activities according to a prognosis model (the Cox model). This problem is analysed not only from a modelling point of view, but also from an algorithmic perspective to efficiently solve this novel class of non-convex MINLP problems. Particular emphasis is given to the global optimality of this class of optimization problems. Section 4.2 extends the stochastic formulation with decision-dependent uncertainties to multiple production campaigns that introduce the features of the decision-dependent structure. In fact, in this formulation not only the probabilities of the uncertain scenarios are adjusted according to the decision variables but also the timing of the realization of the uncertain parameters (and therefore the structure of the scenario tree) is defined by the decision maker.

Part IV provides a summary of this thesis by drawing some conclusions and discussing the outlooks of this work in Chapter 5. All the parameters of the presented formulations are given in Appendix .1-.4.

1.2 Industrial Demand Side Management

Traditionally, in the process industry production and energy management are handled sequentially. This means that a production schedule is defined and given as input to the energy management that minimizes the electricity purchasing cost to realize the given schedule. This sequential approach can easily lead to sub-optimal solutions since possible synergies are not taken into account. An integrated approach that considers simultaneously production scheduling and energy management can be very beneficial since the electricity cost can be further reduced by exploiting the additional degrees of freedom that are provided by the production decisions or/and by a power plant (if present) that generates electric power.

This is in fact the goal of industrial Demand-Side Management (iDSM) that aims at exploiting the financial incentives that are set up by the grid operator by adapting the production levels to dynamic market or supply conditions, e.g. the time-varying electricity prices coming from the spot market (Merkert et al., 2014, Siano, 2014, Zhang and Grossmann, 2015). Apart for the consumer's perspective, iDSM is expected to play a crucial role to support operations of the power grid in a more efficient way coping with the possible drawbacks of the integration of renewable energy sources (Paulus and Borggrefe, 2011). The difficulties of relying on renewable energy sources are related to the volatile and largely uncontrollable power feed due to the nature of the sources, e.g. wind energy, that are not linked to the power needs. This drastically affects the electricity price in the spot market and generates a supply-demand mismatch that may compromise the stability of the power grid. From the grid operator's perspective, whose main objective is to increase efficiency, operate economically and ensure stability of the power grid, iDSM is a mean to define financial programs and incentives (e.g. interruptible loads, ancillary service market) to reduce electricity demand peaks and quickly react to supply-demand imbalances.

Undoubtedly, adopting an iDSM strategy is beneficial for both the electricity consumers to reduce the electricity cost and the grid operator to stabilize the power grid by shaping the electricity demand. An overview of advances and challenges in the area of iDSM can be found in (Zhang and Grossmann, 2015).

1.3 Predictive maintenance

Maintenance activities include all those actions (technical and administrative) aiming at retaining and restoring an item to a state that is necessary to perform a specific function (British Standards Institute, 1993). Therefore, maintenance activities include not only turnarounds that are performed in production plants every 5-10 years, but also cleaning operations, equipment inspections or substitutions needed to restore the health of the equipment that degrade over time due to its usage. According to the way of determining the timing of the maintenance, different maintenance strategies

can be identified: fixed-interval (or periodic) maintenance policy, reliability-based maintenance, run-to-failure strategy and condition-based maintenance.

In this thesis, we focus on the Condition-based maintenance (CBM) strategy, also called predictive maintenance, that is based on the idea of performing the maintenance activities according to the health of the equipment. The core of such a strategy is a degradation model that is able to estimate and to predict the health of the equipment according to the operating conditions of the plant. The advantage of a CBM policy over other maintenance strategies (periodic, reliability-based, run-to-failure) results from the ability to predict the equipment health and, consequently, its Remaining Useful Life (RUL) according to the plant operations. A fixed-interval maintenance policy (Tan and Kramer, 1997) based on predetermined maintenance periods in contrast results in unnecessary costly maintenance activities. Reliability-based approaches (Dedopoulos and Shah, 1995), (Sanmarti, Espuna, and Puigjaner, 1997), (Rajagopalan et al., 2017) are based on reliability metrics, as e.g. mean-time-to-failure, but ignore the influence of the operating conditions on the remaining lifetime. Run-to-failure (or break-down) policies perform the maintenance activities only after the break-down of a piece of equipment and, therefore, are mainly adopted for low-cost equipment that can be repaired quickly.

Therefore, the integration of production planning and CBM aims at capturing and exploiting the dependency between equipment health and plant operation to find the best compromise between operating costs and maintenance costs. In fact, a high production rate might generate high throughput but also high maintenance costs due to frequent maintenance activities that are necessary because of the fast degradation rates.

1.4 The challenges addressed in this thesis

The main goal of this thesis is to investigate new approaches for the explicit consideration of uncertainty within the framework of EWO for the process industry. These approaches should be applicable to complex and industrial-size problems and should extend the current state of the art by providing optimization formulations and solution methods that improve the decision making in terms of quality of the solution and computational effort for systems under the presence of uncertainties.
This thesis focuses on the uncertainty challenge for EWO problems by adopting the framework of stochastic programming. Within this challenge, this work proposes novel stochastic programming formulations and suitable solution methods for real-world industrial problems. From an application perspective, the concept of EWO is brought into the topics of industrial Demand-Side Management (iDSM) and Condition-Based Maintenance (CBM) that have been approached with mixed-integer linear and non-linear optimization techniques.

To realize the concept of iDSM, a novel two-stage mixed-integer stochastic formulation is proposed to integrate energy management and production scheduling to simultaneously optimize the day-ahead electricity procurement and the process operations, accounting for the mechanisms of the electricity markets (e.g. the bidding process). The advantages of the proposed stochastic formulation are analysed taking into consideration the additional complexity of the optimization problem compared

to the deterministic counterpart. While a case of a continuous production plant shows the benefit of the proposed integration and the need of a risk management strategy to reduce the electricity purchase during price peaks, the example of a real-world batch process shows that the large-scale nature of the stochastic programs can be handled via ad-hoc solution methods. In this case, a scenario-based decomposition technique has revealed to be the most suitable approach to find good-quality sub-optimal solutions of the resulting large-scale problem drastically reducing the required computational effort and the optimality loss (that has been estimated a-posteriori).
Following the concept of EWO, the thesis further integrates strategic long-term power contracts decisions and short-term operations for a combined heat and power (CHP) production plant by proposing a multi-stage stochastic formulation. The inherit additional multi-scale challenge has been faced by proposing some judicious approximations. The multi-stage optimization is approximated via a series of two-stage stochastic programs that are solved in a shrinking-horizon fashion. The multi-scale nature is modelled by introducing two time grids: a detailed one with an hourly discretization for the short-term horizon and an aggregated one (defined by the features of the power contracts) for the long-term future.

While an integration of different functions (i.e. energy management and production scheduling) has been realized in the context of iDSM via the framework of stochastic programming with exogenous uncertainty, the integration of production planning and condition-based maintenance optimization requires the introduction of endogenous uncertainties to model the couplings between the two decision levels. To simultaneously optimize the production levels and the health of the equipment of a continuous production plant, a multi-stage stochastic program with endogenous uncertainty (i.e. decision-dependent probabilities) is formulated without assuming fixed and known probabilities of the scenarios but adjusting the probability of the realization of the uncertain parameters according to the decisions at one point in time. Due to the introduction of non-convex terms to describe the endogenous uncertainty, this approach faces not only the uncertainty challenge but also the computational challenge that has been tackled by adopting two primal decomposition techniques to handle the trade-off between global optimality and computational effort.
Furthermore, the extension of the proposed model to a medium term horizon (that is able to handle multiple production campaigns) leads to a stochastic formulation with multiple types of endogenous uncertainties (Type-I and Type-II). A similar formulation (with combined types of endogenous uncertainties) has never been presented in the literature. This work proposes two novel optimization approaches that are able to simultaneously model the features of the decision-dependent probabilities and the decision-dependent structure of the scenario-tree. The complexity of the resulting formulations is analysed in terms of the computational effort needed to reach the global optimum of the non-convex MINLP problems. A global solver is enhanced with different custom branching strategies with the goal of temporarily simplify the non-linear non-convex terms and speed up the solution phase. This novel approach faces all the challenges of EWO. In fact, by introducing multiple types of endogenous uncertainties (uncertainty challenge) the proposed formulation requires a modelling approach that is able to capture these features (modelling challenge) and to enable the application of advanced decomposition methods to reach the global optimum of the resulting MINLP problem (computational challenge). Moreover, the optimization of multiple production campaigns requires to simultaneously consider short-term and long-term decisions (multi-scale challenge).

1.4.1 Achievements and contributions of this thesis

Chapter 3 achieves the integration of production and energy management for industrial-size problems accounting for the uncertainty of the power grid. The major contribution of Section 3.1 is the accurate characterization of the bidding process of the day-ahead market and its integration into a production scheduling model via a risk-averse stochastic mixed-integer optimization. The novel formulation is applied to the industrial size stainless steel-making process and is efficiently solved by adopting a scenario-based decomposition approach.

Section 3.2 provides an online strategy that allows the simultaneous optimization of the electricity procurement from different sources of electric power and the short-term operations of industrial-size combined heat and power plants. The proposed realistic online strategy enables the application of stochastic integer programming approaches to real-world industrial problems by solving the stochastic problems in reasonable amount of time and by handling realizations of the uncertain parameters there were not included in the set of the defined scenarios. The proposed online strategy enables the optimization of multi-scale models by combining short-term and long-term decisions.

Chapter 4 introduces several contributions on the topic of predictive maintenance optimization. First of all, it couples the concepts of predictive maintenance and prognosis by embedding for the first time the Cox model into a stochastic program. The resulting optimization framework that is described in Section 4.1 is based on endogenous uncertainties and can be applied to any production system that degrades over time. This section proposes as well different alternatives and insights to solve this class of problems.

The main contribution of Section 4.2 is the stochastic programming formulation with endogenous uncertainty where both Type-I and Type-II features are present. A similar formulation has never been presented in literature. It enables the simultaneous long-term production planning and predictive maintenance optimization. Additionally, this section proposes and evaluates two different modelling approaches to build efficient mathematical formulations of this novel class of optimization problems.

Part II

Theoretical Foundations

Is it better to approximately solve a correct model or to correctly solve an approximated model?

Chapter 2

Optimization under uncertainty

2.1 Stochastic programming

A stochastic program is a mathematical program (optimization model) where some of the data is uncertain and can be described by a probability distribution. It is assumed that the random variables have a countable number of realizations that are modelled by a discrete set of scenarios $s = 1, ..., S$. In a stochastic program with recourse, corrective decisions or recourse actions can be taken after the uncertainty has partly realized. Each point in time at which a decision is made is called a stage. Stochastic programming was introduced by (Birge and Louveaux, 1997) with a multi-stage stochastic formulation. In the two-stage stochastic formulation (Birge and Louveaux, 2011) the decision maker takes some actions in the first stage, after which the uncertainties affect the outcome of the first-stage decisions. Recourse decisions can then be made in the second stage to adapt to the realization of the uncertainty. A typical example is the planning of a production or distribution facility under uncertainty of the future market, and the later operation according to the real demand. The first stage decisions are optimized under the assumption that recourse decisions will optimally be adapted in the second stage after new information has become available. Thus the total set of n decisions is divided into two groups:

- Decisions that have to be taken before the uncertainty is realized. These are called first-stage or *here-and-now* decisions and they have to be made at the beginning and cannot be changed over the decision horizon;
- Decisions that can be taken after the uncertainty has been disclosed. These are called second-stage or *wait-and-see* decisions and they are a means to react after the realization of the uncertainty.

Figure 2.1 shows the scenario-tree representation for multi-stage (2.1a) and two-stage (2.1b) stochastic problems. Each scenario is defined by a path from the root node to a leaf node. In the more general multi-stage stochastic formulation the uncertainty is modelled by a scenario tree with N stages that branches at each stage. The decision process progresses along this scenario tree. In stage i, the decision is based on the information on the realization of a path in the tree up to this node whereas the future evolution is only known probabilistically. The decisions at stage i are optimized under the assumption that the later decisions are optimally adapted to the information which becomes available after the realization of the uncertainty (Engell, 2009).

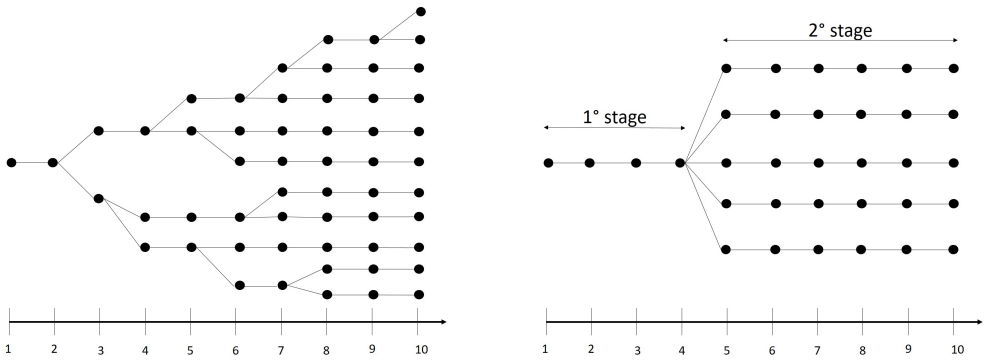

(a) (b)

FIGURE 2.1: Multi-stage (a) and two-stage (b) stochastic optimization problems represented by scenario trees. Source: (Leo and Engell, 2019b).

An alternative representation of the scenario tree was introduced in (Ruszczyński, 1997) using the non-anticipativity constraints (NACs) formulation. In this formulation, as shown in Figure 2.2 for a four-stage problem, each scenario at each stage is represented by a node. This means that different sets of decision variables are associated to each scenario. The NACs enforce that the nodes of the same stage have the same information by forcing the decision variables to be identical. In Figure 2.2b the NACs are represented by the horizontal lines that connect the nodes of the same stage.

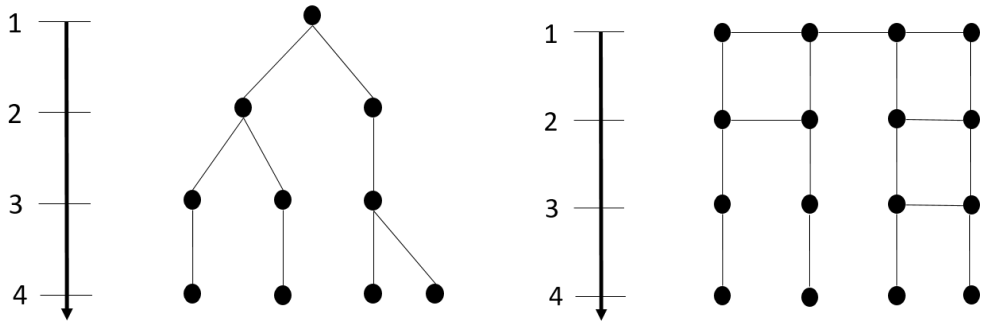

(a) (b)

FIGURE 2.2: Standard scenario tree (a) and scenario tree of the NACs formulation (b) for a multi-stage stochastic optimization problem.

2.1.1 Stochastic integer programming

When integrality requirements are present, a stochastic program is called Stochastic Mixed-Integer Program (SIP). For linear models and a scenario-based representation of the uncertainties, a deterministic equivalent of a two-stage stochastic integer program (2-SSIP) can be stated as the following mixed-integer linear program (MILP) (2.1):

$$\min_{x,y_s} \quad f(x,y_s) = c^T x + \sum_{s=1}^{S} \phi_s q_s^T y_s \tag{2.1a}$$

$$\text{s.t.} \quad Ax \leq b \tag{2.1b}$$

$$T_s x + W_s y_s \leq h_s \tag{2.1c}$$

$$x \in X, y_s \in Y, s = 1, ..., S \tag{2.1d}$$

The objective of a two-stage stochastic mixed-integer linear program (Eq. 2.1a) consists of the first-stage cost and of the expected value of the second-stage cost. The first-stage cost and the second-stage costs are calculated as a linear combination of the first-stage variables x and the second-stage variables y_s with cost parameters c and q_s. The expected value of the second-stage costs is calculated by the sum over all the scenarios of the second-stage costs weighted by the corresponding probabilities ϕ_s. The constraints are divided into two groups: the constraints of the first stage (Eq. 2.1b) are related only to the first-stage decisions, the constraints of the second-stage (Eq. 2.1c) include variables of the first-stage and of the second-stage. The matrices A and b describe the first-stage parameters and T_s, W_s, h_s represent the parameters of each scenario s of the second-stage. When a solution of the first stage x is always feasible in the second-stage, the stochastic problem has complete recourse. The first-stage variables x and the second-stage variables y_s belong to the polyhedral sets X and Y (Eq. 2.1d). Both the sets X and Y can present integer requirements. In case only the polyhedral set X of the first-stage variables x presents integer requirements, this class of problems are called stochastic problems with continuous recourse. When the polyhedral set Y of the second-stage variables y presents integer requirements, the problems are called stochastic problems with integer recourse and the solution becomes harder since the scenario sub-problems lose the property of convexity that is a crucial property for the application of mathematical programming decomposition methods.
In a multi-stage program the uncertainty reveals sequentially and the decision maker can make corrective decisions over a sequence of stages. As in a two-stage stochastic program, the multi-stage case optimizes the cost of the decisions taken at the first-stage and the expected cost of the recourse actions.

2.1.2 Risk-averse optimization

Considering the expected value of the second-stage cost implies that the realizations of the random parameters have no qualitatively different effect. This however is not always true: even a low probability of large losses may not be acceptable. A remedy is to integrate the concept of risk into the optimization problem. We distinguish between two classes of risk measures according to whether they are defined via quantiles or via deviation measures (Rockafellar, 2015). Quantile risk measures are based on the quantiles of the probability distributions of the costs. Types of quantile-based risk-measures include the conditional value-at-risk (CVaR), which measures the expectation of the worst outcomes for a given fraction of the total outcomes, and the excess probability (EP), which measures the probability of exceeding a prescribed target level. Deviation risk measures are given by the expectations of the deviations of the relevant random variable from its mean or from some prescribed target. Examples of deviation-based risk-measures include the expected excess (EE), which measures

the expected value of the excess over a given target, and the semi-deviation (SD), which measures the expected value of the excess over the mean.

Variance

The most intuitive risk measure is the variance of the scenario costs. The variance is a measure of how broad the distribution of the scenario costs is. High variance reflects the chance that the actual costs may largely differ from the expected cost. It is defined as

$$\sigma(Z) = E[(Z - \hat{Z})^2] \tag{2.2}$$

where $\hat{Z}$ is the arithmetic mean of the scenario costs. However, the variance introduces non-linearities in the optimization problem that then becomes harder to be solved.

Value-at-Risk and Conditional Value-at-Risk

In this thesis, we adopt here the CVaR, since it is a coherent risk measure (it preserves convexity). Since the definition of CVaR relies on the concept of VaR, it is worth to first introduce the definition of VaR. Let us consider that Z is a random variable with the meaning of loss. VaR_α is defined as the maximum loss that will not be exceeded at a given confidence level α (with $\alpha \in (0,1)$) (Uryasev, 2000). An equivalent interpretation of VaR_α is the α-quantile of the distribution of the random variable Z. Eq. 2.3 shows the mathematical definition of VaR_α

$$VaR_\alpha(Z) := \min\{c : P(Z \leq c) \geq \alpha\} \tag{2.3}$$

Although VaR is a very popular measure of risk (for instance in financial applications), it has undesirable properties such as non-convexity. CVaR is an alternative measure of risk, with more attractive mathematical properties (Uryasev, 2017). CVaR is defined as the expected loss, conditional on the fact that the loss exceeds the VaR at the given confidence level α. The mathematical definition of CVaR is given by Eq. 2.4.

$$CVaR_\alpha(Z) := E[Z \mid Z \geq VAR_\alpha(Z)] \tag{2.4}$$

CVaR is a coherent risk measure and it is more conservative than VaR. Most importantly, CVaR can be expressed by a minimization formula proposed in (Rockafellar and Uryasev, 2000) and shown by Eqs. 2.5-2.6.

$$CVaR_\alpha(Z) = \min_\psi F_\alpha(Z, \psi) \tag{2.5}$$

$$F_\alpha(Z, \psi) = \psi + \frac{1}{1-\alpha} E[(Z - \psi)^+] \tag{2.6}$$

where $E[\cdot]$ is the expectation and $(Z - \psi)^+ = max\{0, Z - \psi\}$. The variable ψ takes the value of VaR_α when the $CVaR_\alpha$ is computed by the above formula. Eqs. 2.5-2.6 can be formulated as linear constraints in an optimization problem and this provides a computationally efficient way to integrate the CVaR into optimization problems. Figure 2.3 provides a qualitative representation of the $CVaR_\alpha$ and VaR_α.

Expected excess

Expected excess (EE) reflects the expected value of the excess over a given target γ and is defined as:

$$EE(Z) = E[\max\{f(Z(\psi), \psi) - \gamma, 0\}] \tag{2.7}$$

Semi-deviation

Semi-deviation (SD) is similar to the expected excess, but with the prefixed target replaced by the mean of the random variable $\hat{Z}$, and is defined as:

$$SD(Z) = E[\max\{f(Z(\psi), \psi) - (\hat{Z}), 0\}] \tag{2.8}$$

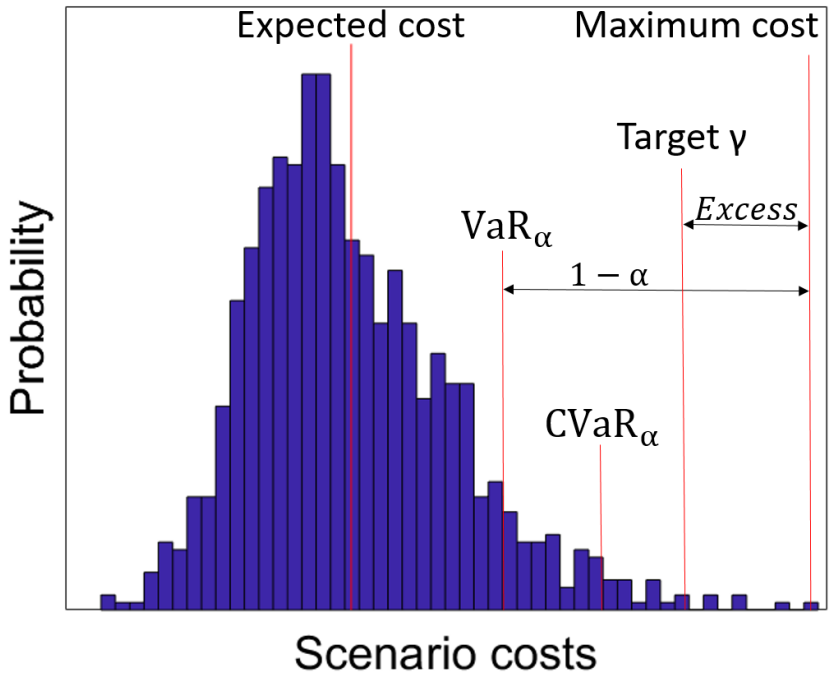

FIGURE 2.3: Illustration of the risk measures $CVaR_\alpha$ and VaR_α and of the excess for the scenario with the maximum cost.

Risk measures for multi-stage programs

For two-stage stochastic programs, the risk-averse model extends immediately from the risk-neutral model by augmenting the expectation of the second stage cost with a risk measure. When it comes to multistage models, however, there is no natural way of measuring risk: risk measures can be applied at every stage additively or to a complete scenario path or be measured in a nested form (Mello and Pagnoncelli, 2016). The definition of a risk measure for multi-stage problems has to enforce the property of time-consistency. Intuitively, the property of time-consistency can be defined such that given the optimal solutions from previous stages, resolving the problem results in the same solutions for the later stages if the optimal solutions are unique. If the

optimal solutions are not unique, resolving the problem at the later stages gives the same optimal objective as computed by the original optimal solutions. Risk-neutral and two-stage risk-averse stochastic programs are time- consistent. For multistage risk-averse stochastic programs, however, time-consistency is not guaranteed and depends on how the risk measure is computed. The risk-averse models with risks measured at every stage separately or measured for the complete scenario path are shown to be time-inconsistent (Pflug and Pichler, 2016). In (Mello and Pagnoncelli, 2016) the authors address this drawback by proposing a class of expected conditional risk measures (ECRMs) which proves to be time-consistent.

2.1.3 The Value of the Stochastic Solution

The value of the stochastic solution (VSS) measures the advantage of using a stochastic program over using the deterministic counterpart where the stochastic parameters have been replaced by their mean values. In other words, it measures the advantage of accounting for the uncertainty and taking into account the recourse decisions. The VSS and the relative $\overline{VSS}$ are defined by Eqs. 2.9-2.10 for a minimization problem.

$$VSS = z^*_{RP} - z^*_{SP} \tag{2.9}$$

$$\overline{VSS} = \frac{z^*_{EP} - z^*_{SP}}{z^*_{RP}} \tag{2.10}$$

where z^*_{SP} is the optimal solution of the stochastic problem and z^*_{RP} is the optimal solution of the recourse problem (RP) that is defined as the stochastic problem with first-stage variables obtained by the optimal solution of the Expected Value Problem (EVP) where the stochastic parameters have been replaced by their mean values.

In risk-averse optimization, the objective is to minimize a weighted sum of the expected cost and a measure of risk, e.g. the CVaR. Therefore, the VSS is defined by Eq. 2.11 for a minimization problem.

$$VSS = \eta(z^*_{RP} - z^*_{SP}) + (1-\eta)(CV^*_{RP} - CV^*_{SP}) \tag{2.11}$$

where CV^*_{SP}, CV^*_{RP} represent the optimal values of the risk measure for the stochastic problem and the recourse problem (RP). The parameter η is a scalar coefficient that the decision maker can tune to assign priorities to the expected cost and to the risk measure. Analogously, Eq. 2.12 defines the relative $\overline{VSS}$.

$$\overline{VSS} = \frac{\eta(z^*_{RP} - z^*_{SP}) + (1-\eta)(CV^*_{RP} - CV^*_{SP})}{\eta z^*_{RP} + (1-\eta)CV^*_{RP}} \tag{2.12}$$

The VSS for multi-stage programs

The natural extension of the VSS from two-stage to multi-stage programs (MSSP) is defined in (**VSS_MSP**) for each stage t for a minimization problem as

$$VSS_t = z^*_{RP_t} - z^*_{MSSP} \tag{2.13}$$

where z^*_{MSSP} is the optimal solution of the multi-stage stochastic program and $z^*_{RP_t}$ is the optimal solution of the recourse problem where all the variables from stage one until stage t are fixed to the optimal solution of the expected value problem. For each stage t the following inequality holds:

$$0 \leq VSS_t \leq VSS_{t+1} \tag{2.14}$$

This sequence of non-negative values represents the cost of ignoring uncertainty until stage t in the decision making of multistage models.

2.2 Stochastic programming with endogenous uncertainty

The standard stochastic programming formulation with recourse assumes the uncertainty to be exogenous. The uncertainty is modelled by a discrete set of scenarios with fixed and known scenario probabilities and the decisions are made at different stages defined by the realization of the uncertainty. The realization of the stochastic parameters is independent of the decision variables. Endogenous uncertainty problems are stochastic problems where the decisions at one point in time can impact the uncertainty realization either in terms of the timing of the realizations or in terms of the probability of the uncertain parameters. According to the influence of the decisions, the endogenous uncertainty formulations can be classified into problems of Type 1, if the decisions can alter the probability distribution by making one uncertain scenario more likely than others, or problems of Type 2, if the decisions determine the timing when the uncertainties are resolved (Jonsbraten, Wets, and Woodruff, 1998). In recent years, the framework of stochastic programming with endogenous uncertainty has received increasing attention (e.g. Hellemo, Barton, and Tomasgard, 2018).

2.2.1 Decision-dependent probabilities - Type-I

The class of stochastic programs with decision-dependent probabilities includes all those stochastic formulations where the probabilities of the uncertainty realizations are affected by the decisions. This includes formulations where the probabilities are selected from a finite number of sets (Peeta et al., 2010, Escudero et al., 2018), formulations where the probabilities can be set continuously according to mathematical expressions of the decision variables (Pflug, 1996, Zhan et al., 2016) and formulations where the parameters of the probability distribution can be modified (Hellemo, Barton, and Tomasgard, 2018). In (Peeta et al., 2010) the authors consider the robust design of a transportation network where the links are subject to random failures. Investments decisions can be made to decrease the probability of a disruptive event. The probabilities are selected from two a-priori-defined sets according to whether the investment takes place. Similarly, in (Escudero et al., 2018) the authors solve a preparedness resource allocation model for the mitigation of natural disasters. A three-stage stochastic mixed 0-1 bilinear optimization problem is presented where the outcomes and the probabilities of the scenarios are influenced by first-stage investment decisions (selection of facilities for commodities storing). In the context of the unit commitment problem, in (Zhan et al., 2016) the authors assume that the electricity prices are dependent on the investment decisions on the generation capacity.

2.2.2 Decision-dependent structure - Type-II

Stochastic programs with decision-dependent structure are optimization models where the structure of the stochastic process can be modified by the decision maker. This covers the case where the timing of the revelation of the uncertain parameters can be altered by the decision variables and the case where stochastic parameters (i.e. the scenarios) can be added and/or deleted. These features are typically modelled with conditional non-anticipativity constraints (NACs) that are NACs that are activated by the decision variables. In (Goel and Grossmann, 2004), the authors optimize the utilization of natural gas resources. The source of uncertainty lies in the production parameters of the wells, and therefore the timing of drilling the wells alters the timing of the revelation of the uncertain parameters (e.g. if the well is not drilled no revelation takes place). In (Boland, Dumitrescu, and Froyland, 2008) the problem of the opening of pit mines is analysed. The quality of the mining blocks is uncertain and therefore its revelation is conditional to the opening of the block (that is a decision variable of the problem). The authors reduced the number of conditional NACs by using structural information of the problem under consideration. The stochastic *R&D* project portfolio optimization problem for the aviation industry in (Solak et al., 2010a) also includes sources of endogenous uncertainty. The uncertain project returns are typically revealed gradually over time according to the decisions on the resource allocation. In (Colvin and Maravelias, 2008), (Colvin and Maravelias, 2009), (Colvin and Maravelias, 2010) the authors study the planning of clinical trials for new drug development where the outcome of the trials represents the uncertain parameter. All these works show that taking into account a decision-dependent structure uncertainty can drastically improve the quality of the solution at the cost of rendering more complex the optimization problem.

2.3 Solution methods and Implementation

Stochastic programming formulations give rise to large-scale optimization problems (2.1) and solving the deterministic equivalent problem can be prohibitive. Decomposition algorithms takes advantage of the special structure of the optimization problem to reduce the computational time. Decomposition methods can be classified into:

- problem-dependent algorithms, which take advantage of the specific properties of the problem at hand (e.g. bi-level decomposition).
- general algorithms, which target a class of problems with similar structures (e.g. Progressive Hedging algorithm, Benders decomposition or L-shaped method).

Focusing on general mathematical programming algorithms, they can be further classified according to the exploitation of complicating constraints or complicating variables (Conejo et al., 2006), as shown in the Figure 2.4. Complicating constraints (Figure 2.4a) involve variables from different blocks (e.g. scenarios in a stochastic formulation with NACs) and complicating variables (Figure 2.4b) link constraints from different blocks. Complicating constraints methods (e.g. Progressive Hedging, Lagrangean decomposition) dualize the complicating constraints to decouple the problem blocks. On the other hand, complicating variables methods (Benders decomposition) temporary fix the complicating variables to obtain easier sub-problems.

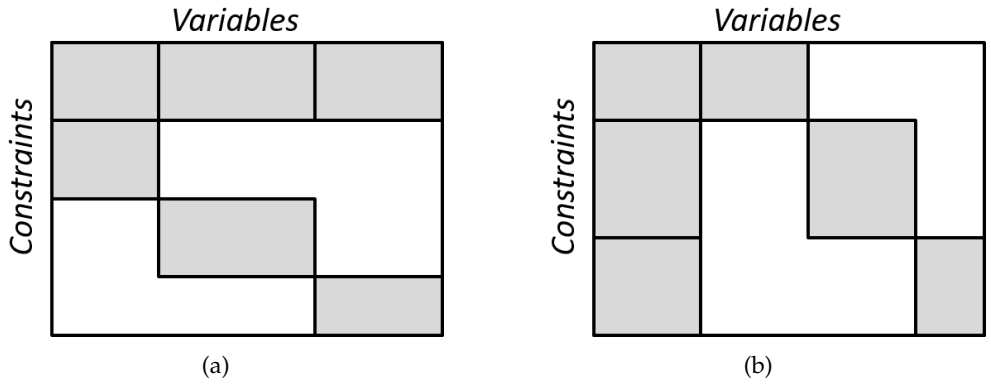

FIGURE 2.4: Schematic representation of the structure of the optimization problems with complicating constraints (a) and complicating variables (b).

The following Sections 2.3.1-2.3.4 describe the mathematical decomposition approaches that were adopted in this thesis and some methods that were used in literature to solve stochastic problems with endogenous uncertainty.

2.3.1 Progressive Hedging

The Progressive Hedging Algorithm (PHA) is a scenario-wise decomposition technique that decomposes the deterministic equivalent formulation of a stochastic program by scenario dualizing the non-anticipativity constraints (NACs) interpreted as complicating constraints. The algorithm iteratively solves modified versions of the sub-problems penalized proportionally to the violation of the dualized NACs (Rockafellar and Wets, 2006). The PHA is proven to converge to the optimal solution only under the condition of convexity of the original problem. In the case of integer variables in the decomposed sub-problems, while convergence to a globally optimal

solution is not guaranteed, the algorithm can reach high-quality solutions within a limited number of iterations (Watson and Woodru, 2011). We consider a two-stage stochastic mixed-integer program of the form

$$\min_{x,y_s} c^T x + \sum_{s=1}^{S} \phi_s q_s^T y_s \tag{2.15a}$$

$$\text{s.t.} \quad (x, y_s) \in X(S) \tag{2.15b}$$

where x represent a vector of first-stage variables, y_s a vector of second-stage variables, and $X(S)$ a set of constraints defining the feasible region. The set S is the set of the scenarios describing the uncertainty. The equivalent formulation with NACs expressed in Problem 2.16 is obtained creating a copy of the first-stage variables into each scenario.

$$\min_{x,y_s} \sum_{s=1}^{S} \phi_s (c^T x_s + q_s^T y_s) \tag{2.16a}$$

$$\text{s.t.} \quad (x_s, y_s) \in X(S) \tag{2.16b}$$

$$x_s = x_{s\prime} \quad \forall s, s\prime \in S \tag{2.16c}$$

where Eq. 2.16c represents the non-anticipativity constraints. The penalized versions of the subproblems are expressed in Problem 2.17.

$$\min_{x,y_s} \sum_{s=1}^{S} \phi_s (c^T x_s + q_s^T y_s + w_s^k x_s + \frac{\rho}{2} \left\| x_s - \hat{x}^k \right\|^2) \tag{2.17a}$$

$$\text{s.t.} \quad (x_s, y_s) \in X(S) \tag{2.17b}$$

where ρ is the penalty parameter that weights the violation of the NACs and w_s^k are the Lagrange multipliers associated to the NACs. The algorithm terminates when the maximum number of iterations (or a time limit) is reached or if the sum of the NAC violations is less than a predefined tolerance. The statement of the PHA for two-stage stochastic mixed integer programs is given in Algorithm 1. The convergence of the

Algorithm 1 Progressive Hedging algorithm

1: **Initialization**: Let $k \leftarrow 0$ and $w^k(s) \leftarrow 0, \forall s \in S$. For each s $\in S$ solve 2.15a-2.15b
2: **Iteration Update**:$k \leftarrow k + 1$
3: **Aggregation**: $\hat{x}^k \leftarrow \sum_{s \in S} \phi_s x_s^k$
4: **Dual price Update**: $w_s^k \leftarrow w_s^{k+1} + \rho(x_s^k - \hat{x}^k)$
5: **Decomposition**: For each $s \in S$ solve 2.17a-2.17b
6: **Convergence test**: If all scenario solutions x_s are equal, stop. Else, go to step 2.

PHA and the quality of the solution are significantly affected by the choice of the penalty parameter ρ. Large values of ρ lead to small number of iterations of the PHA to achieve primal convergence. However, the quality of the final solution can be relatively poor. In contrast, low values of ρ increase the number of the iterations of the PHA but the quality of the resulting primal solutions can be significantly improved. Numerical tested showed that for the problem studied in this thesis (see Section 3.1.5) the convergence is improved when the value of ρ is different for each variable

involved in the dualized NACs. In other words, the parameter ρ in Eq. 2.17a is substituted by the set of parameters ρ_s.

To speed up the convergence of the algorithm, we implemented a heuristic known as variable slamming (Watson and Woodru, 2011). The heuristic fixes decision variables once their value has stabilized to a fixed value over the last $n_{slamming}$ iterations. Low values of $n_{slamming}$ result in an immediate variable fixing with the risk of a poor quality solution. The same heuristic is applied in case some variables have not converged when a termination criterium is activated in order to ensure primal feasibility.

Progressive Hedging and CVaR

Introducing a risk measure can increase the complexity of the optimization problem, not only because of the additional constraints needed to define the risk, but also for the possible lack of separability of the additional constraints that are needed to model the risk-measure (Schultz and Tiedemann, 2006). Here we shown how the progressive hedging algorithm can be applied to solve risk-averse optimization problems with a Conditional-Value-at-Risk measure. We report in Eqs. 2.18-2.21 the constraints defining the CVaR according to a non-anticipativity formulation. These constraints can be separated interpreting the variable ψ as an additional first-stage variable and a copy ψ_s is introduced in each scenario s. Consequently, the set of non-anticipativity constraints (Eq. 2.21) is enlarged to ensure primal feasibility of the solution.

$$CVaR_s = \psi_s + (1-\alpha)^{-1} \sum_s \phi_s * \zeta_s \quad \forall s \in S \tag{2.18}$$

$$Cost_s - \psi_s \leq \zeta_s \quad \forall s \in S \tag{2.19}$$

$$\zeta_s \geq 0 \quad \forall s \in S \tag{2.20}$$

$$\psi_s = \psi_{s\prime} \quad \forall s, s\prime \in S \tag{2.21}$$

2.3.2 Benders decomposition

The Benders decomposition was proposed by Benders (Benders, 1962) to solve large-scale MILP problems with complicating variables that when temporarily fixed give rise to a problem that is significantly easier to handle. When applied to a two-stage stochastic program, the Benders decomposition is also called L-shaped method (Louveaux and Birge, 2008). The complicating variables are the first-stage variables that when fixed render the scenario sub-problems decoupled. We consider the general

MILP formulation in Problem 2.22:

$$\min_{x,y} \quad c^T x + f^T y \tag{2.22a}$$
$$\text{s.t.} \quad Ax = b \tag{2.22b}$$
$$Bx + Dy = d \tag{2.22c}$$
$$y \geq 0 \tag{2.22d}$$
$$x \in Z_+^n \tag{2.22e}$$

where x are the integer complicating variables. The continuous variables y must satisfy along with the complicating variables x the linking constraint in Eq. 2.22c. When the complicating variables x are fixed, the Problem 2.22 can be separated into two decoupled optimization problems in the x and y variables. Problem 2.22 can be re-formulated as:

$$\min_{\hat{x} \in X} \{ c^T \hat{x} + \min_{y \geq 0} \quad \{ f^T y : Dy = d - B\hat{x} \} \} \tag{2.23}$$

where $\hat{x}$ are the fixed values of the complicating variables that satisfy the constraint set $X = \{x : Ax = b, x \in Z_+^n\}$. Since the inner minimization is a continuous linear program, it can be dualized with the dual variable $\lambda \in R^n$ that is associated to the constraint $Dy = d - B\hat{x}$ as shown in Problem 2.24.

$$\max_{\lambda \in R^n} \{ \lambda^T (d - B\hat{x}) : \lambda^T D \leq f \} \tag{2.24}$$

The Benders decomposition algorithm exploits the duality theory reformulating Problem 2.23 into Problem 2.25, where the inner primal optimization problem is substituted with its equivalent dual formulation.

$$\min_{\hat{x} \in X} \{ c^T \hat{x} + \max_{\lambda \in R^n} \quad \{ \lambda^T (d - B\hat{x}) : \lambda^T D \leq f \} \} \tag{2.25}$$

The feasible region of the inner maximization problem ($\Lambda = \{\lambda \mid \lambda^T D \leq f\}$) does not depend on the choice of the complicating variables $\hat{x}$. If Λ is not empty, the inner maximization problem can be either unbounded or feasible. If the inner optimization is unbounded, it exists a direction of unboundedness r_q, $q \in Q$ for which $r_q^T (d - b\hat{x}) > 0$. The set Q represents the set of the extreme rays of the feasible region Λ. To avoid an unbounded inner problem (which indicate an infeasible solution of the complicating variables $\hat{x}$), Eq. 2.26 can be added to the outer optimization problem.

$$r_q^T (d - B\hat{x}) \leq 0 \tag{2.26}$$

If the inner optimization problem is feasible, the optimal point is one of the extreme points λ_e, $e \in E$ (where E is the set of the extreme point of Λ). If all the cuts in Eq. 2.26 are added to the outer minimization problem, the optimal solution of the inner maximization problem is one of the extreme points. Therefore, Problem 2.25 can be

re-expressed as the Benders Master Problem 2.27:

$$\min_{x,\eta} \quad c^T x + \eta \tag{2.27a}$$

$$\text{s.t.} \quad Ax = b \tag{2.27b}$$

$$\eta \geq \lambda_e^T (d - Bx) \quad \forall e \in E \tag{2.27c}$$

$$0 \geq r_q^T (d - Bx) \quad \forall q \in Q \tag{2.27d}$$

$$x \in Z_+^n, \eta \in R^1 \tag{2.27e}$$

where Eq. 2.27c represents the optimality cuts and Eq. 2.27d the feasibility cuts. Since the enumeration of these cuts is not practical for large-scale problems, the Benders decomposition proposes a relaxation of the master problem and an iterative approach. The Benders algorithm solves the relaxed Benders master problem, which includes only a subset of the optimality (Eq. 2.27c) and feasibility cuts (Eq. 2.27d), to obtain a first trial value of the complicating variables $\hat{x}$. Then, it solves the Benders subproblem that is defined in 2.24, where the complicating variables x are fixed to the solution of the relaxed Master problem $\hat{x}$. If the sub-problem is feasible an optimality cut (Eq. 2.27c) is added to the relaxed master problem, otherwise an infeasibility cut is generated to exclude the current solution from the relaxed master problem. Since the relaxed master problem contains fewer constraints than the Benders reformulation in 2.27, its optimal objective function provides a lower bound of the final solution. On the other side, the optimal objective function of the Benders sub-problem (added to the term $c^T \hat{x}$) provides an upper bound of the final solution. The algorithm alternates between the relaxed master and the sub-problem until an optimal solution is found where the upper- and lower-bounds of the problem coincide.

The application of the Benders decomposition to a stochastic program generates as many independent sub-problems as the number of scenarios. The solution of the sub-problems generates the optimality cuts to be inserted into the relaxed master problem. A single-cut L-shaped method inserts into the relaxed master problem only one cut at each iteration. A multi-cut version (Birge and Louveaux, 1998) augment the relaxed master problem with multiple cuts (i.e. one cut per scenario) at each iteration.

The global optimality of the Benders decomposition requires convexity of the original problem in order to reformulate the inner optimization problem in 2.22 into the equivalent dual formulation. When the inner optimization in 2.22 presents integer variables (also called integer recourses for a stochastic program) the property of convexity is lost and the optimality cuts in Eq. 2.27c might not be valid cuts. A modification of the cut generation scheme (Laporte and Louveaux, 1993a, Carøe and Tind, 1998, Sherali and Fraticelli, 2002, Sen and Sherali, 2006, Li and Grossmann, 2019) is needed to handle integer sub-problems. A recent review of the Benders decomposition with an emphasis on combinatorial optimization can be found in (Rahmani et al., 2017).

2.3.3 Generalized Benders Decomposition

The Benders decomposition algorithm was generalized by Geoffrion (Geoffrion, 1972) to handle non-linear convex problems of the form:

$$\min_{x\in X, y\in Y} \quad f(x,y) \tag{2.28a}$$

$$\text{s.t.} \quad g(x,y) \leq 0 \tag{2.28b}$$

where x and y are the decision variables, X and Y the feasible sets of these variables and $g(x,y)$ a set of inequality constraint functions. As for the Benders decomposition, the original problem can be reformulated into an inner and outer optimization problem as shown in Problem 2.29 where the variables x are considered as complicating variables.

$$\min_{x\in X} \quad v(x) \tag{2.29a}$$

$$\text{s.t.} \quad v(x) = \min_{y\in Y} f(x,y) \quad \text{s.t.} \quad g(x,y) \leq 0 \tag{2.29b}$$

$$x \in X \cap V \tag{2.29c}$$

where

$$V \equiv \{x : g(x,y) \leq 0 \quad \textit{for some} \quad y \in Y\} \tag{2.30}$$

The Generalized Benders Decomposition (GBD) assumes that the set Y is convex and the functions $f(x,y)$, $g(x,y)$ are convex with respect to y. As for the Benders Decomposition, the GBD invokes the dual problem of $v(x)$ to obtain the Master Problem 2.31,

$$\min_{\eta\in R^1, x\in X} \quad \eta \tag{2.31a}$$

$$\text{s.t.} \quad \eta \geq \inf_{y\in Y}\{f(x,y) + \lambda^T g(x,y)\} \qquad \forall \lambda \geq 0 \tag{2.31b}$$

$$\inf_{y\in Y}\{u^T g(x,y) \leq 0\} \qquad \forall u \in U \tag{2.31c}$$

and the primal sub-problem 2.32

$$\min_{y\in Y} \quad f(\hat{x},y) \tag{2.32a}$$

$$\text{s.t.} \quad g(\hat{x},y) \leq 0 \tag{2.32b}$$

where $\hat{x}$ is a fixed point in X and $U = \{u \in R^m : u \geq 0 \;\; and \;\; \sum_{i=1}^m u_i = 1\}$. Therefore, if the set Y is not convex or the functions $f(x,y)$, $g(x,y)$ are not convex with respect to y, a dual gap might exist between the problem $v(x)$ and its dual.
Even when a relaxed master problem is considered by ignoring some of the constraints in Eqs. 2.31b-2.31c, Problem 2.31 still involves an inner optimization problem that is parametric in the variables x. For this reason, the GDB assumes that the solution of the inner optimization problem can be found independently of x.
Therefore, the practical implementation of the GBD solves the sub-problem 2.32 with an initial guess of the complicating variables $\hat{x}$. The optimal objective function of the

primal sub-problem represents an upper-bound of the solution of original problem 2.28. Then, it solves the relaxed master problem 2.33 where the variables y^k and the Lagrange multipliers λ^k are fixed to the optimal solution of the sub-problem at iteration k. The optimal objective function η^* is a lower-bound of the optimal value of Problem 2.28.

$$\min_{\eta \in R, x \in X} \quad \eta \tag{2.33a}$$

$$\text{s.t.} \quad \eta \geq f(x, y^k) + \lambda^{kT} g(x, y^k) \quad k = 1, \ldots, i, \tag{2.33b}$$

$$u^{kT} g(x, y^k) \leq 0 \quad k = 1, \ldots, j \tag{2.33c}$$

Eqs. 2.33b-2.33c correspond to the optimality and feasibility cuts of the Benders decomposition, respectively. The right-hand-side of Eq. 2.33b can also be seen as the Lagrange function of the relaxed master problem $L(x, y^k, \lambda^k)$ at iteration k. In terms of global optimality of the solution it is crucial to analyse the Lagrange function $L(x, y^k, \lambda^k)$ when non-linear terms are present, as shown in Section 2.3.4. The index i represents the *i-th* iteration of the GBD while the index j the iterations where the sub-problem is infeasible. The algorithm alternates between the relaxed master problem and the sub-problem with fixed complicating variables until the upper- and lower-bounds coincide (or differ for a pre-defined tolerance $\epsilon > 0$). If the sub-problem is infeasible for some fixed complicating variables $\hat{x}$, the values of (y, u) that satisfy $u^T g(\hat{x}, y) > 0$ must be inserted into the relaxed master problem.
The presented version of the GBD differs from the one presented in (Geoffrion, 1972) since it avoids to solve the inner optimization problem by fixing the variables y and the Lagrange multipliers λ to the optimal solution of the primal sub-problem. This is a valid implementation if the original problem is convex and is often adopted in practice, in particular, when non-convex terms are present (even though it might lead to a non-optimal point) (Sahinidis and Grossmann, 1991, Floudas and Visweswaran, 1990).

2.3.4 Global Optimization (GOP) algorithm

A crucial assumption of the GBD algorithm to guarantee global optimality is that the solution of the inner optimization problem in 2.31 can be found independently on the variables x. Therefore, the GBD fixes the variables y in 2.31 to the solution of the primal sub-problem y^k in order to eliminate the inner optimization. When non-convex terms are present (e.g. bi-linear terms), this assumption does not hold and the GBD might lead to a local optimal solution (Sahinidis and Grossmann, 1991).

We focus here on a class of non-convex problems where the assumption of the GBD on the inner optimization problem (i.e. its solution is independent on the x variables) is not valid. We introduce the Global Optimization (GOP) algorithm (Floudas and Visweswaran, 1990) that is able to handle (when particular conditions hold) problems of the form of 2.28 where non-linear non-convex terms are present in the functions $f(x, y)$ and/or $g(x, y)$. The GOP is based on a similar algorithmic procedure to the GBD by alternating between a relaxed master problem that provides a lower-bound of the final solution, and a sub-problem with fixed-complicating variables that provides an upper-bound of the final solution. The difference between the two algorithms is related to the way of handling the inner optimization problem in 2.31: the GOP makes a series of rigorous simplifications to reformulate the inner optimization problem in

2.31 and to guarantee global optimality of the final solution when non-convex terms are present.

For the case of feasible primal sub-problems (or complete recourse for a stochastic program), the inner optimization problem in 2.31, also denoted as Inner Relaxed Dual problem, can be expressed as

$$\min_{y \in Y} \quad L(x, y, \lambda^k) \tag{2.34a}$$

$$\text{s.t.} \quad L(x, y, \lambda^k) = f(x, y) + \lambda^{kT} g(x, y) \tag{2.34b}$$

where $L(x, y, \lambda^k)$ is the Lagrange function of Problem 2.32 at iteration k. If the original problem is convex, fixing the variables y to the solution of the primal sub-problem y^k (that defines a local support of $v(x)$ in 2.29 around the point y^k) represents a valid under-estimator for all values of x, and it can be used within the iterative procedure of the GBD algorithm. However, when non-convexities are present, the linear Lagrange function with fixed y^k ($L(x, y^k, \lambda^k)$) does not ensure an under-estimation of $v(x)$ for all the variables x and, therefore, might lead to local solutions.

The GOP is restricted to the class of non-convex problems where the Lagrange function $L(x, y, \lambda^k)$ is convex in y for $x = \overline{x}$ and is convex in x for $y = \hat{y}$. This is for example the case of non-convex bi-linear terms that appear in the objective function of a stochastic program with decision-dependent probabilities. When a variable of the non-convex bi-linear terms is fixed, the bi-linear terms become linear and therefore convex. For this class of problems, the linearization of the Lagrange function around the solution of the primal sub-problem y^k ($L^{lin}(\overline{x}, y, \lambda^k) \mid_{y^k}$) is therefore a valid under-estimator when the complicating variables are fixed to $\overline{x}$.

$$\min_y L(\overline{x}, y, \lambda^k) \geq \min_y L^{lin}(\overline{x}, y, \lambda^k) \mid_{y^k} \quad \forall \overline{x} \tag{2.35}$$

The linearization of the Lagrange function around the solution of the primal sub-problem y^k is expressed in Eq. 2.36:

$$L^{lin}(x, y, \lambda^k) \mid_{y^k} = L(x, y, \lambda^k) \mid_{y^k} + \sum_i \nabla_y L(x, y_i, \lambda^k) \mid_{y_i^k} (y_i - y_i^k), \tag{2.36}$$

where y_i is the *i-th* y variable. When the Lagrange function is replaced by its linearization, the authors in (Floudas and Visweswaran, 1990) proved that the solution of the Inner Relaxed Dual problem depends only on the variables y_i that are involved in the non-convex terms with the variables x. This sub-set of variables is called *connected variables*. This property implies that for such problems the computational effort does not depend on the total number of variables but on the number of connected variables (which can be limited to a small number).
Moreover, when the Lagrange function is linearized, the optimal solution of the Inner Relaxed Dual problem lies at the bounds (upper- or lower-bounds) of the connected variables. According to the definition of the linearized Lagrange function given in Eq. 2.36, it is straightforward to see that for a minimization problem if the gradient of the Lagrange function is positive ($\nabla_y L(x, y, \lambda^k) \mid_{y^k} > 0$) the solution lies on the lower-bounds of the connected y variables, and if negative ($\nabla_y L(x, y, \lambda^k) \mid_{y^k} < 0$) on the

upper-bounds. Therefore, as indicated in 2.37, for the discretized variables $x = \overline{x}$ the solution of the inner relaxed dual problem can be obtained by evaluating the Lagrange function over all the possible combinations of the bounds of the connected variables with the corresponding constraints on the sign of the gradients $\nabla_y L(x, y_k, \lambda^k) \mid_{y^k}$. The non-negativity and non-positivity of the gradient of the Lagrange function are known as *qualifying constraints* of the Lagrange function.

$$\min_y L(x, y, \lambda^k) \geq \min_{b_j \in B} \left\{ \begin{array}{lll} L^{lin}(x, y^{b_j}, \lambda^k) \mid_{y^k} & & \\ \text{with} & \nabla_y L(x, y, \lambda^k) \mid_{y^k} \geq 0 & \forall y_i^{b_j} = y_i^{LB} \\ & \nabla_y L(x, y, \lambda^k) \mid_{y^k} \leq 0 & \forall y_i^{b_j} = y_i^{UB} \\ & \forall x = \overline{x} & \end{array} \right\} \tag{2.37}$$

The set B represents the set of the upper- (y_i^{UB}) and lower-bounds (y_i^{LB}) of the connected variables y_i. With these rigorous simplifications, the GOP algorithm provides a way to handle the inner optimization problem in 2.31.
The last step of the GOP algorithm is to determine which Lagrange functions from the previous iterations can be included into the relaxed master problem. This is accomplished by evaluating the qualifying constraints of the previous Lagrange functions at the fixed value of the current (at iteration k) complicating variable $\overline{x}^k$. If the qualifying constraint is satisfied, the Lagrange function along with the satisfied qualifying constraint is added to the current relaxed master problem. Therefore, at iteration k the relaxed master problem 2.31 can be rigorously reformulated as Problem 2.38 to eliminate the inner optimization problem.

$$\min_{b_j \in B} \left\{ \begin{array}{lll} \min\limits_{\eta \in R^1, x \in X} & \eta & \\ \text{s.t.} & & \\ \eta \geq L^{lin}(x, y^{b_j}, \lambda^{k'}) \mid_{y^{k'}} & & \\ & \nabla_y L(x, y, \lambda^{k'}) \mid_{y^{k'}} \geq 0 & \forall y_i^{b_j} = y_i^{LB} \\ & \nabla_y L(x, y, \lambda^{k'}) \mid_{y^{k'}} \leq 0 & \forall y_i^{b_j} = y_i^{UB} \\ & \forall k' = \{1, 2, \ldots, k-1\}, k' \in LS(k) & \\ \eta \geq L^{lin}(x, y^{b_j}, \lambda^k) \mid_{y^k} & & \\ & \nabla_y L(x, y, \lambda^{k'}) \mid_{y^{k'}} \geq 0 & \forall y_i^{b_j} = y_i^{LB} \\ & \nabla_y L(x, y, \lambda^{k'}) \mid_{y^{k'}} \leq 0 & \forall y_i^{b_j} = y_i^{UB} \end{array} \right\} \tag{2.38}$$

The set $LS(k)$ is the set of Lagrange functions over the iterations $1, 2, \ldots, k-1$ whose qualifying constraints are satisfied for $x = \overline{x}^k$. The GOP algorithm can be stated in the following steps:

- *Step 0*: Initialization of the complicating variables $\overline{x}^k = x^0$ with $k = 0$ and of the upper- and lower-bounds of the final solution $UB^k = +\inf, LB^k = -\inf$
- *Step 1*: Iteration update $k \leftarrow k + 1$
- *Step 2*: Solution of the sub-problem 2.32 with fixed complicating variables $\overline{x}^k = \overline{x}^{k-1}$ obtaining the optimal Lagrange multipliers λ^k
- *Step 3*: Creation of the relaxed master problem 2.38 by adding the Lagrange function of the previous iterations $k' \in \{1, \ldots, k-1\}$ if the qualifying constraints evaluated at $\overline{x}^k$ are satisfied

- *Step 4*: Solution of the relaxed master problem 2.38 for each combination of the bounds of the connected variables $y_i^{b_j}$. The optimal objective function values are stored in the vector z^*_{MP}.
- *Step 5*: Bounds update according to $LB^k = min\{z^*_{MP}\}, UB^k = min\{UB^{k-1}, z^{SP*}\}$
- *Step 6*: Convergence test to verify if the upper- and lower-bounds are sufficiently close. If $UB^k - LB^k < \epsilon$, stop. Else, go to step 3.

2.3.5 Solution methods for stochastic programs with endogenous uncertainty

Stochastic programs with decision-dependent probabilities give rise to non-convex MINLP problems. Given the complexity of the formulation it is unrealistic to solve the deterministic equivalent problem up to global optimality. In (Peeta et al., 2010) the authors approximate the original problem by relaxing the integrality of investment variables and applying Taylor series expansion with the idea of sacrificing global optimality to gain tractability for the problem under investigation. In (Zhan et al., 2016) the authors introduce a quasi-exact solution approach to reformulate the non-linear multistage stochastic investment model to a mixed-integer linear programming (MILP) model. The reformulation-linearization technique is based on the work proposed in (Meyer and Floudas, 2006). In (Escudero et al., 2018) the authors present the Cluster Dual Descent Algorithm to solve the stochastic mixed 0-1 bilinear optimization problem with decision dependent uncertainty. In (Hellemo, Barton, and Tomasgard, 2018) the authors propose a global solution method combining McCormick-Based Relaxations of Algorithms (Mitsos, Chachuat, and Barton, 2009) and Benders decomposition, where the non-convex bi-linear terms are iteratively under- and over-estimated. However, the algorithm solves the non-convex MINLP problem as fast as the global solver BARON (Kilinc and Sahinidis, 2018) when a branching priority scheme is implemented.

Stochastic programs with decision-dependent structure are typically modelled with conditional non-anticipativity constraints (NACs) that are NACs that are activated by the decision variables. In (Goel and Grossmann, 2004) the optimization problem of utilization of natural gas resources is solved locally using a tailored decomposition method that searches in a sub-space of the feasible region of the original optimization problem by iteratively fixing some investment decisions. The resulting exogenous multi-stage tree is solved in a shrinking-horizon fashion. This formulation was further extended in (Goel and Grossmann, 2006) to exogenous uncertainty sources. The authors identify a set of theoretical properties that lead to reduction in the size of the model and propose a branch and bound algorithm that is based on Lagrangean duality. In (Solak et al., 2010a) good-quality heuristic solutions of the multi-stage integer stochastic project portfolio optimization are found by applying the Lagrangian relaxation and the sample average approximation algorithm. In (Colvin and Maravelias, 2008), (Colvin and Maravelias, 2009), (Colvin and Maravelias, 2010) the authors reduce the size of the problem by proving the redundancy of a large number of conditional NACs. In (Apap and Grossmann, 2017) the authors review existing formulations and solution methods to solve stochastic problems with decision-dependent structure and propose two solution approaches. The first approach is a sequential scenario decomposition heuristic that sequentially solves

endogenous MILP subproblems to determine the decisions that influence the uncertainty revelation, fix these decisions, and then solve the resulting sub-problem to obtain a feasible solution. The second approach is the Lagrangean decomposition.

From these works, it is evident that endogenous uncertainty sources drastically increase the complexity of stochastic programs and that custom solution algorithms that are able to exploit the specific structure of the problem at hand are needed to reduce the required computational effort.

Part III

Case studies and results

All models are wrong but some are useful

George Box

Chapter 3

Integrated electricity procurement and production scheduling

This chapter studies the challenges faced by large electricity consumers to simultaneously determine the optimal production schedule and the electricity procurement. The electricity purchase options include different types of power contracts (Base load, Time-of-Use) and different spot markets (day-ahead market, intra-day market, futures market, Over-the-Counter market). These options mainly differ in the time shift delay between trading and delivery time:

- Long-term contracts (base load) define a constant price and a constant amount of electricity delivered over a time horizon of at least one year;
- Time-of-Use contracts (TOU) are characterized by price levels consisting of a time-dependent component and an amount-dependent component and cover a period of time between one week and three months. They can include penalties if they are exceeded and peak load costs;
- The day-ahead market trades electricity for the following day defining daily an hourly-varying electricity price;
- The intraday market continuously trades electricity to avoid supply-demand unbalances. The lead time for trading can be down to five minutes.

Integrating electricity procurement and production scheduling enables the simultaneous optimization of the electricity purchasing decisions and the adjustment of the production rates to time-varying price signals. The electricity procurement decisions must be made at a point in time before the operations. Therefore, accounting for uncertainty is crucial. Modelling different electricity purchase options within an optimization under uncertainty framework gives rise to different formulations according to the procurement features. In Section 3.1 we focus on the day-ahead electricity market and the related bidding process to procure electricity. The inherit uncertainty of the bidding process is modelled via a two-stage stochastic formulation. Section 3.2 extends the two-stage stochastic formulation to a multi-stage problem to include TOU power contracts as source of electricity procurement.

Literature review

The importance of the optimal energy procurement for large electricity consumers is reflected in the large amount of literature on the topic. We review some existing

works highlighting the differences between an integrated and a sequential approach.

In (Beraldi et al., 2011) the authors focus on the optimal electricity procurement strategy by solving in a rolling horizon fashion a stochastic program to determine the amount of electricity purchased from the TOU contracts and from the spot markets. In (Carrión et al., 2007) the authors define the day-ahead bidding curves for a large consumer purchasing electricity from the day-ahead market. The same problem is solved in (Jalal Kazempour, Conejo, and Ruiz, 2015) formulating a complementary bi-level model. In these works the main aim is to define the optimal electricity procurement plan and the electricity demand of the consumer is considered as a known or uncertain parameter. The optimizer does not have the capability to exploit the process flexibility adjusting the production rates to time-varying price signals.

From a process scheduling point of view, a number of contributions emphasized the importance of adapting the production level to the time-varying price signals of the spot markets in order to reduce the energy cost. In (Nolde and Morari, 2010), a scheduling solution for electrical load tracking of a steel plant is proposed. The schedule is defined such that the total electricity consumption tracks the load curve as closely as possible while respecting all production constraints. In (Hadera et al., 2015, Hadera et al., 2019), the authors take into account multiple electricity sources (day-ahead market and on-site generation) and the load deviation problem to determine the optimal production schedule for a steel-making plant. Additional works on scheduling models that take into account the time-varying electricity price can be found in the literature (Mitra et al., 2013, Ramin, Spinelli, and Brusaferri, 2018, Wenzel et al., 2019) emphasizing the large potential for load shifting in case of process flexibility. In these contributions, the main focus is the process scheduling, and the electricity procurement decisions are assumed as given and are not optimized. Toward an integrated formulation, in (Dalle Ave, Harjunkoski, and Engell, 2018) the authors solve deterministically a two-day horizon problem defining the optimal energy-aware schedule for the first day (following a predefined commitment) and the optimal future load prediction for the second day.

The main challenge of the integration of the electricity procurement and the production scheduling results from the delay between the decisions. The procurement decisions must be made before the operations and, therefore, uncertain market conditions (e.g. electricity prices, demand) or uncertain process conditions (e.g. processing times of tasks) can have an important impact on the energy cost. A pioneering work integrating electricity procurement and production scheduling is described in (Zhang et al., 2016). The authors apply stochastic programming to define the optimal electricity profile purchased from the power contracts and the optimal schedule of an air separation plant. Considering a medium-term electricity procurement problem, the authors neglect the day-ahead commitment problem for the day-ahead market.

3.1 Stochastic short-term integrated electricity procurement and production scheduling for a large consumer

This section is based upon

- *Leo E. and Engell S., Integrated day-ahead energy procurement and production scheduling, Automatisierungtechnik 2019*
- *Leo E., Dalle Ave G., Harjunkoski I. and Engell S., Stochastic short-term integrated electricity procurement and production scheduling for a large consumer, Computers & Chemical Engineering, Volume 145, February 2021.*

Here we focus on the day-ahead electricity market and the challenge faced by large electricity consumers to simultaneously determine the optimal day-ahead electricity commitment and the optimal energy-aware production schedule. The inherent uncertainty of the problem, due to the bidding process in the day-ahead market, is dealt with by means of the stochastic programming modelling framework. In particular, a two-stage problem is formulated with the aim of establishing the optimal bidding strategy and the optimal production schedule hedging against price uncertainty. The optimal integrated solution is defined to minimize the overall cost and to control the risk of high cost scenarios due to uncertain price peaks. The stochastic model is solved with a scenario-decomposition approach. Extensive numerical experiments have been carried out to assess the performance of the proposed decision approach. The results collected when considering an industrial relevant case-study show the superiority of the proposed methodology in comparison with a deterministic approach.

The figures and the tables of this section are adapted from (Leo et al., 2021).

3.1.1 Problem statement

We consider an energy-intensive plant that produces a given set of products. The product demand is assumed to be known for the optimization horizon. The plant parameters (e.g. batch time, resource consumption) are fixed and known. The operating cost consists of the electricity purchasing cost. Electricity can be purchased from the day-ahead market and/or from the balancing market.

The day-ahead electricity purchasing is performed via a bidding process. The plant has to provide bids a day in advance, before the time when the market is cleared. A bid consists of the amount of electricity and the corresponding purchasing price. After the market is cleared, the day-ahead equilibrium prices for every hour of the following day are announced and participants are informed whether their bids were accepted or rejected. For each hour of the following day the bids at a price higher than the clearing price are accepted. The clearing prices represents the hourly rate charged to the customer, while the accepted bids for every hour represent the consumer load commitment. The problem of submitting bids to the day-ahead market will be referred to as the bidding problem. Load deviations in the following day are dealt with by the balancing market.

The goal is to optimally define simultaneously the production scheduling and the electricity procurement, accounting for electricity market mechanisms and the realistic revelation of the market information. Bidding decisions have to be made with uncertain information on the day-ahead market price, whereas scheduling decisions can be postponed until complete information on the clearing day-ahead price is fully available. We consider uncertainty in the clearing price of the day-ahead market and, therefore, in the proposed formulation the here-and-now decisions are the bidding decisions since they have to be made before the realization of the price uncertainty.

The wait-and-see decisions are the scheduling decisions, the actual electricity consumption and the load deviations with respect to the day-ahead commitment since these decisions can be adjusted in response to the realization of the uncertainty.

The main idea of the energy-aware scheduling formulation is to flatten the electricity consumption profile according to the electricity price by shifting the consumption from the price peaks to the price valleys. Since the electricity price is uncertain, only an estimation of the timing of the price peak is available. To also account for the uncertain price of the peaks, rather than only average the cost over the price scenarios, we integrate a risk measure in the optimization problem. Here we adopt the Conditional Value at Risk (CVaR), since it is a coherent risk measure defined by convex equations. Namely, the objective function of the proposed formulation is a linear combination of the total expected cost and the CVaR.

Value of the stochastic solution

The value of the stochastic solution (VSS) measures the advantage of accounting for uncertainty adopting a two-stage stochastic program over using the deterministic counterpart where the uncertain parameters have been replaced by their expected values. In other words, it measures the advantage of taking decisions aware of possible uncertainty realizations and reacting to the these realizations with recourse variables. The definition of the VSS and of the relative $\overline{VSS}$ are given in Eqs. 2.9-2.10. As already described, in the proposed formulation the first-stage variables are the electricity volumes and the prices of the hourly bids. Therefore, the computation of the VSS requires to fix the bids volumes and bids prices of the Recourse Problem (RP) to the solutions of the EVP that, however, is not aware of price uncertainty and of the possibility that the bids might not be accepted if the bid price is lower than the price that realizes. In fact, the bidding strategy of the EVP would propose a bid price equal to the expected day-ahead price and, therefore, a price realization (scenario) of the RP higher than the expected day-ahead price would result in a rejected bid and in high load deviations and high scenario costs. Hence, this computation would show high but unrealistic values of the VSS. To overcome this issue we define $VSS^{inelastic}$, in which the volumes of the bids of the RP are fixed to the volumes obtained from the EVP, but the prices of the bids of the RP are fixed to the maximum prices. In other words, the decision maker is willing to accept any possible realization of the day-ahead price (inelastic bidding). It is straightforward to prove that the following relation always holds $0 \leq VSS^{inelastic} \leq VSS$ if the load deviation prices are higher than the day-ahead prices as assumed in this work. The proposed definition of the $VSS^{inelastic}$ reflects also the common industrial practice of inelastic bidding.

Scenario generation

To generate the set of electricity price scenarios we identify a day-ahead electricity price model from price data (*Gestore Mercati Energetici* 2019) applying the ARIMA methodology as described in (Fleten and Kristoffersen, 2007, Nogales et al., 2002). More information on the ARIMA identification can be found in (Aggarwal, Saini, and Kumar, 2009). The scenarios are generated according to the following steps:

- Identification of the ARIMA model from historical data (Fig. 3.1a)

- Validation of the model against the electricity price data (Fig. 3.1b)
- Monte Carlo simulation to generate a large number of scenarios (Fig. 3.1c)
- Scenario-reduction procedure (Fig. 3.1d).

The different scenario generation steps are carried out with the software MATLAB. Monte Carlo sampling has been used to simulate 100 scenarios, that however for the industrial-size case study have been reduced applying the scenario reduction routine SCENRED in GAMS (Heitsch and Römisch, 2001, Dupačová, Gröwe-Kuska, and Römisch, 2003). Note that the scenario reduction routine most likely returns a reduced set of scenarios with different probabilities.

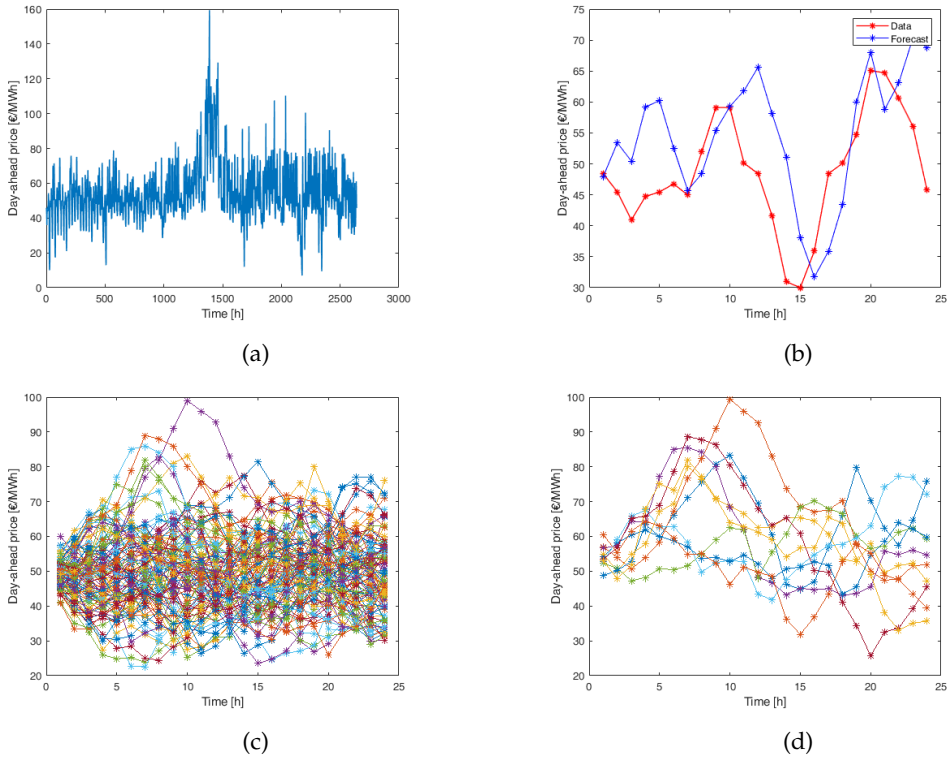

FIGURE 3.1: (a) Day-ahead price from 01.01.2018 to 01.04.2018 from the Italian electricity market (*Gestore Mercati Energetici* 2019), (b) Validation of the identified price model against the price data of the 02/04/2018 from the Italian electricity market, (c) Day-ahead electricity price scenarios, (d) Reduced set of day-ahead electricity price scenarios. Source: (Leo et al., 2021).

Features of the electricity markets and modelling assumptions

The features of the considered electricity markets define the structure of the proposed stochastic formulation. In particular, the timing of the bid submission and the information on the auction results are key factors that need to be carefully analysed For the day-ahead market, the trading is executed as a uniform price, double-sided call auction. Buyers and sellers submit bids (i.e. a combination of volume and price) for every hour of the following day. All supply and demand curves are aggregated and the uniform market clearing price is determined. After the market is cleared,

the participants are informed whether their bids for every hour of the following day were accepted or rejected. The accepted bids define the amount of electricity that the buyers commit to purchase and the sellers agree to provide.

The balancing market ensures that the power grid is balanced if short-term imbalances occur because of unforeseen plant outages, incorrect demand predictions or stochastic feed-in from the renewable energies. Imbalance prices reflect the real-time system balancing costs and according to the quality of the traded balancing power (primary control reserve, secondary control reserve and minute reserve) they are defined after the imbalance has realized.

In this work, the model of the day-ahead market accurately reflects the market regulations by considering unknown and uncertain clearing prices by the time the hourly bids have to be submitted. The day-ahead prices become known only after the market has been cleared. Regarding the balancing market, the proposed formulation assumes that a certain estimation of the balancing prices (or load deviation prices) is available. The estimation depends on the uncertain scenario assuming a positive correlation between the day-ahead prices and the balancing prices. In particular, for each scenario the imbalance prices are considered to be higher than the uncertain day-ahead prices. In other words, when a peak of the day-ahead price realizes, we assume that deviating from the load commitment in the same time step is more expensive. In fact, a lower value of the balancing prices compared to the day-ahead prices of the same scenario would drive the optimization solution to drastically deviate from the load commitment, purchasing more electricity from the balancing market. The load deviation prices for over- and under- consumption are listed in Table 3 in Appendix .1.

Nomenclature	
Indices	
i	products
$t, t\prime$	time steps
$m, m\prime$	operating modes
$s, s\prime$	scenarios
j	vertices of the mode production region
h	steel heats
u	steel production units
k	steel production stages
g	steel heat groups
r	resources
Sets	
I	products
T	time periods
M	operating modes
S	scenarios
H	steel heat
U	steel production unit
K	steel production stage
G	steel heat group
R	resources
Parameters	
v_{mjis}	production of i at vertex j of mode m in scenario s [kg]
$\theta_{m,m\prime,t}$	minimum stay time in mode m after transition from mode $m\prime$ [h]
δ_m	fix electric power consumption in mode m [kWh]
γ_{mi}	electric power consumption coefficient for product i in mode m [kWh/kg]
$IV_{it}^{max}, IV_{it}^{min}$	upper and lower bounds of the inventory level of product i at time period t [kg]
$IV_i^{initial}, IV_i^{final}$	initial and final inventory level of product i [kg]
$y_{m,initial}$	initial active operating mode
D_{it}	demand of product i at time period t [kg]
$p_{ts}^{day-ahead}$	day-ahead electricity price for time period t in scenario s [€/kWh]
P^p	electricity price at price index p [€/kWh]
ϕ_s	probability of scenario s
p_{st}^+, p_{st}^-	load deviation penalties for over- and under- electricity consumption at time period t in scenario s [€/kWh]
p_i	price of purchasing product i [kg]
α	quantile in the definition of the CVaR CV
η	objectives priorities
μ_{rit}	structural RTN parameter to define the interaction between resource s and task i at time t
$power_{hu}$	power consumption to execute the heat h on the unit u
$maxtrfuu\prime/mintrfuu\prime$	maximum/minimum transfer time from unit u to $u\prime$
Continuous variables	
PR_{its}	total production of i at time t in scenario s
$\overline{PR}_{mits}$	production of i at time t in mode m in scenario s
λ_{mjts}	coefficients for extreme point j of the feasible region in mode m at time period t for scenario s
EU_{ts}	electric power consumption at time t in scenario s
$EU\_r^{el}{}_{ts}$	total electricity consumption (resource r^{el}) at time t in scenario s for the RTN formulation
IL_{its}	amount of inventory of product i at time t in scenario s
SO_{its}	amount of product i sold at time t in scenario s
PU_{its}	amount of product i purchased at time t in scenario s
BA_{pts}	day-ahead bid volume accepted at time t, at price level p in scenario s
B_{pts}	day-ahead bid volume at time t, at price level p in scenario s
$\delta e_{ts}^+, \delta e_{ts}^-$	electricity mismatches (over-consumption and under-consumption) at time t in scenario s
z	expected second-stage cost
$\overline{z}$	linear combination of the expected second-stage cost and the CVaR
$CVaR$	conditional value at risk
ψ, ζ_s	auxiliary variables for the definition of $CVaR$
R_{rts}	non negative continuous variables to define the amount of resource r at time t for scenario s
Binary variables	
y_{mt}	one if the operating mode m is active in time period t
$z_{m,m\prime,t}$	one if transition from mode m to mode $m\prime$ occurs at time t
N_{its}	one if the task i starts at time t in scenario s

3.1.2 Illustrative example

MILP formulation

To highlight the features and the advantages of the proposed approach and to discuss the results independently from the optimization algorithm used, we apply it to a continuous production plant. The process constraints are described in (Zhang et al., 2016) and the stochastic programming version for the short-term electricity procurement was proposed in (Leo and Engell, 2019b). For completeness we describe here the entire optimization formulation including the bidding model.

Plant model

The plant produces two products i (P_i) and it presents three different operating modes m: *on*, *off* and *start-up*. The variable $\overline{PR}_{mits}$ defines the production for each mode m for each product i at time t of the horizon T for scenario s. The production for each mode m is computed by Eq. 3.2 as the convex combination of the extreme points v_{mjis} of the mode feasible region. The sum of the coefficients of the convex combination of the extreme points v_{mjis} is forced to be equal to the binary variable y_{mt} that defines whether the mode m is active in time period t. The total hourly production is defined by Eq. 3.1 as the sum over the operating modes m of $\overline{PR}_{mits}$. Only one mode can be active at each time period t (Eq. 3.4). The possible mode transitions (*off* to *start-up*, *start-up* to *on*, and *on* to *off*) are identified by the binary variable $z_{mm\prime,t}$ that is equal to one if and only if the plant switches from mode m to mode $m\prime$ in time period t. The mode transition can happen only after fixed periods of time ($\theta_{mm\prime}$) that have been spent in mode m (Eqs. 3.5-3.6). Note that while the decisions on the operating modes and on the shut down of the plant (identified by the variables y_{mt}, $z_{m\prime m,t}$) have to be made the day before the operation and, therefore, are classified as first-stage variables, whereas the production levels (identified by the variables PR_{its}, $\overline{PR}_{mits}$) can be adjusted according to the realization of the uncertain parameters. The electricity consumption at time period t for scenario s is defined by EU_{ts} as the sum of a fixed term δ_m for the active mode and a variable term proportional to the hourly production $\overline{PR}_{mits}$. All the data are listed in Appendix .1.

$$PR_{its} = \sum_{m} \overline{PR}_{mits} \quad \forall i \in I, t \in T, s \in S \tag{3.1}$$

$$\overline{PR}_{mits} = \sum_{j} \lambda_{mjts} * v_{mjis} \quad \forall i \in I, t \in T, s \in S, m \in M \tag{3.2}$$

$$\sum_{j} \lambda_{mjts} = y_{mt} \quad \forall t \in T, s \in S \tag{3.3}$$

$$\sum_{m} y_{mt} = 1 \quad \forall t \in T \tag{3.4}$$

$$\sum_{m\prime} z_{m\prime m,t-1} - \sum_{m\prime} z_{mm\prime,t-1} = y_{mt} - y_{m,t-1} \quad \forall m \in M, t \in T \tag{3.5}$$

$$\sum_{k=1}^{\theta_{mm\prime}} z_{mm\prime,t-k} \leq y_{m\prime t} \quad \forall (m, m\prime) \in M, m \neq m\prime, t \in T \tag{3.6}$$

$$EU_{ts} = \sum_{m} \left(\delta_m * y_{mt} + \sum_{i} \gamma_{mi} * \overline{PR}_{mits} \right) \quad \forall t \in T, s \in S \tag{3.7}$$

Inventory balance

The produced products *P1* and *P2* can be stored independently and the amount of inventory of product i at time t for each scenario s, IL_{its}, is defined as the amount of inventory of product i at the previous time step $(t-1)$ increased by the produced quantity of product i at time t, represented by PR_{its}, minus the product i sold at time period t, indicated by SO_{its}. These variables are defined for each scenario s since they represent the second-stage variables (*wait-and-see* decisions). The inventory levels cannot exceed the upper and lower bounds as described in Eq. 3.9. A demand satisfaction constraint (Eq. 3.10) ensures that the sum of sold product i, SO_{its}, and the purchased product i, PU_{its}, covers the product demand i. The variable PU_{its} can also be seen as a penalty for not meeting the demand.

$$IL_{its} = IL_{i,t-1,s} + PR_{its} - SO_{its} \quad \forall i \in I, t \in T, s \in S \tag{3.8}$$

$$IL_{it}^{min} \leq IL_{its} \leq IL_{it}^{max} \quad \forall i \in I, t \in T, s \in S \tag{3.9}$$

$$SO_{its} + PU_{its} = D_{it} \quad \forall i \in I, t \in T, s \in S \tag{3.10}$$

Initial and final conditions

Eqs. 3.11-3.12 set the plant initial conditions in terms of products inventory and active operating mode. Eq. 3.14 provides the history of the mode transitions before the optimization horizon. A terminal constraint is imposed for the inventory levels by Eq. 3.13.

$$IL_{i,0,s} = IL_{i}^{initial} \quad \forall i \in I, s \in S \tag{3.11}$$

$$y_{m,0} = y_{m,initial} \quad \forall m \in M \tag{3.12}$$

$$IL_{i,t^{final},s} \geq IL_{i}^{final} \quad \forall i \in I, s \in S \tag{3.13}$$

$$z_{mm\prime,t} = z_{mm\prime t}^{initial} \quad \forall (m, m\prime) \in M, -\theta^{max} + 1 \leq t \leq -1 \tag{3.14}$$

Day-ahead electricity market constraints

The electric power can be purchased from the day-ahead market. To model the double-sided call trading in the day-ahead electricity market, the bidding model developed in (Fleten and Kristoffersen, 2007) is adopted. Buyers have to submit step-wise demand curves for every hour of the following operation day. The consumer is assumed to act as a price-taker and therefore not able to influence the realization of the market clearing price. To formulate the bidding model as a linear program, bid prices are considered to be fixed parameters. Thus, the optimization solution has to decide which volume to bid for each price. Bid volumes at each price index p and hour t are represented by the continuous variables $B_{p,t} \geq 0$. Eq. 3.15 enforces that

the bidding curve is monotonically decreasing according to the operating rules of the market.

$$B_{p,t} \geq B_{p+1,t} \qquad \forall p \in P, t \in T \tag{3.15}$$

Whether a bid is accepted depends on the uncertain day-ahead clearing price at hour t and scenario s, $p_{t,s}^{day-ahead}$. The accepted bids, represented by the variables $BA_{p,t,s}$, are defined in Eq. 3.16.

$$BA_{p,t,s} = B_{p,t} \qquad if \;\; P_p \leq p_{t,s}^{day-ahead} \leq P_{p+1} \tag{3.16}$$

Eq. 3.16 models the realization of the uncertain day-ahead prices by ensuring that the accepted bid volumes are the bid volumes associated to a bid price P_p equal to the price realization $p_{t,s}^{day-ahead}$ for each time t and scenario s. Note that the bid volumes that are associated to bid prices lower than the price realization are not accepted and, therefore, no electric power is purchased from the day-ahead market. It is worth to highlight that the bid prices are modelled as fixed parameters to obtain linear bidding equations and, consequently, to avoid the introduction of binary variables for the implementation of the *if-statement* in Eq. 3.16.

The sum of the accepted bids over the price indexes p identifies the consumer electricity commitment at each hour t. Electricity over-consumption and electricity under-consumption, δe_{ts}^{+}, δe_{ts}^{-}, represent the load mismatches respect to the day-ahead electricity commitment and therefore expressed as the difference between the actual consumption of electric power, EU_{ts} and the accepted bid (see Eqs. 3.17-3.18-3.19). The load deviations represent the electricity purchased from the balancing market. As previously discussed, here no uncertainty is considered for the load deviations prices. No restrictions are imposed on the over-consumption and under-consumption of electric power. Since the day-ahead electricity commitment has to define the amount of energy to be purchased for a period of 24 hours one day in advance the actual day-ahead electricity price is realized, the bidding volume decisions are first-stage variables and the accepted bids and the load deviations are recourse decisions reacting to the price realization.

$$EU_{t,s} - \sum_{p} BA_{p,t,s} = \delta e_{t,s}^{+} - \delta e_{t,s}^{-} \quad \forall t \in T, s \in S \tag{3.17}$$

$$\delta e_{t,s}^{+} \geq 0 \quad \forall t \in T, s \in S \tag{3.18}$$

$$\delta e_{t,s}^{-} \geq 0 \quad \forall t \in T, s \in S \tag{3.19}$$

Objective function

The objective function of the optimization problem is defined by Eq. 3.20 as the linear combination of total expected cost z and the risk measure Conditional Value at Risk (CVaR). Since this generates a multi-objective optimization, the scalar parameter $\eta \in [0, 1]$ implements a scalarization of the objective function prioritizing the two objectives.

$$\bar{z} = \eta * z + (1 - \eta) * CVaR \tag{3.20}$$

Eq. 3.21 defines the total cost, z, as the expected second stage cost since the first stage (bidding) has no cost. The second stage cost consists of the cost of the accepted bids (electricity purchasing) on the day-ahead market, the cost of load deviations (balancing market) and the cost of purchasing products externally at the price p_i to cover the demand.

$$z = \sum_t \left(\sum_s \phi_s * \left(p_{t,s}^{day-ahead} \sum_p BA_{p,t,s} + p_{st}^+ * \delta e_{ts}^+ + p_{st}^- * \delta e_{ts}^- + \sum_i p_i * PU_{its} \right) \right) \tag{3.21}$$

where $p_{t,s}^{day-ahead}$ represents the day-ahead electricity price and p_{st}^+, p_{st}^- the load deviations costs for over consumption and under consumption; ϕ_s represents the probability of scenario s.
According to (Rockafellar and Uryasev, 2000), the linear programming constraints defining the CVaR for the quantile α are reported in Eqs. 3.22-3.24 (see Section 2.1.2 for the definition of the CVaR).

$$CVaR = \psi + (1-\alpha)^{-1} \sum_s \phi_s * \zeta_s \tag{3.22}$$

$$\sum_t \left(p_{t,s}^{day-ahead} \sum_p BA_{p,t,s} + p_{st}^+ * \delta e_{ts}^+ + p_{st}^- * \delta e_{ts}^- + \right.$$
$$\left. + \sum_i p_i * PU_{its} \right) - \psi \leq \zeta_s \forall s \in S \tag{3.23}$$

$$\zeta_s \geq 0 \quad \forall s \in S \tag{3.24}$$

where ψ, ζ_s are continuous variables. When the cost of scenario s is greater than the variable ψ, the difference between the scenario cost and the variable ψ is computed with the variable ζ_s; otherwise ζ_s takes the value of zero.

Solution method

The proposed two-stage stochastic formulation was solved by generating the deterministic MILP equivalent problem. The deterministic equivalent has 1 498 113 constraints and 557 284 variables (209 discrete variables).

The proposed formulation was implemented within the algebraic modelling environment GAMS and the resulting MILPs were solved using the commercial solver CPLEX 12.7 on an Intel Core i7-2600 machine at 3.40 GHz with 8 processors and 8 GB RAM running Windows 7 Professional.

Results

We solve the problem for the original scenario set (100 scenarios) and for the reduced one (10 scenarios). The original scenario set allows us to analyse the effect of the risk model on the optimal solution. The introduction of the CVaR defines a multi-objective optimization problem and therefore the optimal solution lies on the Pareto front (if the problem is solved to optimality). The Pareto front is shown in Figure 3.2.

The comparison of the hourly scenario cost distribution for the risk neutral solution (optimization of the expected second stage cost) and the risk-averse solution is given in Figure 3.3a. The data above the top edge of the box (dash line and cross marker) represent the scenario costs over the 75th percentiles. We can see that the risk-averse solution reduces the probability of high cost scenarios, namely, purchasing electricity during uncertain price peaks. The shaded area highlights the time between ($t = 7$ and $t = 10$) where the influence of the risk measure on the distribution of the hourly scenario costs is pronounced since in these time steps the uncertain price peaks are more likely realize (as shown in Figure 3.1d). Figure 3.3b shows the scenario cost distribution at time $t = 8$ emphasizing that the probability of purchasing electricity during a price peak, namely the probability of a cost greater or equal to 220 €, drops from 8 % for the risk-neutral solution to 0 % for the risk-averse solution.

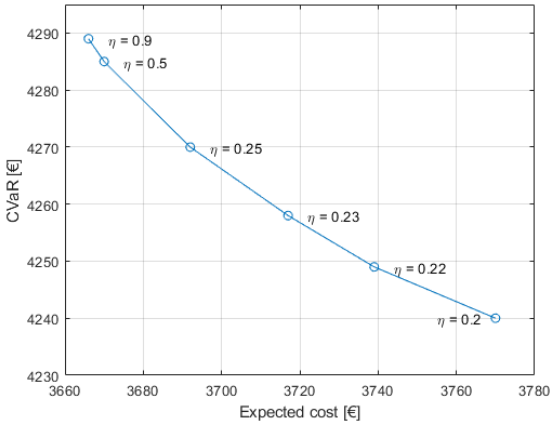

FIGURE 3.2: Pareto curve of risk-averse stochastic optimization ($\alpha = 0.9$) for 100 scenarios. Source: (Leo et al., 2021).

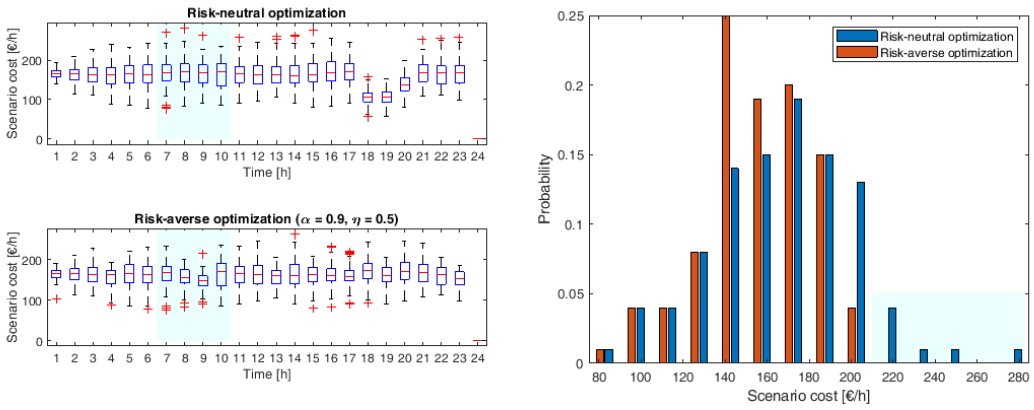

(a) (b)

FIGURE 3.3: (a) Distribution of the hourly scenario costs with risk-neutral and risk-averse stochastic optimization ($\alpha = 0.9$ and $\eta = 0.5$) for 100 scenarios, (b) Scenario costs distribution with risk-neutral and risk-averse stochastic optimization ($\alpha = 0.9$ and $\eta = 0.5$) at $t = 8$ for 100 scenarios. Source: (Leo et al., 2021).

Finally for the case with reduced number of scenarios we compute the relative Value

of the Stochastic Solution ($\overline{VSS}$) to estimate the benefit to adopt a stochastic formulation instead of the deterministic counterpart. Table 3.1 shows that the $\overline{VSS}^{inelastic}$ can be quite significant. Note that the recourse problem cost with elastic bidding is higher than the recourse problem cost with an inelastic bidding $z^{RP}_{elastic} \gg z^{RP}_{inelastic}$ and therefore the standard computation of the $\overline{VSS}$ would result is in a larger value $\overline{VSS} \gg \overline{VSS}^{inelastic}$, as already discussed in Section 3.1.1. Therefore, we adopt the $\overline{VSS}^{inelastic}$ to have a conservative and realistic estimation of the potential savings reachable applying the proposed stochastic formulation.

TABLE 3.1: Relative Value of the Stochastic Solution for 10 scenarios. Source: (Leo et al., 2021).

z^{EVP}	$z^{RP}_{elastic}$	$z^{RP}_{inelastic}$	z^{SP}	$\overline{VSS}^{inelastic}$	η
4 395,854	46 602,3	5 364,7	4 482,8	3,3 %	0,8
	32 705,0	5 001,4	4 647,9	7 %	0,5
	80 757,1	5 606,9	4 922,4	12,2 %	0

TABLE 3.2: Detailed results of the stochastic solution for 10 scenarios. Source: (Leo et al., 2021).

$CVaR^{RP}$	$E[cost]^{RP}$	$CVaR^{SP}$	$E[cost]^{SP}$	η
5 606,9	4 395,8	4 934,8	4 369,8	0,8
		4 922,6	4 373,5	0,5
		4 922,4	4 922,4	0

Bidding curves of a given hour ($t = 5$) have been drawn in Figure 3.4c. The curves are shown for the stochastic problem (step-wise curve) and for the expected value problem (vertical line). The horizontal lines represent the uncertain price realizations. Figure 3.4c shows that the optimal solution proposes price-elastic bids, namely different bidding volumes at different prices. Figures 3.4a-3.4b show respectively the expected electricity consumption of the stochastic solution and of the expected value problem. Since the stochastic solution is aware of price uncertainty, and therefore of peak price uncertainty, it is able to better adjust the electricity consumption and therefore to reduce the electricity cost (see Table 3.2).

3.1.3 Industrial case study

In Section 3.1.2 the efficacy of the proposed approach was shown using a relatively simple continuous production plant. In this section, the proposed method is applied to the industrially relevant problem of stainless steel-making in order to analyse whether the proposed stochastic approach will suffer from the complexity of large-scale scheduling problem. Steel-making was chosen as a motivating industrial example for several reasons. On the one hand, it is recognized as one of the most difficult industrial processes to schedule as it is a large-scale multi-stage, multi-product batch process with parallel equipment and critical production-related constraints. On the other hand, it is a very energy intensive process which stands to greatly benefit from iDSR.

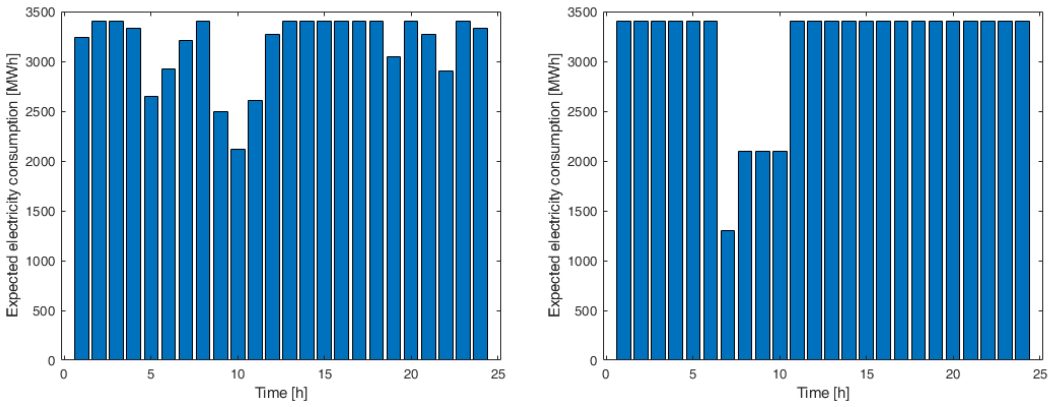

(a) (b)

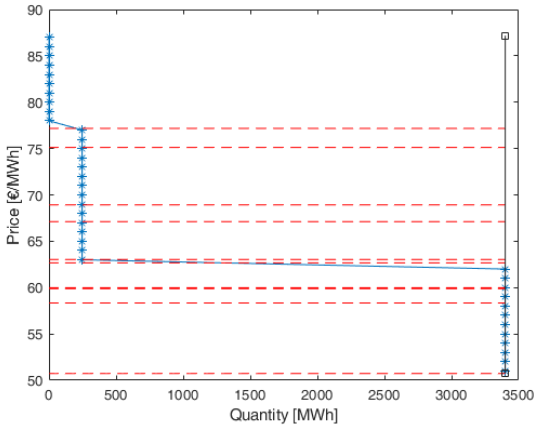

(c)

FIGURE 3.4: (a) Expected electricity consumption stochastic formulation, (b) Electricity consumption expected value problem, (c) Bidding curve of a given hour (t=5) of the stochastic solution (blue line), inelastic bidding (black line) and price realizations (horizontal red dashed lines). Source: (Leo et al., 2021).

The first step in steel production is the melt shop, where solid metal scrap is melted, endowed with its steel characteristics and cast into slabs. The melt shop consists of four consecutive production stages. The first stage is the electric arc furnace (EAF), in which electricity is used to melt a batch of metal scrap (also known as a heat). Next, the heat is transported to an Argon Oxygen Decarburizer (AOD) where the carbon content of the melt is reduced in order to form steel. The heat is then moved to a Ladle Furnace (LF) where the heat and chemistry of the heat are further adjusted. The last step in the process is to cast the heats sequentially, one directly after another, in a predefined sequence in order to form a slab of steel. This process is performed by the Continuous Caster (CC). Heats that produce to the same slab are known as a group of heats. A CC cannot process two heat groups back-to-back but requires a setup time in between the two.

The scheduling model for this plant is formulated using a Resource-Task Network (RTN) (Pantelides, 1994). In this work, two identical parallel machines are considered for the first three stages of production while two unique CCs are modelled. Between each stage, a heat is transported with some minimum and maximum time

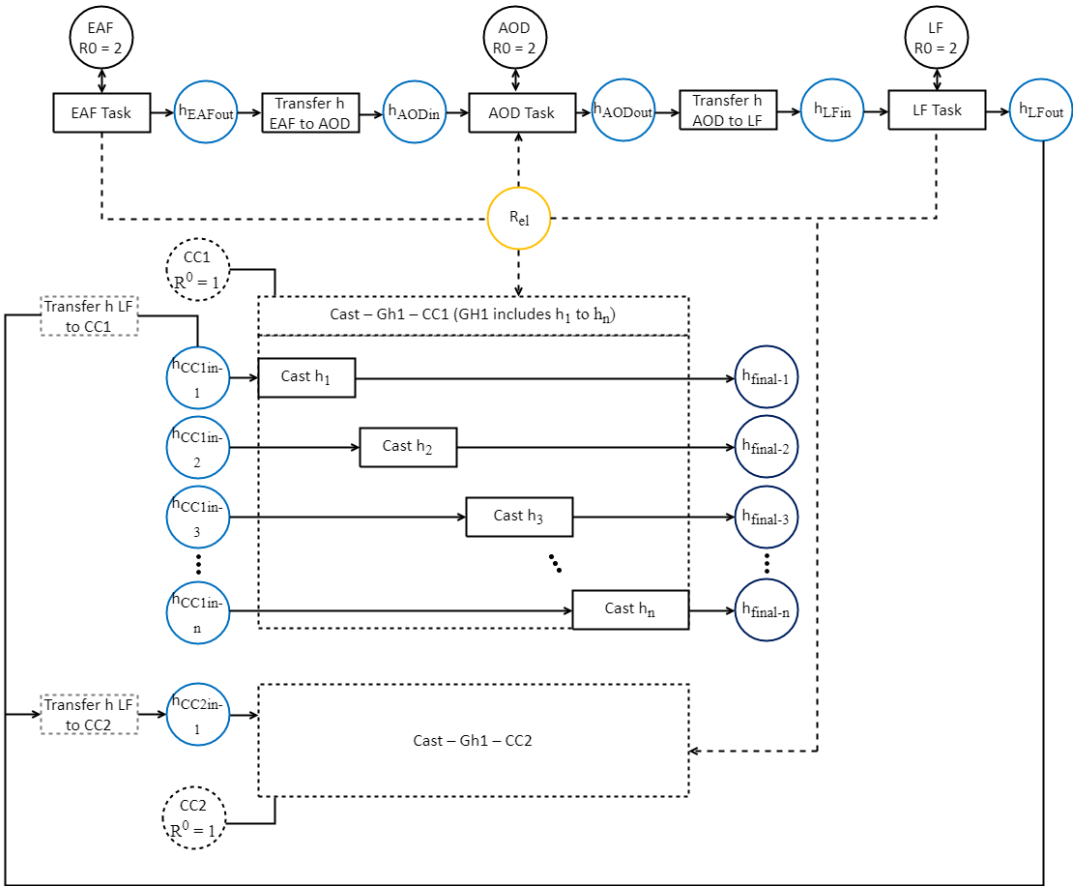

FIGURE 3.5: The RTN diagram of the steel plant considered. Source: (Leo et al., 2021).

requirements. An RTN process diagram can be seen in Figure 3.5. The RTN model implemented here follows the formulation that is presented in (Castro, Sun, and Harjunkoski, 2013).

In the RTN model, a discrete-time grid is used, which allows for straightforward modelling of intermediate events (such as a change in electricity pricing or power availability). In discrete-time scheduling formulations, the scheduling horizon is divided into $t \in T$ slots of size δ (chosen to be equal to 15 minutes).

The RTN formulation represents the entire scheduling model as a set of task (I), which produce and consume sets of resources (R). Due to the fact that heats in steel production are discrete-entities, this model only considers the discrete-interaction of a task with its resources. This discrete interaction is modelled by the binary variable $N_{i,t,s}$, and the discrete-interaction parameter $\mu_{r,i,t}$. $N_{i,t,s}$ assigns the start of a task $i \in I$ to time point $t \in T$, while the parameter $\mu_{r,i,t}$, describes the interaction of the execution of said task with its resources over the duration of the task τ_i. The excess value of a resource $r \in R$ at time point $t \in T$ is accounted for through the non-negative continuous variables $R_{r,t,s}$. The availability of the resources over the time grid is enforced by the resource balance constraint which can be seen in Eq. 3.25. In the proposed stochastic formulation, the scheduling decisions represent recourse decisions and therefore they are defined for each scenario s.

$$R_{r,t,s} = R^{0}_{r|t=1,s} + R_{r\notin r^{el},t-1,s} + EU_{r^{el},t,s} + \sum_{i\in I}\sum_{\theta=0}^{\tau_i} \mu_{r,i,\theta} N_{i,t-\theta,s}$$
$$\forall r \in R, t \in T, s \in S \quad (3.25)$$

In this case, the term $R_{r,t-1,s}$ does not apply to the resource balance for electricity in order to ensure that energy does not propagate over time. Conversely, the non-negative continuous variable $EU_{r^{el},t,s}$ only applies to the electricity resource and is used to track the total electricity consumption at any given time.

In order to account for the steel-specific constraints this base-RTN model needs to be expanded as shown in (Castro, Sun, and Harjunkoski, 2013). Eq. 3.26 ensures that a heat ($h \in H$) is executed in one unit ($u \in U$) at each stage ($k \in K$). Eq. 3.27 similarly follows for a group of heat ($g \in G$) in the CCs. Note that the set $I_{h,u}$ indicates the set of tasks that process heat h on unit u.

$$\sum_{u\in U_k}\sum_{i\in I_{h,u}}\sum_{t} N_{i,t,s} = 1 \quad \forall h \in H, s \in S, k = 1,2,3 \quad (3.26)$$

$$\sum_{u\in U_k}\sum_{i\in I_{g,u}}\sum_{t} N_{i,t,s} = 1 \quad \forall g \in G, s \in S, k = 4 \quad (3.27)$$

Eq. 3.28 imposes bounds on the execution of transfer tasks in a similar manner to the processing tasks. In order to approximate the maximum transfer times between stages, the resource availability for all heats at the exit location of a stage (R^{OL}) is set to be zero. Therefore, only the heats at the input location (R^{IL}) to a stage are allowed to exist for multiple time periods. Eq. 3.29 is then used to approximate the maximum transfer time of a heat by placing restrictions on the lifetime of its inlet intermediate resources based on the max and min transfer times between the stages ($maxtrf_{u,u'}$ and $mintrf_{u,u'}$ respectively).

$$\sum_{u\in U_k}\sum_{u'\in U_{k+1}}\sum_{i\in I_{h,u,u'}}\sum_{t} N_{i,t,s} = 1 \quad \forall h \in H, s \in S, k \neq 4 \quad (3.28)$$

$$\sum_{r\in R^{IL}_{h,u'}}\sum_{t} R_{r,t,s} \leq \left\lceil \max_{\substack{u\in U_k \\ u'\in U_{k+1}}} (maxtrf_{u,u'} - mintrf_{u,u'})/\delta \right\rceil \quad \forall h \in H, s \in S, k \neq 4 \quad (3.29)$$

To re-iterate, the link between the electricity-related concerns and the scheduling model is described in Eqs. (3.17, 3.18, 3.19). As before, the total electricity consumption must be equal to the amount of electricity actually purchased from the day-ahead market (based on the accepted bids ($BA_{p,t,s}$) plus the over- and under-consumption ($\delta e^{+}_{t,s}$ and $\delta e^{-}_{t,s}$ respectively).

The bidding model is the same as described in Section 3.1.2 for the illustrative example. It is defined by Eqs. 3.15-3.16. Lastly, the upper bound on the electricity

consumption is given in Eq. 3.30.

$$EU_{r^{el},t,s} \leq \sum_{u \in U} (\max_{h \in H}(power_{h,u})) \quad \forall t \in T, s \in S \tag{3.30}$$

3.1.4 Solution method

The stochastic programming formulation of the industrial size steel-making problem gives rise to an intractable large-scale deterministic equivalent MILP. To ensure a reasonable solution time and online feasibility of the solution, the optimization problem is decomposed by applying the Progressive Hedging algorithm (PHA) as described in Section 2.3.1. To apply the PHA, a formulation that is based on the NACs is generated by making a copy of the first-stage variables for each scenario s. For the steel-making problem, the copies of the first stage variables identify for each scenario s the bid volumes at price level p and hour t ($B_{p,t,s}$) and the continuous variables (ψ_s) to define the risk measure CVaR. The NACs couple the scenarios by forcing the copies of the first-stage variables to be equal to each other (Eq. 3.31 for the bid volumes and Eq. 2.21 for the NACs of the first-stage variable associated to the risk measure).

$$B_{p,t,s} = B_{p,t,s\prime} \quad \forall s, s\prime \in S \tag{3.31}$$

The PHA dualizes the non-anticipativity constraints (NACs) that couple the scenarios in order to solve the scenario sub-problems independently. The scenario sub-problems are penalized proportionally to the violation of the dualized NACs (according to the penalty parameter ρ_s) and are solved iteratively until a termination criterium is met.
The convergence of the PHA and the quality of the solution are significantly affected by the choice of the penalty parameter ρ_s. Numerical tests showed that for the problem at hand the convergence is improved when the value of ρ_s is different for each variable of the NACs. The chosen value of ρ_s is equal to the expected day-ahead electricity price multiplied by a factor of 0.001.
Furthermore, as described in Section 2.3.1, the heuristic known as variable slamming was implemented to speed up the convergence of the algorithm. The heuristic the fixes decision variables once their value has stabilized (with a tolerance of 0.5) to a fixed value over the last $n_{slamming}$ iterations. The best results were obtained with the value of $n_{slamming}$ equal to 4.

Computational Environment

The progressive hedging algorithm is implemented within the algebraic modelling language Julia/JuMP. The MILPs and MIQPs models were solved using the commercial solver CPLEX 12.6.3 on an Intel Core i7-2600 machine at 3.40 GHz with 8 processors and 8 GB RAM running Windows 7 Professional. We consider as termination criteria a maximum time limit equal to 7200 seconds and a maximum number of iterations equal to 15. The NAC violation tolerance is set to 0.01.

3.1.5 Results

In this section we discuss the results obtained with the proposed formulation. We solve the stochastic formulation for different values of the parameter η that weighs the importance of the expected value cost and the risk measure, as described in section 3.1.3. The deterministic equivalent problem has approximately 487 010 variables (149 760 binary variables) and 2 306 020 linear constraints. The best solution of the deterministic equivalent problem ($\alpha = 0.9$ and $\eta = 0.5$) is equal to 1 503 610 with a gap of 60 % after 24 hours of computation time.

Tables 3.3-3.4 shows the improvement that can be achieved by solving the stochastic model (10 scenarios) instead of the deterministic counterpart in terms of the Value of the Stochastic Solution ($VSS^{inelastic}$). In particular, Table 3.3 shows the optimal objective function value of the stochastic problem (z^{SP}) and of the recourse problem with inelastic bidding ($z^{RP}_{inelastic}$), the absolute and relative Value of the Stochastic Solution ($VSS^{inelastic}$, $\overline{VSS}^{inelastic}$) for different values of the scalar parameter η that prioritizes the expected cost and the risk measure in the objective function. Table 3.4 provides detailed results of the same optimization solutions for the different values of the parameter η ($\eta = 0$ minimizes only the risk measure). The values of the risk measures and the expected costs are shown for the stochastic problem ($CVaR^{SP}$, $E[cost]^{SP}$) and the recourse problem with inelastic bidding ($CVaR^{RP}$, $E[cost]^{RP}$). Moreover, the computational times and the number of iterations of the Progressive Hedging Algorithm (PHA) are listed. It is worth to highlight that several values of the time limit termination criterion (up to 24 hours) and of the parameter $n_{slamming}$ (that fixes the decision variables once their optimal value has been stable over $n_{slamming}$ iterations) were tested. The best results were obtained with a time limit equal to 7200 [s] and the value of $n_{slamming}$ equal to four. For larger time limits and larger values of the parameter $n_{slamming}$, the solution of the PHA begins to fluctuate over the iterations due to the presence of integer recourse variables and the algorithm does not converge to a solution better than the one presented in Tables 3.3-3.4. A solution time larger than 24 hours is impractical since the day-ahead bids have to be submitted every day to purchase electric power from the day-ahead market. Lower values of the parameter $n_{slamming}$ reduce the computational effort but lead the convergence to a poor quality solution. Additionally, numerical tests showed that for the problem at hand the convergence is improved when the value of the penalty parameter ρ is different for each variable involved in the dualized NACs. The chosen value of ρ is proportional to the expected day-ahead electricity price by a factor of 0.001.
Even though the solution obtained with the PHA cannot be guaranteed to be the global optimum (in other terms a duality gap might exist), the obtained $VSS^{inelastic}$ values are quite significant. For this application the $VSS^{inelastic}$ can also be interpreted as the potential daily savings of the electricity consumer obtainable adopting the SP formulation instead of the Expected Value Problem (EVP) one. The results of the SP formulation in Table 3.4 do not lie on the Pareto front since the problems are not solved to the global optimum. To estimate the loss of optimality, we compare in Table 3.5 the optimal solution obtained with the PHA (z^{SP}) and the best linear programming relaxation (best LB) obtained by solving the deterministic equivalent with a time limit of two days. It is worth to highlight that this represent an upper bound of the duality gap (UB^{loss}), since the best linear programming relaxation is only a lower bound of the original problem. Table 3.5 shows that the optimality loss resulting with the PHA is lower than 2.1% if the expected cost is prioritized over the risk measure and lower than 4.4% if the risk measure has a larger weight in the objective function. The risk

measure complicates the convergence of the decomposition algorithm.

TABLE 3.3: Value of the Stochastic Solution with 10 scenarios. Source: (Leo et al., 2021).

z^{SP}	$z^{RP}_{inelastic}$	$VSS^{inelastic}$	$\overline{VSS}^{inelastic}$	η
773 567,9	837 648,5	64 080,5	7,6 %	0,7
795 154,1	870 566,4	75 412,3	8,6 %	0,5
830 784,4	910 392,4	79 608,5	8,7 %	0,3
860 668,0	999 532,6	138 864,6	13,8%	0

TABLE 3.4: Detailed results for the stochastic solution with 10 scenarios. Source: (Leo et al., 2021).

$CVaR^{SP}$	$E[cost]^{SP}$	$CVaR^{RP}$	$E[cost]^{RP}$	$CPUs$	$iterations$	η
849 718,7	740 931,9	1 023 128,8	758 156,9	7 200	11	0,7
850 984	739 342,2	994 928,7	746 204,1	7 200	10	0,5
866 826	746 687,3	979 162,5	749 930,5	7 200	10	0,3
860 668,0	-	999 532,6	-	7 200	8	0

TABLE 3.5: Estimation of the duality gap. Source: (Leo et al., 2021).

z^{SP}	best LB	UB^{loss}	η
773 567,9	758 505,9	1,9 %	0,7
795 154,1	778 641,4	2,1 %	0,5
830 784,4	796 708,6	4,2 %	0,3
860 668,0	824 367,3	4,4 %	0

Interestingly, the PHA solution converges to a inelastic bidding solution, however, with a different hourly bidding volume compared to the EVP solution as shown in Figures 3.6a-3.6b. As previously described, the electricity commitment represents the electricity volume purchased from the accepted bids. To highlight how the stochastic solution can differ from the corresponding deterministic counterpart solution, Figures 3.7a-3.7b show the energy-aware scheduling solutions for the stochastic programming formulation for scenario 1 and the expected value problem. The stochastic solution further reduces the electricity consumption over the time range where the electricity peak is more likely to happen.

We analyse how the risk measure influences the electricity purchased profile. Figure 3.8 shows different electricity commitment profiles for different values of the parameter η that influences the importance of the risk over the expected value cost. Values of η close to one mean that the consumer is concerned about the average costs over the scenarios and willing to take the risk of high cost scenarios. In other words, the consumer accepts the possibility to not shift electricity during price peaks for some scenario realizations. On the other hand, values of η close to zero define a completely risk-averse decision maker that tries to avoid important electricity consumptions during price peaks for all the scenario realizations. The effect of the risk measure is particularly visible in Figure 3.8 in the time range between $t = 7$ h and $t = 10$ h. In this time range the solution with high weight of the risk measure in the objective

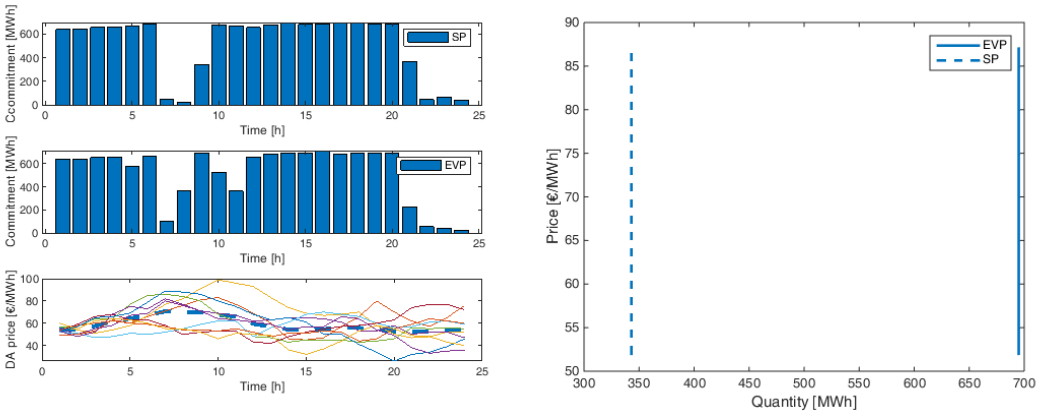

(a) (b)

FIGURE 3.6: (a) Comparison of the day-ahead electricity commitments obtained with the EVP formulation and the SP formulation ($\eta = 0.5$), (b) Bidding curve at a given hour (t = 9) of the stochastic solution (dashed line) and the EVP solution (continuous line). Source: (Leo et al., 2021).

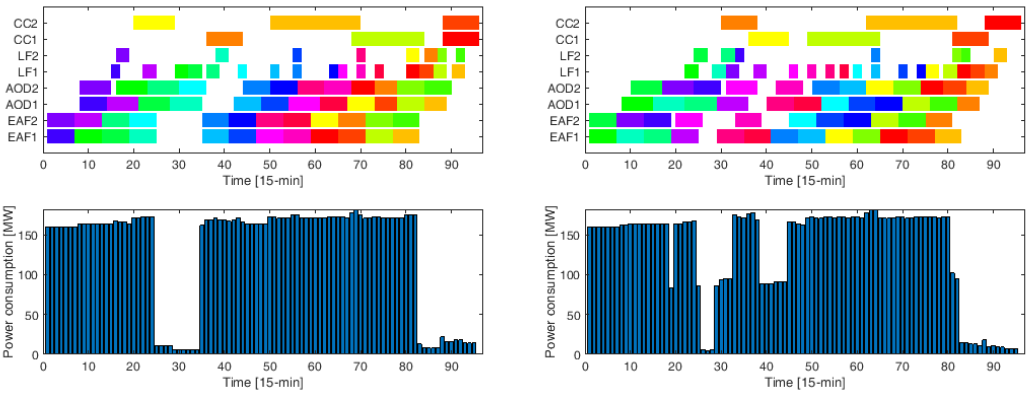

(a) (b)

FIGURE 3.7: (a) Energy-aware scheduling Scenario 1, (b) Energy-aware scheduling EVP. Source: (Leo et al., 2021).

function ($\eta = 0.5$, $\eta = 0$) reduces the electricity commitment to avoid possible price peaks and therefore high electricity costs for some price scenarios. On the other hand, the solution with low weight of the risk measure ($\eta = 0.7$) does not account for scenarios with high costs as long as the expected cost over all the scenarios is minimized. In fact, the electricity commitment is drastically reduced only at time $t = 10$ where the highest price peak might realize accepting the possibility to not shift the commitment during the remaining possible price peaks.

Discussion

The results presented in Sections 3.1.2-3.1.5 show that considering price uncertainty drastically impacts the operating costs of the plant. Relatively high values of the $VSS^{inelastic}$ point at a large potential for cost savings by adopting the proposed stochastic formulation. The results were presented for a relatively small continuous plant

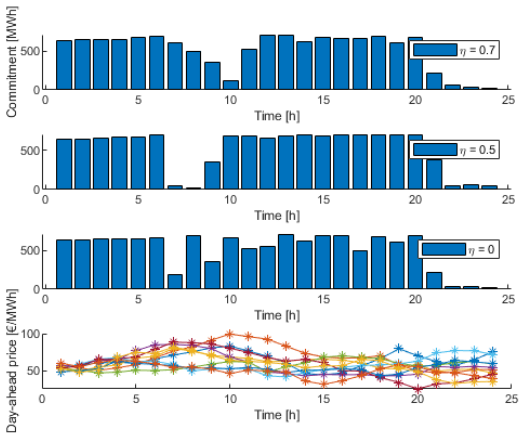

FIGURE 3.8: Comparison of day-ahead electricity commitment for different levels of risk aversion. Source: (Leo et al., 2021).

and for an industry-relevant case study.

The introduction of a bidding model, on the other hand, has shown opposite results for the two case studies. The optimal solution of the continuous plant case-study, obtained solving the deterministic equivalent problem, showed that price elastic bids are able to further reduce the electricity cost. On the other hand, the solution of the decomposition algorithm for the large-scale steel making case-study converged to inelastic bids. Conceptually, the solution with a bidding model (and therefore with elastic bids) would never be worse than the solution with inelastic bids since the bidding model only introduces additional degrees of freedom. However, the introduction of the bidding model further complicates the optimization problem for a large-scale industrial case study such that a monolithic solution is impractical. By decomposing the monolithic problem into scenario subproblems, the bidding model introduces additional NACs that complicates the convergence of a decomposition algorithm to a global optimum solution. In other words, the decomposition algorithm converges to a local optimum or to a feasible solution and therefore the inelastic solution obtained with the PHA might not be the global optimum. The reason is that the decomposed subproblems are not convex due to the integrality requirements. It is worth to mention that a primal decomposition with Lift and Project cuts (Balas, Ceria, and Cornuéjols, 1993, Carøe and Tind, 1997), that would in theory guarantee the convergence to the global optimum, has shown very poor convergence performances due to the high number of binary variables needed for the RTN scheduling formulation. Lagrange-like algorithms that are able to close the duality gap of the Lagrangean relaxation (Carøe and R Schultz, 1999, Kim and Zavala, 2015) could also be applied to solve the problem to global optimality.
Therefore, we can conclude that the introduction of the bidding model can further reduce the operating costs in the case the stochastic optimization is solved via the deterministic equivalent formulation. For a large-scale formulation, whose monolithic solution is impracticable, the required decomposition algorithm might have difficulties to converge to a better solution than the inelastic one. However, even without elastic bidding, the solution of a large scale problem can benefit from price uncertainty awareness. Further work on decomposition algorithms for non-convex problems is needed to converge to the global optimum and therefore to properly exploit price-elastic bids.

3.2 Medium- and short-term electricity procurement

When in addition power contract decisions are optimized, the stochastic formulation that was proposed in the previous section becomes a multi-stage program. In fact, while for the day-ahead market the consumer has to commit a day in advance to the amount of electricity that will be used during the following day, to purchase electricity from the power contracts the load commitment for the corresponding contract horizon has to be announced at the beginning of the contract horizon.
To model the electricity procurement from the power contracts and from the day-ahead market, we propose a multi-stage mixed-integer stochastic programming approach (Leo and Engell, 2018, Leo and Engell, 2019a). The first-stage represents the TOU electricity commitment and the following stages model the daily integrated production scheduling and day-ahead electricity procurement. Due to the size of the problem and the application of the proposed approach to a real-world industrial power plant, the resulting multi-stage formulation is approximated via a series of two-stage programs that are solved in a shrinking horizon fashion. To reduce the approximation error, at each iteration of the shrinking horizon strategy we combine a detailed model to make accurate decisions for the short-term future (e.g. day-ahead commitment) and an aggregated model to account for the long-term future (e.g. production levels at the end of the time horizon).

This section partly follows *Leo E. and Engell S., Applying Stochastic Optimization to Demand-Side Management of a Combined Heat and Power Plant, ECCE12, The 12th European Congress of Chemical Engineering Florence 15-19 September 2019*.

3.2.1 Problem statement

We consider the combined heat and power (CHP) plant that is located at INEOS in Köln (Rahimi-Adli et al., 2021). The CHP plant consists of a set of plant components $c \in C$ (steam turbines, boilers, pre-heaters and by-pass valves) that can produce the products $p \in P$: electricity (EL) and steam at different pressure levels (60 bar, 30 bar, 15 bar, 5 bar) and condensate at 1.8 bar. The CHP plant has to satisfy the fixed hourly demand of electricity and steam coming from the production site. Electricity can be purchased from the electricity grid by TOU power contracts and on two different markets (the future-market and the day-ahead market) with different purchasing conditions. The TOU power contract and the future market have fixed pre-agreed electricity prices and commitments, while the day-ahead market is subject to the regulations already introduced in Section 3.1.1. The goal is to maximize the profit of the CHP plant by making the following decisions over the time horizon of one week:

- the amount of electricity purchased from the power contract and from the future-market
- a daily day-ahead commitment with hourly discretization to purchase electricity from the day-ahead market
- the hourly production levels of steam and electricity
- the amount of fuels stored and of off-gases incinerated.

We account for uncertainty in the day-ahead electricity price. Since the electricity purchased from the TOU contract and the future market must be defined before the

beginning of the time horizon of interest, they are modelled as first-stage variables. Note that the profile of electricity purchased from these two options must be defined for the whole horizon of one week. The uncertain day-ahead electricity price realizes every day for the following day. Therefore, recourse variables model the day-ahead hourly electricity commitment, the load deviations of the following day respect to the load commitment along with the production levels of the CHP plant. We implement an inelastic bidding strategy for the day-ahead electricity market (see Section 3.1 for more details on elastic and inelastic bidding) .

3.2.2 MILP formulation of the CHP plant

Production plants are typically equipped with a combined heat and power (CHP) plant that incinerates wastes to provide steam and electricity. When the energy content of the waste streams that are used as fuels is not sufficient to satisfy the steam demand of the production plants, additional fuels as Naphtha and crack-oil are used. As shown in Figure 3.9, the CHP plant that is considered in this thesis consists of five boilers and several multi- and single-stage turbines. There are four steam networks with different pressure headers (60, 30, 15 and 5 bar) that satisfy the demand of steam coming from the production plants. In addition, the power plant has a condensation turbine which produces electric power by using steam at 5 bar. For large production sites, the electricity production of the CHP plant is not able to satisfy the entire electric power demand of the production plants and additional electricity is purchased from the public grid.

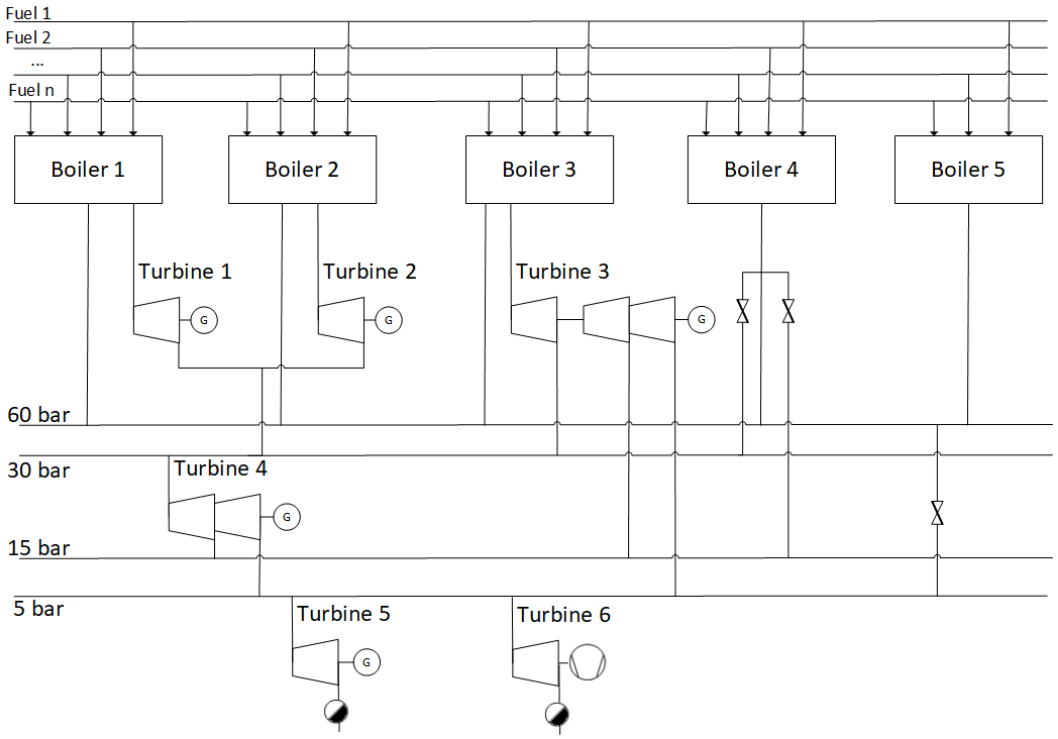

FIGURE 3.9: The schematic of the CHP plant.

The MILP model of the CHP plant has been developed under the following assumptions:

TABLE 3.6: Nomenclature of the MILP formulation of the CHP

Indices	
p	plant product (electricity and steam at different levels)
st	steam pressure level (60 bar, 30 bar, 15 bar, 5 bar, 1.8 bar)
$h, h\prime$	hour
h^{TOU}	TOU period
c	plant component (steam turbine, boiler, pre-heater)
$m, m\prime$	operating mode
f	fuel
s	scenario
br	burner
b	boiler
n	node
bl	contract block
i, i^{IN}, i^{OUT}	plant stream
Sets	
P	Set of products
H	time periods
$H_{h^{TOU}}$	TOU periods
S	scenarios
C	plant components
$C^{turbines}$	steam turbines
$C^{boilers}$	boilers
C^{steam}	subset of plant components that produce steam
N	nodes
B^{TOU}	contract blocks
ST	steam pressure levels
M	operating modes
NAC^{MSSP}	matrix to describe the structure of the scenario tree for the NACs
Parameters	
$H^{MB}_{n,i}$	Mass Balance matrix
$H^{EB}_{n,i}$	Energy Balance matrix
$UB_{c,i}, LB_{c,i}$	Upper- and lower-bounds of each mass stream i of component i
$h_{n,i}$	entalphy of stream i at node n
α_c, β_c	parameters of the Willans line for the turbine c
$UB_{f,b,br}, LB_{f,br}$	Upper and lower bounds of the mass flow of fuel f to burner br of boiler b
IV^0_f, LHV_f	initial inventory level and lower heating value of fuel f
$\eta_{b,br}$	efficiency of burner b of boiler b
N^{fuels}	number of fuels
$\theta_{m,m\prime}$	minimum time in mode $m\prime$ after switching from m
$D^{steam}_{st,h}$	hourly demand of the steam pressure level st
$D_{EL,h}$	hourly demand of the electricity
$price^{day-ahead}_{h,h}$	Clearing day-ahead electricity price at hour h and scenario s
$p^{+,DA}_h, p^{-,DA}_h$	day-ahead penalties for over and under consumption
$p^{+,TOU}_h, p^{-,TOU}_h$	TOU penalties for over and under consumption
EC^{bl}_{max}	Upper bound of electricity for the TOU block bl
$p^{+,fm}_h, p^{-,fm}_h$	future-market penalties for over and under consumption
$price^{naphtha}, price^{crack-oil}$	Price of naphtha and crack-oil as fuels
$p^{feed}, p^{+,st}_{steam}$	Price of feed water and to purchase externally steam at the pressure level st
p^{TOU}_b	TOU price component for the block bl
α	Quantile for the definition of the risk measure CV
η	Scalar parameter to define objectives priorities
ϕ_s	probability of scenarios s
Continuous variables	
$m_{n,i,h,s}$	mass flow of stream i at node n at time h for scenario s
$m^{fuel}_{f,b,br,h,s}$	mass flow of fuel f to burner br of boiler b at time h for scenario s
$IV_{f,h,s}$	inventory level of fuel f at time h for scenario s
$P^{burner}_{f,b,br,h,s}$	power generated by the combustion of fuel f at time h for scenario s on the burner br of boiler b
$P^{boiler}_{b,h,s}$	power generated by the boiler b at time h for scenario s
EC_{bl}	TOU electricity commitment for the block bl
$E^{TOU}, E^{contract}_h$	total electricity purchased from the TOU contract and hourly TOU commitment
$\hat{E}^{contract}_{h^{TOU}}$	TOU commitment per TOU period
C^{TOU}	TOU quantity component cost
$Q_{h,s}, E^{fm}_h, E^{day-ahead}_{h,s}$	total electricity commitment, hourly electricity purchased from the future market and the day-ahead market for scenarios s
$PR_{c,st,h,s}, PR_{c,EL,h,s}$	steam and electricity production for component c scenario s at time h and steam level st
$\Delta^{steam}_{st,h,s}, \Delta^{steam,-}_{st,h,s}, \Delta^{steam,+}_{st,h,s}$	total, positive and negative steam deviations for scenario s at time h and steam level st
$\delta^{el}_{h,s}, \delta^{-,DA}_{h,s}, \delta^{+,DA}_{h,s}$	total, positive and negative electricity day-ahead deviations for scenario s at time h
$\delta^{-,contract}_{h,s}, \delta^{+,contract}_{h,s}, \delta^{-,fm}_{h,s}, \delta^{+,fm}_{h,s}$	positive and negative electricity deviations for scenario s at time h for the TOU contract and the future market
$cost_s, cost^{el}_{h,s}, cost^{steam}_{h,s}, cost^{fuel}_{h,s}$	total cost, electricity cost, steam cost and fuel cost for scenario s and time h
z	total expected cost
$\bar{z}$	weighted sum of the total expected cost and the CVaR
$CVaR$	conditional value at risk
ψ, ζ_s	continuous variables to define $CVaR$
Binary variables	
$y_{c,h,s}$	1 if the component c is active in time period h for scenario s
$y^{burner}_{f,b,br,h,s}$	1 if the fuel f is allocated to the burner br of the boiler b in time period h for scenario s
$y^{fuel}_{f,b,h,s}$	1 if the fuel f is allocated to the boiler b in time period h for scenario s
$z_{m,m\prime,t}$	1 if transition from mode m to mode $m\prime$ occurs at time t
x_{bl}	1 if the contract block bl is chosen

- the process dynamics of the considered components are faster then the chosen time discretization (one hour) and, therefore, negligible;
- to keep the model linear, the enthalpy of the steam is considered as a fixed property of the steam streams and the turbine efficiency is considered as a fixed and known parameter;
- the Lower Heating Value (LHV) of the fuels is a known and fixed parameter.

Mass balance constraints

The mass balance constraints are enforced at a component level and at a network level. At a component level, the mass balance constraints ensure that the sum of the inflow streams equals the sum of the outlet streams. The network mass balance constraints define the interactions among the difference components of the power plant (e.g. the extraction flows of the steam turbines are used as hot streams in the pre-heaters of the boilers). For confidentiality reasons the exact layout of the plant will not be described and the set of the mass balance constraints will be summarized by Eq. 3.32. The mass balance equations are enforced for each node $n \in N$ of the CHP plant. A node represents a component of the plant $c \in C, C \subset N$ (pre-heaters of the boilers, combustion chambers, steam turbines) or any point of the plant where two or more streams are mixed or divided.

$$\sum_{n \in N} \sum_{i \in I} H^{MB}_{n,i} * m_{n,i,h,s} = 0 \quad \forall h \in H, s \in S \tag{3.32}$$

$H^{MB}_{n,i}$ is an appropriate matrix of Boolean parameters that select the streams of the plant involved in the mass balances. The continuous variable $m_{n,i,h,s}$ represents the hourly mass flow of steam for stream i of node n for scenario s. To give an idea of the size of the plant, 20 plant components have been considered and approximately 1000 streams. For the plant components, the upper- and lower-bounds of the steam mass flows ($UB_{c,i}, LB_{c,i}$) are enforced by Eq. 3.33. The binary variable $y_{c,h,s}$ describes if the component c at time h and scenario s is in operation ($y_{c,h,s} = 1$) or shut down ($y_{c,h,s} = 0$). If the component c at time h is shut down, Eq. 3.33 forces the mass flow of steam $m_{c,i,h,s}$ to zero.

$$LB_{c,i} * y_{c,h,s} \leq m_{c,i,h,s} \leq UB_{c,i} * y_{c,h,s} \quad \forall h \in H, c \in C, i \in I, s \in S \tag{3.33}$$

Energy balance constraints

Similarly to the mass balance constraints, linear energy balances are enforced at each node n to describe the change of the enthalpy of the steam flows (e.g. heat-exchangers of the boilers, mixing of streams with different thermodynamic properties). As already explained, the enthalpies of the steam flows are considered as fixed and known parameters.

$$\sum_{n \in N} \sum_{i \in I} H^{EB}_{n,i} * h_{n,i} * m_{n,i,h,s} = 0 \quad \forall h \in H, s \in S \tag{3.34}$$

$H^{EB}_{n,i}$ is an appropriate matrix of Boolean parameters that select the streams of the plant involved in the energy balances and $h_{n,i}$ represents the enthalpies that are associated to the selected streams.

Steam turbines constraints

The steam turbines $c \in C^{turbines}$, $C^{turbines} \subset C$ (two multi-stage turbines and three single-stage turbines) are described by the Willans line (Willans, 1888) by Eq. 3.35 that couples the power output ($P_{c,el,s}$) and the steam mass flow ($m_{c,i,h,s}$) via a linear relation. The model parameters (α_c, β_c) were identified from plant data. The binary variable $y_{c,h,s}$ multiplies the constant term β_c to force to zero the power output of the turbines that are not in operation. Figure 3.10 shows the identification of a Willans line for a single-stage turbine. Multi-stage turbines can be seen as a cascade of Willans lines.

$$PR_{c,EL,h,s} = \alpha_c * m_{c,i,h,s} + \beta_c * y_{c,h,s} \quad \forall c \in C^{turbines}, h \in H, s \in S \tag{3.35}$$

It is worth to highlight that the Willans line, although described by a linear equation, accounts for non-linear variations in the turbine efficiency, assuming that the efficiency losses are a fixed percentage of the maximum power output (Willans, 1888).

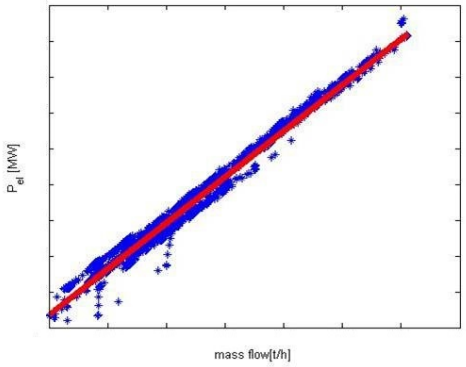

FIGURE 3.10: Model identification of the Willans line for a single-stage turbine.

Boilers constraints

The power plant consists of five boilers producing steam at different pressure levels. According to the steam pressure level, the boilers have several pre-heaters to heat up the feed water before the combustion chamber. The water streams are pre-heated via the extractions of the steam turbines. Each of the three boilers producing high pressure steam (60 bar) has seven pre-heaters. As mentioned before, the enthalpies of the water/steam streams are considered as known and fixed parameters to avoid non-linear energy balances. Each boiler has several burners to burn the different fuels (crack-oil, naphtha, waste gases). The variable $m^{fuel}_{f,b,br,h,s}$ models the mass flow of fuel f to the burner br of the boiler b at time h and scenario s. Eq. 3.36 imposes the upper- and lower-bounds of the mass flow of fuel f to the burner br of boiler b. The binary variable $y^{burner}_{f,b,br,h,s}$ is equal to one if the fuel f is allocated to the burner br

of the boiler b at time h and scenario s. If a fuel f cannot be burned on the burner br the corresponding upper- and lower-bounds ($UB_{f,b,br}$, $LB_{f,b,br}$) are set to zero and therefore the corresponding fuel mass flow $m^{fuel}_{f,b,br,h,s}$ is forced to be zero. Eq. 3.37 computes the inventory level for each fuel f as the inventory level at the precedent time ($IV_{f,h-1,s}$) or an initial inventory value (IV^0_f) if $h = 1$ minus the amount of fuel burned by all the burners of the CHP plant ($\sum_{b \in C^{boilers}} \sum_{br \in B} m^{fuel}_{f,b,br,h,s}$).

$$LB_{f,b,br} * y^{burner}_{f,b,br,h,s} \leq m^{fuel}_{f,b,br,h,s} \leq UB_{f,b,br} * y^{burner}_{f,b,br,h,s} \quad \forall f \in F, b \in C^{boilers}, br \in B, h \in H, s \in S \tag{3.36}$$

$$IV_{f,h,s} = IV^0_f|_{h=1} + IV_{f,h-1,s} - \sum_{b \in C^{boilers}} \sum_{br \in B} m^{fuel}_{f,b,br,h,s} \quad f \in F, h \in H, s \in S \tag{3.37}$$

Eq. 3.38 computes the power generated from the combustion of the fuel f on the burner br at time h for scenario s. The parameters LHV_f, $\eta_{b,br}$ represent a constant lower heating value of the fuel and the efficiency of the burner. For each boiler b, the power is computed as the sum of the power of the burners of the boiler (Eq. 3.39). Eq. 3.40 implements for each boiler b and time h and scenario s an energy balance to enforce that the change of the enthapy of the steam flow over the combustion chamber of the boiler is due to the power generated by the combustion of the fuels.

$$P^{burner}_{f,b,br,h,s} = m^{fuel}_{f,b,br,h,s} * LHV_f * \eta_{b,br} \quad \forall f \in F, b \in C^{boilers}, br \in B, h \in H, s \in S \tag{3.38}$$

$$P^{boiler}_{b,h,s} = \sum_{br \in B} \sum_{f \in F} P^{burner}_{f,b,br,h,s} \quad \forall b \in C^{boilers}, h \in H, s \in S \tag{3.39}$$

$$P^{boiler}_{b,h,s} = m_{b,\hat{i}^{OUT},h,s} * h^{b,\hat{i}^{OUT}} - m_{b,\hat{i}^{IN},h} * h^{b,\hat{i}^{IN}} \quad \forall h \in H, b \in C^{boilers}, s \in S \tag{3.40}$$

The parameters $h^{b,\hat{i}^{IN}}$, $h^{b,\hat{i}^{OUT}}$ are the enthalpies of the stream before ($\hat{i}^{IN}$) and after ($\hat{i}^{OUT}$) the combustion chamber. Note that the mass flows of the steam $m_{b,\hat{i}^{IN},h,s} = m_{b,\hat{i}^{OUT},h,s}$ are set equal to each other via the mass balance constraints.

Logic fuels constraints

The following constraints allocate the different fuels ($f \in F$) to the different burners ($br \in B$) of the boilers ($b \in C^{boilers}$, $C^{boilers} \subset C$). The binary variables $y^{fuel}_{f,b,h,s}$ are equal to one if the fuel f is allocated to the boiler b at time h and scenario s. Eq. 3.41 ensures that at least one fuel f is allocated to the boiler b if the boiler is in operation ($y_{b,h,s} = 1$). Eq. 3.42 states that no fuel f must be allocated at time h to a boiler b that is not in operation ($y_{b,h,s} = 0$). The parameter N^{fuels} is a *big-M* parameter identifying the number of fuels that are considered.

$$\sum_{f \in F} y^{fuel}_{f,b,h,s} \geq y_{b,h,s} \quad \forall h \in H, b \in C^{boilers}, s \in S \tag{3.41}$$

$$\sum_{f \in F} y^{fuel}_{f,b,h,s} \leq N^{fuels} y_{b,h,s} \quad \forall h \in H, b \in C^{boilers}, s \in S \tag{3.42}$$

If the fuel f is not allocated to the boiler b at time h ($y^{fuel}_{f,b,h,s} = 0$), it cannot be allocated to any of the burners br of the boiler b (Eq. 3.43). Similarly, if a fuel f is allocated to a boiler b ($y^{fuel}_{f,b,h,s} = 1$) it must be allocated to one of the burners br of the boiler b (Eq. 3.44).

$$y^{burner}_{f,b,br,h,s} \leq y^{fuel}_{f,b,h,s} \quad \forall h \in H, b \in C^{boilers}, br \in B, f \in F, s \in S \tag{3.43}$$

$$\sum_{br \in B} y^{burner}_{f,b,br,h,s} \geq y^{fuel}_{f,b,h,s} \quad \forall h \in H, b \in C^{boilers}, f \in F, s \in S \tag{3.44}$$

At each time step h only one fuel f can be assigned to a burner br as imposed by Eq. 3.45.

$$\sum_{f \in F} y^{burner}_{f,b,br,h,s} \leq 1 \quad \forall h \in H, b \in C^{boilers}, br \in B, s \in S \tag{3.45}$$

Minimum stay constraints

The plant components have two modes of operation $m \in M$ ($M = \{on, off\}$). The binary variable $z_{c,m,m\prime,h,s}$ takes value of one if and only if the plant component c switches from mode m to mode $m\prime$ at time period h for scenario s. This is modelled by Eqs. 3.46-3.49. The mode transitions can happen only after fixed periods of time that have been spent in the modes. Eqs. 3.50-3.51 restrict the plant component c to remain in a certain mode $m\prime$ for an amount of time equal to $\theta_{m,m\prime}$ after the transition from mode m (Mitra et al., 2013). For instance, Eqs. 3.50- 3.51 force the boilers to be at least 24 hours in operation once they are turned on.

$$z_{c,off,on,h,s} = y_{c,h,s} \quad \forall c \in C, h \in H, s \in S \tag{3.46}$$

$$z_{c,on,off,h,s} = 1 - y_{c,h,s} \quad \forall c \in C, h \in H, s \in S \tag{3.47}$$

$$z_{c,on,off,h,s} - z_{c,off,on,h,s} = y_{c,h-1,s} - y_{c,h,s} \quad \forall c \in C, h \in H, s \in S \tag{3.48}$$

$$z_{c,off,on,h,s} - z_{c,on,off,h,s} = y_{c,h,s} - y_{c,h-1,s} \quad \forall c \in C, h \in H, s \in S \tag{3.49}$$

$$\sum_{k=0}^{\theta_{off,on}-1} z_{c,off,on,h-k,s} \leq y_{c,h,s} \quad \forall c \in C, h \in H, s \in S \tag{3.50}$$

$$\sum_{k=0}^{\theta_{on,off}-1} z_{c,on,off,h-k,s} \leq 1 - y_{c,h,s} \quad \forall c \in C, h \in H, s \in S \tag{3.51}$$

Power contracts and future markets constraints

The following constraints model the electricity purchasing options of the plant. The plant can purchase electricity from the TOU contracts $E^{contract}_h$, from the future markets E^{fm}_h and from the day-ahead market $E^{day-ahead}_h$. According to the timing of the decisions, the different purchasing options belong to different stages of the stochastic formulation: TOU commitment decisions and future market decisions are first-stage variables and day-ahead commitment decisions are recourse variables. The TOU contract price depends on the time and on the amount of the electricity that is purchased from the contract. The more electricity is purchased the lower is the price. To model the TOU contract discount a set of contract blocks bl is considered and a Boolean variable x_{bl} is introduced. The amount of electricity to be purchased EC^{max}_{bl}

before reaching the next block $bl+1$, which is associated to a lower price β_{bl}, is associated to each contract block bl. The variable x_{bl} is equal to one if block bl is chosen. Eq. 3.52 ensures that only one block is chosen. Eqs. 3.53-3.54 impose the upper- and lower-bounds of electricity ($EC^{max}_{bl-1}, EC^{max}_{bl}$) that can be purchased for the block bl.

$$\sum_{bl \in B^{TOU}} x_{bl} = 1 \tag{3.52}$$

$$EC^{max}_{bl-1} * x_{bl} \leq EC_{bl} \quad \forall bl \in B^{TOU}, bl > 1 \tag{3.53}$$

$$EC_{bl} \leq EC^{max}_{bl} * x_{bl} \quad \forall bl \in B^{TOU} \tag{3.54}$$

The total electricity purchased from the TOU contact is defined by Eq. 3.55 as the sum of electricity purchased over the contract blocks. Eq. 3.56 defines the hourly electricity profile purchased form the TOU contract.

$$E^{TOU} = \sum_{bl \in B^{TOU}} EC_{bl} \tag{3.55}$$

$$E^{TOU} = \sum_{h \in H} E^{contract}_{h} \tag{3.56}$$

The TOU contracts require a constant electricity commitment over the TOU period (corresponding to six hours) as imposed by Eq. 3.57. In other words, the TOU commitment can be defined with a TOU period discretization. We use here an hourly discretization ($E^{contract}_{h}$) since we also model the hourly day-ahead commitment.

$$E^{contract}_{h} = \hat{E}^{contract}_{h^{TOU}} \quad \forall h^{TOU} \in H^{TOU}, h \in \hat{H}_{h^{TOU}} \tag{3.57}$$

H^{TOU} represents a set of TOU periods and $\hat{H}_{h^{TOU}}$ a matrix that links hours and TOU periods. Eq. 3.58 defines the cost of purchasing electricity from the power contract according to the amount that is purchased.

$$C^{TOU} = \sum_{bl \in B^{TOU}} p^{TOU}_{bl} * EC_{bl} \tag{3.58}$$

The parameter p^{TOU}_{bl} represents the amount-dependent price component. Eq. 3.59 defines the total hourly electricity commitment of the plant. The future-day market presents a constant price over the whole week and requires an electricity commitment profile before the beginning of the time horizon of interest. Note that while the TOU and the future market commitments ($E^{contract}_{h}, E^{fm}_{h}$) are first stage decisions (they do not present a subscript s indicating the scenarios), the day-head commitment ($E^{day-ahead}_{h,s}$) is a recourse decision and therefore can be different for each scenario s.

$$Q_{h,s} = E^{contract}_{h} + E^{fm}_{h} + E^{day-ahead}_{h,s} \quad \forall h \in H, s \in S \tag{3.59}$$

Steam and electricity demand satisfaction constraints

The plant must satisfy the steam and electricity demands. Eq. 3.60 imposes that the steam demand $D_{st,h}$ must be covered by the produced steam ($Pr_{c,st,h}$) or by the

steam that is purchased from external sources ($\Delta^{steam,+}_{st,h,s} \geq 0$). The plant has also the possibility to vent a surplus of steam ($\Delta^{steam,-}_{st,h,s} \geq 0$). There is no possibility to purchase externally steam at high pressure level (60 bar) as imposed by Eq. 3.62. The set ST indicates the different pressure levels of the steam (60 bar, 30 bar, 15 bar, 5 bar and condensate at 1.8 bar).
Eqs. 3.63-3.64 compute for each scenario s the hourly deviations $\delta^{el}_{h,s}$ between the total electricity commitment $Q_{h,s}$, the electricity produced by the CHP plant $Pr_{c,EL,h,s}$ and the electricity demand $D_{EL,h}$. The electricity deviations are the over- and under-consumption respect to the day-ahead electricity commitment ($\delta^{+,DA}_{h} \geq 0, \delta^{-,DA}_{h} \geq 0$) and to the power contracts commitment ($\delta^{+,contract}_{h} \geq 0, \delta^{-,contract}_{h} \geq 0$). The deviations related to the TOU power contracts and to future market are more expensive than the ones related to the day-ahead market since they are associated to a longer term commitment. Note that the steam and electricity deviations $\Delta^{steam}_{st,h,s}, \delta^{el}_{h,s}$ are continuous free variables.

$$\sum_{c \in C^{steam}} Pr_{c,st,h,s} + \Delta^{steam}_{st,h,s} = D^{steam}_{st,h} \quad \forall h \in H, st \in ST, s \in S \tag{3.60}$$

$$\Delta^{steam}_{st,h,s} = \Delta^{steam,+}_{st,h,s} - \Delta^{steam,-}_{st,h,s} \quad \forall h \in H, st \in ST, s \in S \tag{3.61}$$

$$\Delta^{steam}_{st,h,s} = 0 \quad \forall h \in H, s \in S, st = 60bar \tag{3.62}$$

$$\sum_{c \in C^{turbines}} Pr_{c,EL,h,s} + Q_{h,s} - D_{EL,h} = \delta^{el}_{h,s} \quad \forall h \in H, s \in S \tag{3.63}$$

$$\delta^{el}_{h,s} = \delta^{+,DA}_{h,s} - \delta^{-,DA}_{h,s} + \delta^{+,contract}_{h,s} - \delta^{-,contract}_{h,s} + \delta^{+,fm}_{h,s} - \delta^{-,fm}_{h,s} \quad \forall h \in H, s \in S \tag{3.64}$$

$$\Delta^{steam,+}_{st,h,s}, \Delta^{steam,-}_{st,h,s}, \delta^{+,DA}_{h}, \delta^{-,DA}_{h}, \delta^{+,contract}_{h}, \delta^{-,contract}_{h} \geq 0 \quad \forall h \in H, s \in S, st \in ST \tag{3.65}$$

Non-anticipativity constraints

The non-anticipativity constraints (NACs) equate to each other the recourse variables that belong to the same stage. Note that the first stage variables that are related to the TOU power contracts and the future market are modelled without creating copies for the scenarios and, therefore, they do not present an index $s \in S$. As an example of the implemented constraints, Eq. 3.66 enforces the NACs for the day-ahead electricity commitment $E^{day-ahead}_{h,s}$

$$E^{day-ahead}_{h,s} = E^{day-ahead}_{h,s\prime} \quad \forall (s, s\prime, h) \in NAC^{MSSP} \tag{3.66}$$

where NAC^{MSSP} is a matrix that defines the structure of the multi-stage tree by connecting the stages of the stochastic formulation to the scenarios and the time. It is interesting to highlight that, due to the nature of the problem, variables that refer to different days belong to the same stage. In fact, as discussed later in Section 3.2.3, the operational decisions for the current day d and the day-ahead electricity commitment for the following day $d+1$ belong to the same stage.

Objective function

Since the importance of a risk-averse optimization for iDSM problems has been shown in Section 3.1, the model minimizes the weighted sum of the expected total operating cost and the risk measure adopted, the CVaR as shown by Eq. 3.67. The parameter η priorities for the decision maker the importance of the total expected cost and risk measure.

$$\bar{z} = \eta * z + (1 - \eta) * CVaR \tag{3.67}$$

Eq. 3.68 defines for each scenario s the total operating cost of the plant as the sum of the cost of the electricity purchasing, the cost of the steam and the cost of the fuels.

$$cost_s = \sum_{h \in H} cost^{el}_{h,s} + cost^{steam}_{h,s} + cost^{fuel}_{h,s} \quad \forall s \in S \tag{3.68}$$

Eq. 3.69 computes the electricity cost as the cost of purchasing electricity from the day-ahead market, the TOU power contracts and the future market plus the corresponding over- and under-consumptions penalized by the parameters p^{+}_{DA}, p^{-}_{DA}, p^{+}_{TOU}, p^{-}_{TOU}, p^{+}_{fm}, p^{-}_{fm}.

$$\begin{aligned} cost^{el}_{h,s} = {} & p^{day-ahead}_{h,s} * E^{day-ahead}_{h,s} + p^{+,DA}_{h} * \delta^{+,DA}_{h,s} + p^{-,DA}_{h} * \delta^{-,DA}_{h,s} \\ & + E^{TOU} + p^{contract}_{h} * E^{contract}_{h} + p^{+,TOU} * \delta^{+,contract}_{h,s} + p^{-,TOU} * \delta^{-,contract}_{h,s} \\ & + p^{fm} * E^{fm}_{h} + p^{+,fm} * \delta^{+,fm}_{h,s} + p^{-,fm} * \delta^{-,fm}_{h,s} \quad \forall h \in H, s \in S \end{aligned} \tag{3.69}$$

The parameter $p^{day-ahead}_{h,s}$ represents the uncertain day-ahead electricity price and $p^{contract}_{h}$ the known time-dependent price component of the TOU power contract. Note that the TOU power contract present a time-dependent price component $p^{contract}_{h}$ and an amount-dependent price component p^{TOU}_{bl}. Eq. 3.70 computes the steam cost as the sum of the cost of the feed water entering the boilers and the cost of purchasing steam from external sources.

$$cost^{steam}_{h,s} = \sum_{b \in C^{boilers}} p^{feed} * m_{b,in,h,s} + \sum_{st \in ST} p^{+,st}_{steam} * \Delta^{steam,+}_{st,h,s} \quad \forall h \in H, s \in S \tag{3.70}$$

The fuel cost is defined as the price that the CHP plant must pay to use crack-oil and naphtha as fuels. The waste gases produced by the production site must be incinerated and do not generate a cost.

$$\begin{aligned} cost^{fuel}_{h,s} = {} & \sum_{b \in C^{boilers}} \sum_{br \in B} p^{naphtha} * m^{fuel}_{naphtha,b,br,h,s} + p^{crack-oil} * m^{fuel}_{crack-oil,b,br,h,s} \\ & \forall h \in H, s \in S \end{aligned} \tag{3.71}$$

Eq. 3.72 computes the expected total cost z

$$z = \sum_{s \in S} \phi_s * cost_s \tag{3.72}$$

where ϕ_s denotes the probability of scenario s. Eqs. 3.73-3.75-3.75 implement the CVaR for the quantile α by imposing that for each scenario s in which the total cost is greater than ψ, the variable ζ_s takes the value of the difference between the total cost and ψ, otherwise ζ_s takes the value of zero (see Section 2.1.2 for the definition of the CVaR).

$$CVaR = \min_{\psi,\zeta_s}\{\psi + (1-\alpha)^{-1}\sum_s \phi_s * \zeta_s\} \tag{3.73}$$

$$cost_s - \psi \leq \zeta_s \quad \forall s \in S \tag{3.74}$$

$$\zeta_s \geq 0 \quad \forall s \in S \tag{3.75}$$

3.2.3 Solution strategy

The described formulation gives rise to a large scale mixed-integer multi-stage optimization. The deterministic equivalent problem is intractable and to overcome the large computational effort, we propose an approximation strategy that consists of solving a series of two-stage stochastic programs within a shrinking horizon framework. The approximation of a multi-stage problem by a two-stage problem can be seen as an optimistic assumption about the future: it is implicitly assumed that after the first-stage decisions have been implemented all the uncertain parameters reveal and the subsequent decisions are the optimal ones for the scenario that materializes. The shrinking horizon framework alleviates this simplification by re-optimizing when new information is available. The approximation of a multi-stage program via a two-stage program within a rolling horizon framework has been already studied in the scientific literature for planning and scheduling problems (Sand et al., 2000, Balasubramanian and Grossmann, 2004, Cui and Engell, 2010) and for the optimal electricity procurement strategy (Beraldi et al., 2011) where, however, the operational decisions of the plant are neglected.

For the integrated medium-term electricity procurement and production scheduling, Figure 3.11 shows the scenario tree associated to the multi-stage program (Figure 3.11a) and the sequence of two-stage trees that are solved at each iteration of the shrinking horizon procedure (Figure 3.11b). At each iteration that is defined by the realization of the uncertain parameter the shrinking horizon algorithm solves a two-stage program assuming that the future uncertain parameters (associated to the following stages) are known. Since the uncertain parameters assumed as known may differ from the values that will later realize, after the two-stage program is solved only the first-stage variables are implemented and the scenario tree is shifted. The first-stage variables of the following iteration are the recourse variables of the current one. The algorithm repeats until the end of the time horizon of interest.

In particular, for the problem under consideration the first iteration solves a two-stage stochastic problem where the first-stage decisions represent the profile of electricity purchased from the TOU contract and the future market for the entire time horizon of interest (one week in this work). The uncertain parameters are the day-ahead electricity prices for the entire week. In this iteration the approximation of a multi-stage program via a two-stage optimization is evident: the two-stage problem assumes that after the TOU contract decisions are made, all the day-ahead prices for the entire week become known. In reality, only the day-ahead price of the first day realizes.

The shrinking-horizon methodology reacts to the error of this approximation by re-optimizing when the electricity price of the first day becomes known and considering as uncertain the day-head price of the following day. Even though this procedure generates high-quality solutions, it is not theoretically ensured that the approximation error will be zero. After the first iteration, each following one solves a two-stage stochastic program with first-stage variables that model the operations of the CHP plant for the current day d and the day-head commitment for the following day $d+1$. A set of uncertain day-ahead prices of the following day $d+1$ is considered. The second stage variables describe the operations of the CHP plant in the remaining horizon $\{d+1,\dots,D\}$ (where D represents the number of days of the week). The day-head prices of the remaining days of the week $\{d+2,\dots,D\}$ are considered as known and they are randomly generated and can differ from their later realizations in the following iterations. After the two-stage program is solved, the operational decisions for the current day d and the electricity commitment for the following day $d+1$ are implemented and they are considered as fixed in the following optimizations. The day-ahead price for the day $d+1$ realizes and the following iteration starts. The shifted scenario tree for the following iteration presents as first stage variables the operational decisions of the CHP for the day $d+1$ and the electricity commitment for the day $d+2$. The day-ahead prices of the day $d+2$ represent the uncertain parameters.

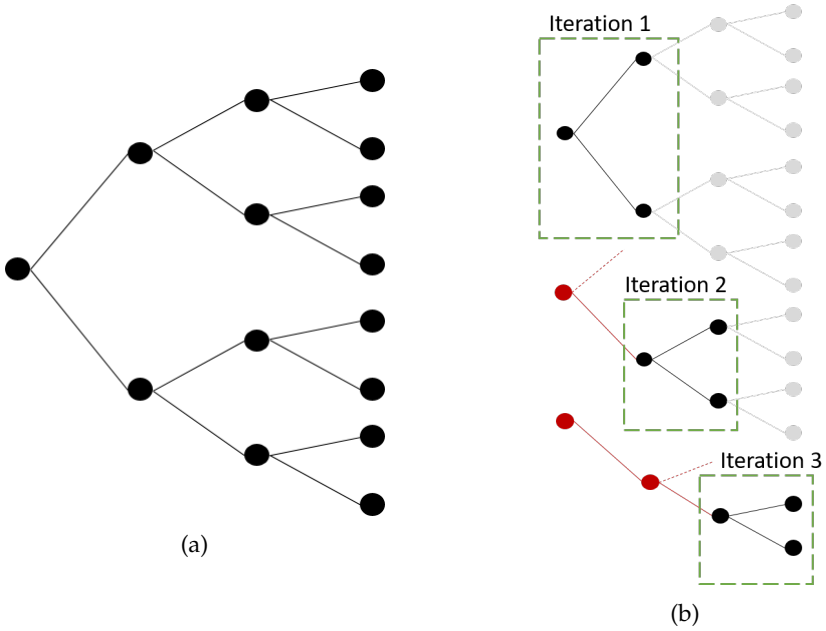

FIGURE 3.11: (a) The scenario tree describing the multi-stage formulation, (b) The illustration of the approximation strategy that approximates a multi-stage program with a series of two-stage problems in a shrinking horizon fashion.

Even after the application of the proposed approximation strategy, the solution of the stochastic problems along the iterations remains challenging due to the long time horizon (1 week) and the fine discretization (1 hour). The time horizon must cover the horizon of the TOU power contract and the fine discretization is required due to the requirements of the day-ahead commitment. Therefore, to balance computational effort and model accuracy, each two-stage model employs two different time grids (Figure 3.12): a fine one with an hourly discretization for the short term future (two

days) and a coarse one with a discretization of six hours (corresponding to a TOU period) for the long term future (i.e. the rest of the week). The implementation of the two different time grids is straightforward within a discrete time formulation: the formulation of the model constraints is not affected but some parameters (e.g. the minimum stay time $\theta_{m,m\prime}$ and the upper- and lower-bounds of the steam mass flow $LB_{c,i}, UB_{c,i}$) must be adjusted to the change of time discretization.

A special treatment is required for the first iteration where the first-stage variables are the decisions regarding the TOU power contract and the future market that define an electricity profile over the whole week with a TOU period (six hours) discretization. Since at this stage none of the two purchasing options requires an hourly commitment, the first iteration solves a two-stage model built only on the coarse time grid (with a time discretization equal to a TOU-period, namely six hours) for the whole time horizon. Moreover, since these first-stage decisions have an impact on the entire remaining week, a bigger scenario tree is considered (40 scenarios) to cope with the uncertain day-ahead price over the entire time horizon (a week). The generation of the scenarios follows the procedure described in Section 3.1.1.

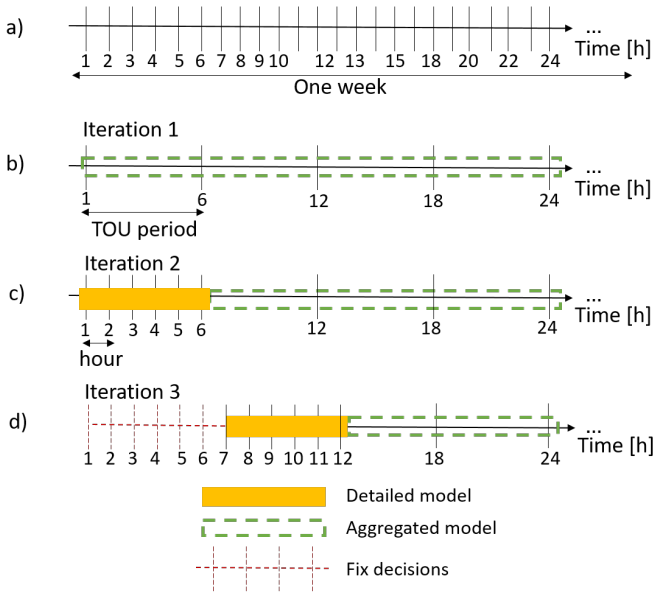

FIGURE 3.12: Illustration of the two different time grids used to model the two-stage stochastic programs. The detailed model is associated to the fine time grid (one-hour-discretization) while the aggregated one to the course grid (TOU-period-discretization).

Figure 3.13 depicts the scenario trees of the two-stage programs associated to the first three iterations of the approximation algorithm highlighting the two-stage and the time approximations.

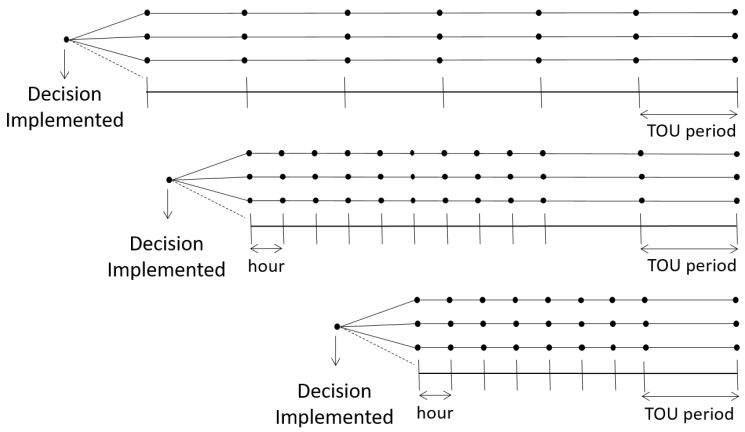

FIGURE 3.13: Illustration of the trees of the two-stage stochastic programs associated to the first three iterations of the approximation strategy. The different time grids that define the detailed and aggregated models are highlighted.

3.2.4 Solution method

The solution strategy discussed in Section 3.2.3 approximates the large-scale multi-stage problem by solving a series of two-stage stochastic programs within a shrinking horizon framework. From a solution perspective, the two-stage stochastic programs are solved by generating the deterministic equivalent MILP problem.

Computational Environment

The proposed formulation and approximation were implemented within the algebraic modelling environment AIMMS and the MILPs were solved using the commercial solver CPLEX 12.7 on an Intel Core i7-2600 machine at 3.40 GHz with 8 processors and 8 GB RAM running Windows 7 Professional. We consider as termination criteria a maximum time limit equal to 7200 seconds and an optimality gap of 1%.

3.2.5 Results

This section shows the results of the proposed solution strategy applied to the power plant model that was previously described to simultaneously define the optimal electricity purchasing strategy and the production planning over a medium-term time horizon hedging again uncertainty of the day-ahead electricity price and adopting a risk-averse strategy (parameter $\eta = 0.5$ to balance risk measure and expected cost and quantile $\alpha = 0.9$).

As previously explained, the first iteration of the approximation algorithm that is based on the shrinking horizon strategy defines for the whole time horizon of interest the profile of electricity purchased from the TOU power contact and the future market. Figure 3.14 shows the electricity prices considered in the first iteration: the constant future market price, the TOU price that presents on-peak and off-peak values and the uncertain day-ahead prices over the entire week. The first iteration considers 40 scenarios. It is worth to highlight that the TOU prices present an amount-dependent

discount: the more electricity is purchased from the contract the larger is the price reduction.

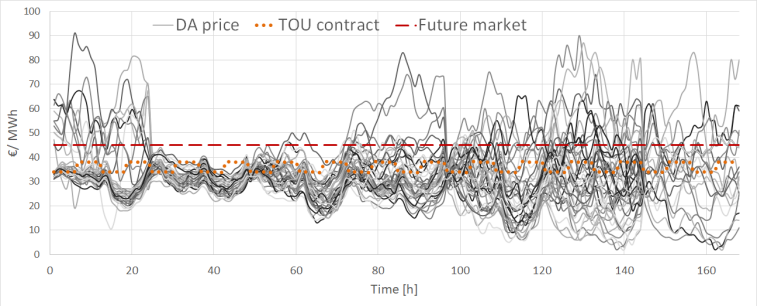

FIGURE 3.14: Known price of the electricity for the TOU power contract and the future market and uncertain price profiles for the day-ahead (DA) market.

To handle the large number of scenarios needed to describe the uncertain prices over a long horizon, the process model employs a TOU-period (six hours) discretization. Figure 3.15 shows the results of the first iteration of the shrinking horizon procedure. The TOU power contracts are used to hedge against the high variability of the day-ahead price (e.g. at the beginning and end of the week): the higher is the uncertainty associated to the day-ahead price the larger is the electricity purchased from the power contact. Due to the higher price, electricity is not purchased from the future market but from the TOU power contract and from the day-ahead market, and it is also generated by the CHP plant. While the first stage variables (TOU and future market profiles) will not change for the rest of the horizon, the day-ahead commitment and the generation profile along with the corresponding operational decisions (e.g. steam mass flows, fuel consumption, . . .) are recourse variables that will be re-optimized after the realization of the uncertain parameters. Figure 3.15 shows the expected profiles over the scenarios for the electricity that is purchased from the day-ahead (DA) market and is generated by the CHP plant. It is worth to highlight once again that the two-stage model for this iteration is built on the coarse time grid (with a discretization equal to a TOU period) according to the requirement of the TOU contract since no operational decisions from this iterations will be implemented.

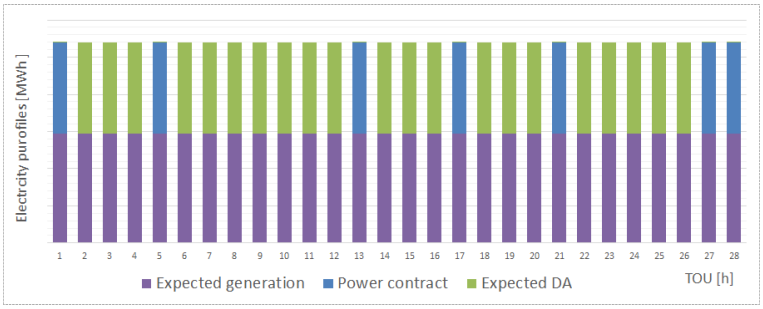

FIGURE 3.15: Iteration 1: electricity purchased from the TOU power contract and expected values of the electricity purchased from the day-ahead market (DA) and generated by the CHP plant.

The second iteration of the shrinking horizon procedure is shown in Figure 3.16. The power contract decisions are fixed to the result of the previous iteration, and the current two-stage stochastic optimization problem models as first-stage decisions the day-ahead bidding volumes for the next day considering an hourly discretization.

Figure 3.16 shows the fixed value of the electricity purchased from the TOU power contract, the day-ahead (inelastic) bidding, the expected electricity generation profile (since it is a second stage variable) and the uncertain day-ahead price. Each iteration (apart from the first one) considers ten price scenarios. The rest of the week (that is not shown here) is modelled adopting the aggregated model with a TOU period (six hours) discretization. The goal of the aggregated model is to consider the impact of the medium-term predicted future on the first-stage variables: for instance, the operational decisions of the boilers (if on or off) needs to take in account the minimum-stay constraints that force the boilers to be in an operational mode for at least 24 hours (period of time that can exceed the horizon of the detailed model).

FIGURE 3.16: Iteration 2: fixed value of the electricity purchased from the TOU power contract, the day-ahead (inelastic) bidding, the expected electricity generation profile and the uncertain day-ahead price.

After the stochastic program is solved, the day-head price profile realizes. Note that the realization of the uncertain parameter can differ from the scenarios that are considered, as shown later in Figure 3.19. The iterations progress sliding the scenario tree until the whole time horizon of one week is covered. The optimal first-stage variables of the second iteration are fixed for the third one. Figure 3.17 shows the results of the third iterations in terms of electricity generation and day-ahead (inelastic) bidding for the fine time grid (detailed model). The day-ahead biddings for the hours 1-24 are fixed to the optimal values of the previous iteration while the same profile for the hours 25-48 models the first stage variables of the third iteration. Conversely, the generation profile for the hours 1-24 represents the operational first stage variables of the third iteration while the hours 25-48 show the expected value over the scenarios.

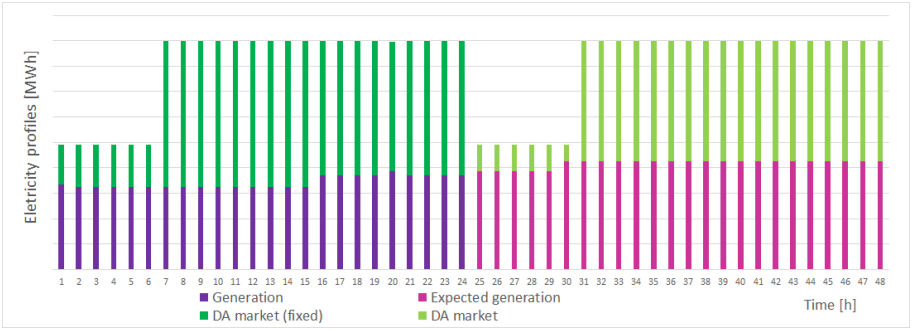

FIGURE 3.17: Iteration 3: fixed value of the day-ahead market commitment, optimal day-head bidding (first stage variable), optimal generation profile (first stage variable) and expected generation profile (recourse variable) over the scenarios.

The remaining of the week for the same iteration is modelled by adopting the coarser time grid (TOU discretization). Figure 3.18 depicts the optimal electricity generation profile for the third iteration with the two different applied discretizations. From hour 1 to 24 the profile shows the optimal values of the first stage variables with an hourly discretization; from hour 25 to 48 the profile corresponds to the optimal expected values of the recourse variables with an hourly discretization; for the remaining time steps it represents the optimal expected values of the recourse variables with a TOU discretization.

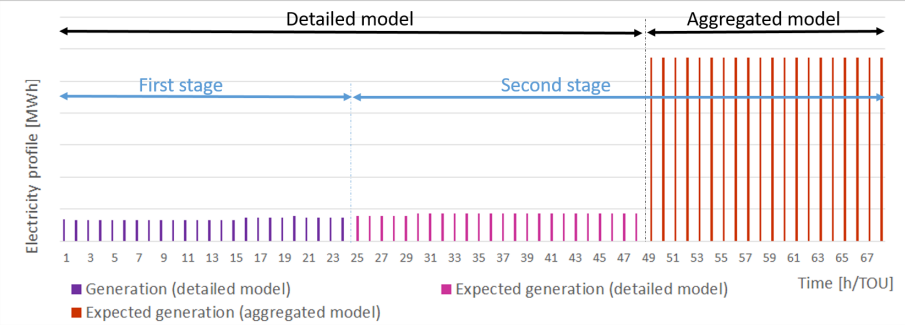

FIGURE 3.18: Iteration 3: optimal first stage variables with an hourly discretization (detailed model), optimal expected values of the recourse variables with an hourly discretization (detailed model); optimal expected value of the recourse variables with a TOU discretization (aggregated model).

The shrinking horizon strategy implements in each iteration only the first-stage decisions being aware of the uncertain day-ahead prices. Collecting the implemented first stage decisions, Figures 3.19a-3.19b show the profiles of electricity that is purchased from the day-ahead market and that is generated by the CHP plant. The figures also show the uncertain day-ahead prices that are considered along the iterations and the realized prices. It is worth to highlight that the realizations of the uncertain parameter can differ from the considered scenarios.

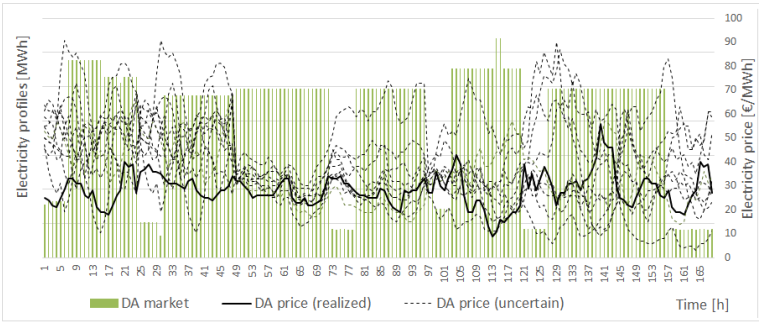

(a)

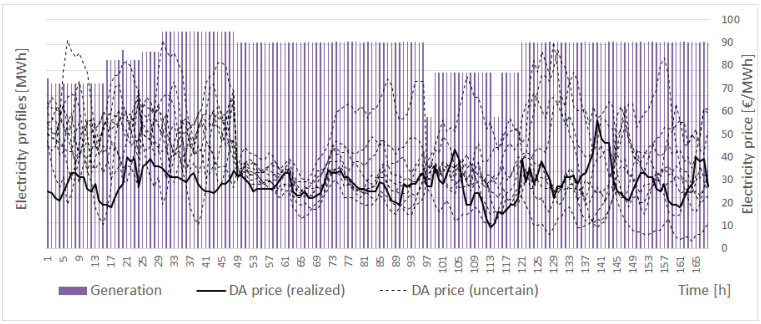

(b)

FIGURE 3.19: (a) Implemented day-ahead purchase profile, (b) Implemented electricity generation profile. In addition, both figures show the uncertain day-ahead prices considered over the iterations and the realized ones.

The proposed approximation strategy enables to solve an intractable large-scale deterministic equivalent problem. The computational statistics for the iterations of the solution procedure of the shrinking horizon algorithm are reported in Table 3.7 in terms of number of variables (#*var*), number of constraints (#*con*), reached optimality gap of the solution (*gap*), computational time (*CPU*), time interval associated to the first stage ($first - stage$) and number of scenarios considered ($|S|$). The average computational time is approximately 17 [min] with a maximum value of approximately 42 [min].

TABLE 3.7: Computational statistics for each iteration of the shrinking horizon procedure. The first stage variables of the first iteration are the contract decisions that have to be made a point in time before the horizon of interest.

it	*#var*	*#con*	*gap*	*CPU* [s]	$first-stage$ [h]	$\|S\|$
1	2 700 442	3 557 014	0,02 %	1 402,5	1-148	40
2	1 159 774	1 588 671	0,36 %	202,7	1-24	10
3	1 643 490	4 770 439	0,00 %	91,3	1-48	10
4	1 546 250	5 232 847	0,99 %	693,4	24-72	10
5	1 449 814	5 105 769	0,07 %	2 397,3	48-96	10
6	1 356 562	4 989 779	0,57 %	2 499,4	72-120	10
7	1 256 918	4 851 595	0,6 %	426,3	96-144	10
8	1 160 474	4 724 511	0,0 %	221,7	120-168	10

To evaluate the stochastic formulation we solve the Expected Value Problem (EVP) and we compute the Value of the Stochastic Solution (VSS) for each iteration. Figure 3.20 compares the results of the stochastic approach (Figure 3.20b) to the optimal electricity profiles of the EVP obtained by solving the deterministic problem in a shrinking horizon fashion (Figure 3.20a). In particular, Figure 3.20 shows the optimal generation profile, the electricity purchased from the day-ahead market and the TOU power contract, the expected and realized day-ahead price and the (known) TOU price. The realizations of the uncertain parameter are identical for the stochastic and deterministic approaches. The expected day-ahead price profile is obtained by averaging over the scenarios that are considered in the stochastic optimizations. Compared to the stochastic solution, the EVP optimization purchases electricity from the TOU power contract only when the TOU price is lower than the expected day-ahead price (e.g. 1-28 hours). On the other side, the stochastic solution is aware of the day-ahead price uncertainty and, therefore, uses the TOU power contracts to hedge against high price variability (e.g. for hours 1-6 and 156-168 of Figure 3.20).
Table 3.8 shows the computation of the absolute (VSS) and relative ($\overline{VSS}$) Value of the Stochastic Solution .

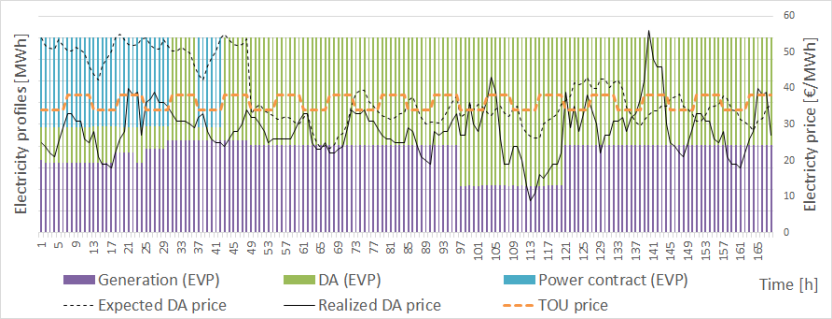

(a) Optimal solution of the Expected Value Problem

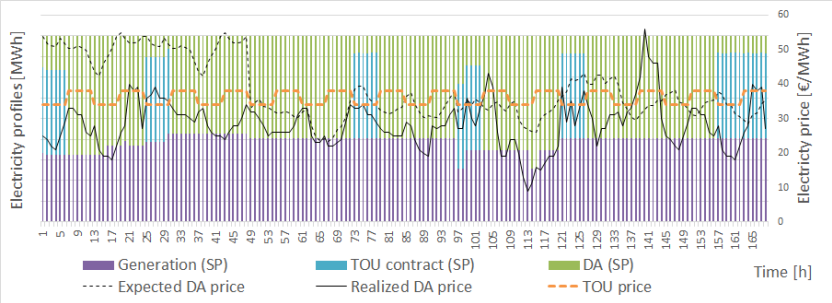

(b) Optimal solution of the stochastic problem

FIGURE 3.20: Electricity profiles: the generation profile, the electricity purchased from the day-ahead market and the TOU power contract, the expected and realized day-ahead price and the TOU price

TABLE 3.8: VSS computation.

it	VSS	$\overline{VSS}$
1	73 555,3	9,9 %
2	274 701,3	19,3 %
3	69 113,6	7,1 %
4	73 555,3	9,9 %
5	31 662,8	11,7 %
6	59 103,1	35,2 %
7	27 343,3	21,3 %
8	24 822,8	13,7 %

Due to the nature of the approximation strategy, no theoretical analysis is possible to estimate a-priori and a-posteriori the (possible) loss of optimality. In fact, since the proposed algorithm is based on a shrinking horizon procedure that considers at each iteration the entire remaining time horizon (and not a part of it as for a rolling horizon procedure) the optimal objective function value of the monolithic deterministic equivalent problem (or if intractable its linear programming relaxation) cannot be used to evaluate a-posteriori the quality of the obtained solution. The sum over the iterations of the optimal total costs cannot be compared to the solution of the deterministic equivalent problem since at each iteration the total cost is computed over

the time horizon starting from the point in time of the current iteration to the end of the week. However, the proposed approximation strategy enables to efficiently solve large-scale industrial size stochastic MILP problems within reasonable computational times and to gain important benefits from the awareness of the sources of uncertainty. Given the generality of the proposed solution strategy, different sources of uncertainty could be taken into account (e.g. the steam demand that typically represents the need of production plants). As previously shown, due to the shrinking horizon procedure the proposed strategy represents an efficient online approach that is also able to react to the realizations of the uncertain parameters that were not considered in the set of scenarios. In fact, in this work at each iteration of the shrinking horizon procedure the realization of the uncertain day-ahead price profile can differ from the scenarios that are considered for the stochastic problem.

Chapter 4

Condition-based maintenance via stochastic programming with endogenous uncertainty

This chapter is based upon

- *Leo E. and Engell S., A novel multi-stage stochastic formulation with decision-dependent probabilities for condition-based maintenance optimization, European Symposium on Computer-Aided Process Engineering 2020 (ESCAPE-30), Volume 48, 1795-1800*
- *Leo E. and Engell S., Condition-based maintenance optimization via stochastic programming with endogenous uncertainty, Computers & Chemical Engineering, Volume 156, January 2022.*
- *Leo E. and Engell S., Handling Type-I and Type-II endogenous uncertainties in simultaneous production planning and condition-based maintenance optimization in continuous production, Computers & Chemical Engineering, submitted July 2022*

In this chapter we address the challenge of integrating production planning and condition-based maintenance optimization, also called predictive maintenance. The goal of the condition-based maintenance strategy is to reduce the maintenance costs by performing the maintenance activities only when necessary according to the prediction of the Remaining Useful Life (RUL) of the equipment that is obtained via a degradation model. The degradation model couples the maintenance decisions and the operations of the plant: harsher operating conditions increase the plant throughput and reduce the RUL of the equipment increasing the frequency of the maintenance activities and the maintenance costs. Therefore, the integration of production planning and condition-based maintenance is a necessary step to optimally balance the plant income, the operating costs and the maintenance costs.
We consider uncertain predictions of the equipment degradation by adopting a stochastic programming formulation with decision-dependent uncertainty. The probability of the uncertainty, in this work the RUL of the plant, is adjusted according to the plant operating conditions by embedding a prognosis model, the Cox model, into the optimization problem. Section 4.1 proposes a multi-stage stochastic problem with decision-dependent probabilities to simultaneously optimize the production planning and the predictive maintenance of a single production campaign. Section 4.2 extends this formulation for multiple production campaigns by modelling a

second class of endogenous uncertainty, the decision-dependent structure uncertainty.

The figures and the tables of Section 4.1 are adapted from (Leo and Engell, 2021).

Literature review on condition-based maintenance optimization

Maintenance is widely recognized as a critical element of asset management to increase profits by avoiding unplanned stoppages and bad quality production (Alsyouf, 2007, De Jonge and Scarf, 2020). The integration of CBM optimization and production planning is necessary to optimally balance production costs and maintenance costs and its importance is evident from the wide literature on this topic. Most of the work in this direction assumes a perfectly known degradation model that is able to predict the degradation trajectory and the Remaining Useful Life of the equipment according to the operating conditions. In (Jain and Grossmann, 1998) the authors propose a cyclic scheduling policy for an ethylene production process that requires maintenance activities to restore the plant operations. The evolution of the degradation is assumed to be proportional to the running time and not dependent on the operating conditions. Similarly, in (Xenos et al., 2015) the authors developed a condition-based maintenance optimization describing the degradation of the compressors as function of the running time only. In (Biondi, Sand, and Harjunkoski, 2017) the authors present an optimization-based modeling framework for the integration of maintenance and short-term production scheduling of multipurpose process plants based on a State Task Network (STN) formulation. The proposed formulation assumes the reduction of the RUL as certain and known and models it as a state that results from the execution of a production task. In (Leo and Engell, 2017) the authors embed in the optimization problem a crack-growth model to simulate a virtual crack propagation as a function of the operating conditions until a critical crack length. The crack-growth model and the resulting prediction of the RUL are assumed as certain and known.

The number of papers that describe CBM optimization under uncertainty is quite limited. In (Basciftc et al., 2018) the authors used a degradation model to create failure scenarios, which then were included into a chance-constraint programming formulation. Since the degradation model is only used to generate the uncertain scenarios, the optimization does not consider the coupling between the operating strategy and the health of the equipment. This is taken into account in (Wiebe, Cecilio, and Misener, 2018) where the authors consider a parametric uncertainty of the degradation model and adopt an adjustable robust optimization formulation. To avoid uncertain time-varying parameters, which result in a very conservative solution, a complete knowledge of the future degradation parameters is assumed after the first collection of measurements.
In this work we build upon our recently proposed MINLP formulation that integrates condition-based maintenance, prognosis and production planning in the multi-stage stochastic programming framework with decision-dependent uncertainty (Leo and Engell, 2020, Leo and Engell, 2021). A similar direction has been taken also in (Basciftci, Ahmed, and Gebraeel, 2019) for the generator maintenance scheduling problem. The authors assume the RULs of the generators to be normally distributed and that the generator loads modify the mean of the RUL distribution. An MILP chance-constraint optimization problem is formulated by linearizing the non-linear terms.
From a mathematical formulation perspective, some analogies can be found with the works on the planning of clinical trials in drug discovery because of the stochastic

nature of the process: a drug might fail a clinical trial stopping its development, or it might pass all trials generating a large profit. Thus, these problems are typically modelled by MILP formulations with endogenous uncertainty of Type-II. The first formulation of this problem that accounts for uncertainty in *R&D* project portfolios was presented in (Colvin and Maravelias, 2008). The authors proposed several ideas to exploit the logical relationships in the problem structure to reduce the size of the problem and the solution time. Later, the authors developed solution procedures to handle larger problem instances proposing relaxation-based heuristic algorithms (Colvin and Maravelias, 2009) and a branch-and-cut method (Colvin and Maravelias, 2010). The same problem was addressed by (Solak et al., 2010b) proposing a formulation technique that enables the application of scenario decompositions as e.g. the sample average approximation method. However, it is worth to highlight that while the planning of clinical trials in drug discovery gives rise to stochastic MILP problems with conditional non-anticipativity constraints, in this work we address the solution of MINLP formulations where the probabilities of the scenarios are modelled as decision variables (Type 1 endogenous uncertainty) and, therefore, introduce non-linear non-convex terms.

Survival analysis and Cox model

Survival analysis is a set of statistical approaches used to estimate the time it takes for an event of interest to occur. For this reason, it is also called time-to-event analysis. Examples of time-to-events are the time until infection or recovery of a disease in health sciences or the time until failure of a part of a machine in reliability engineering (Lawless, 2002). Survival data are commonly described by the survival and the hazard functions. The survival (or survivor) function, $S(t)$, indicates the probability that an event of interest has not yet occurred by time t.

$$S(t) = P(T > t) \quad for \;\; t > 0 \tag{4.1}$$

where T denotes a non-negative random variable representing the time of occurrence of some event of interest. In this work, the random variable T represents the lifetime of the plant. The hazard function gives the instantaneous failure rate of an individual conditioned on the fact that the individual survived until a given time. The hazard function is defined as:

$$h(t) = \lim_{\Delta t \to 0} \frac{P(t \leq T < t + \Delta t | T \geq t)}{\Delta t} \tag{4.2}$$

where Δt represents an infinitesimally small time span. The hazard function is related to a probability density function, $p(t)$, and a survival function, $S(t)$, as follows:

$$h(t) = \frac{p(t)}{S(t)} \tag{4.3}$$

The Cox model, also called Cox proportional hazards model, is a regression model commonly used to estimate the effect of explanatory variables (or covariates) on the

hazard function as described by Eq. 4.4.

$$h(t) = h^0(t) * exp(\beta_1 x_1 + \beta_2 x_2 + \cdots + \beta_n x_n) \tag{4.4}$$

where t represents time, $h(t)$ is the hazard function that is determined by a set of covariates $(x_1, x_2, \ldots, x_p)$. The coefficients $(\beta_1, \beta_2, \ldots, \beta_n)$ measure the effect of the covariates. The term $h^0(t)$ is called the baseline hazard and it corresponds to the value of the hazard if all the covariates $(x_1, x_2, \ldots, x_p)$ are equal to zero. The baseline hazard $h^0(t)$ can vary over time. Typical applications of the Cox model range from clinical investigations, where for instance the difference in survival among individuals may be attributable to genotype or age, to reliability predictions, where the probability of a failure can be altered by the operating conditions of the equipment (Nikulin and Wu, 2016).

4.1 Type-1 endogenous uncertainty

Motivation of the work

The ethylene production by steam cracking is the source of motivation of this work. Steam cracker units produce olefins (ethylene, propylene and heavier hydrocarbons) by cracking the hydrocarbon feeds like naphtha or LPG with the use of steam. The cracking process leads to the formation of coke on the inner surface of the coils of the furnace. The rate of coke deposition depends on the nature of the feed and the operating conditions of the plant (coil outlet temperature, feed rate, steam to naphtha ratio). Due to the coke deposition, the performance of the furnaces decreases over time and, therefore, the furnaces must be shut down for de-coking activities to afterwards restart the operations. Hence, the timing of the cleaning represents a compromise between cleaning costs, running costs and lost production. The identification of the degradation model (coke deposition model for the ethylene production plant) represents a crucial step for the deployment of a CBM strategy. In fact, the degradation depends on complex physical phenomena that evolve on a different time scale compared to production planning. Figure 4.1 shows the identification of a coke deposition model for the furnace coils of an ethylene plant. The coke deposition has a number of negative effects on the performance of the steam cracker. The formed coke layer causes a reduction of the available cross section of the tubes for the process gas, leading to a higher pressure drop over the coils. Moreover, the coke deposition leads to a large increase in the heat transfer resistance across the coil wall and a carburization of the wall structure. Typical indicators of the degradation are the pressure difference between the inlet and the outlet of the coils and the coil skin temperature. The identified model in Figure 4.1 represents a data-driven auto-regressive model with exogenous inputs (ARX). The exogenous inputs that were considered are the feed quality that was estimated from the feed composition and the operating conditions of the furnaces that are described by the mass flow of the hydrocarbon feed, the coil outlet temperature and the steam-to-hydrocarbon ratio. As shown in Figure 4.1, since the coke layer thickness grows over the production campaign the degradation indices increase until the furnace is shut down for the de-coking activities and restarted afterwards. The rapid decrease in the pressure and in the skin temperature represents the decoking activities. Due to the complexity of the

degradation phenomenon, a data-driven model with daily discretization is not able to accurately represent the degradation process and therefore to accurately predict the Remaining Useful Life of the furnaces. For this reason, in this work we integrate production planning and CBM considering an uncertain prediction of the RUL.

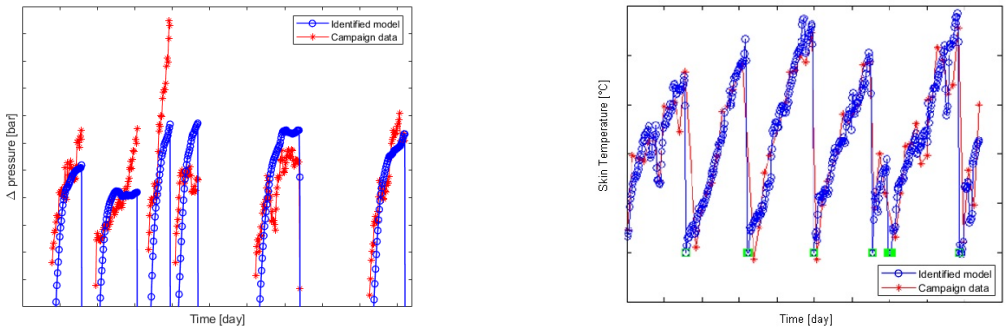

(a) Coil pressure difference

(b) Coil skin temperature

FIGURE 4.1: Identification of two data-driven degradation models for the coke deposition in a steam cracker with feed quality and operating conditions of the furnaces (feed mass flow, coil outlet temperature and steam-to-hydrocarbon ratio) as exogenous inputs. Since the coke layer thickness grows over the production campaign, the degradation indices increase until the furnace is shut down for the de-coking activities and restarted afterwards. Source: (Leo and Engell, 2021).

The process model considered in the simulations in this work is, for confidentiality reasons, a modified version of a data-driven model that was developed at INEOS in Köln. The process model is characterized by linear equations with continuous variables.

While the formulation of the CBM discussed in this work has been developed for units in the process industry, it is worth to emphasize that it can similarly be applied to identify e.g. the optimal replacement policy of components for the manufacturing industry (see e.g. Compare, Baraldi, and Zio, 2020).

4.1.1 Problem statement

In this work, a continuous production plant is considered. The product demand over the planning horizon is fixed and known. The goal is to minimize the total production cost, consisting of the feed purchasing cost, the cost of performing the maintenance activities, the resource consumption cost (i.e. the cost of steam and fuel consumption assumed proportional to the plant inputs as discussed later in Section 4.1.2) and the cost of producing the products in the next campaign or purchasing them from external sources if the demand cannot be covered, e.g. due to shutdowns. The decision variables are:

- the feeds to be purchased
- the plant operating conditions along with the resulting degradation trajectory
- the amount of products to be produced in the next campaign or to be purchased from external sources
- the timing of the maintenance activities.

Uncertainty model

In the proposed formulation, the discrete scenarios represent possible realizations of the uncertain RUL of the equipment, i.e. the predictions of the times when the degradation trajectory reaches the failure threshold. Since the planning problem requires a daily time discretization, the uncertain RULs belong to a finite set, here $RUL_s = \{30, \dots, 39\}$. Figures 4.2-4.3 show the scenario tree of the proposed multi-stage stochastic program (MSSP) and its rigorous simplification that considers a reduced set of scenarios. At each stage, the uncertain parameters are revealed and the information whether the plant reaches the end of the RUL at this stage becomes available (in other words whether the degradation trajectory has reached the failure threshold). The red nodes in Figures 4.2-4.3 represent the time steps when the RUL was exceeded. It is worth to notice that since the uncertainty considered in this work is discrete (the plant at each time step either fails or does not fail) the representation of the uncertainty in this problem is exact and there is no discrete approximation of the probability distribution. When the degradation trajectory reaches the failure threshold, the plant must be shut down to perform the maintenance activities and restore the plant operations. Therefore, since the goal is to plan a production campaign (production time between two consecutive maintenance activities), the scenario tree in Figure 4.2 can be rigorously simplified in the scenario tree in Figure 4.3. In fact, for the scenario tree in Figure 4.2 the time steps after the red nodes (that identify that the RUL has been exceeded) are associated either to further failures of the plant (red nodes) that cannot happen since the RUL has already been exceeded or to time steps when the production is resumed (black nodes) but these belong to a consecutive production campaign that is not considered here. So the decisions associated with these time steps are not relevant here. The nodes in the dashed boxes in Figure 4.2 can be neglected and this leads to the scenario tree depicted in Figure 4.3. As a consequence, the scenarios are associated to different durations of the production campaign and, therefore, different production amounts. To compare the production costs of the different scenarios, we introduce a terminal cost that is proportional to the amount of products needed to cover the demand after the failure has occurred. This terminal cost estimates the production cost of the beginning of the following campaign that might be necessary to cover the demand according to the duration of the current production campaign that differs for each scenario. Another interpretation of the terminal cost is that the not produced products must be purchased from external sources. The challenge of considering also the consecutive production campaign is addressed in Section 4.2. The timing of the realization of the uncertainty of the second production campaign can be modified by maintenance activities introducing the Type-II endogenous uncertainty.

The endogenous uncertainty formulation, instead of considering fixed and known scenario probabilities, adjusts the probabilities of the uncertain RULs according to the degradation trajectory defined by the operating conditions of the plant. In fact, a higher degradation, due to harsher operating conditions, makes scenarios corresponding to shorter RULs more likely. The relation between the probabilities of the scenarios and the degradation trajectory is described by the survival analysis equations and the Cox Model (Cox, 1972).

It is worth to highlight that even though the Cox model is a well-known standard prognosis technique, here for the first time it is integrated into a stochastic programming optimization. Figure 4.4 depicts the multi-stage scenario tree that is associated to the problem under investigation. We consider 10 scenarios and a time horizon of 39 time steps. The time horizon is divided into T^{1stage}, the subset of time steps belonging

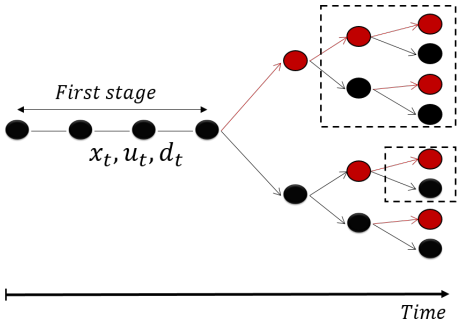

FIGURE 4.2: Scenario tree of the proposed MSSP formulation considering all of the possible uncertainty realizations. The decision associated to the highlighted nodes in the dashed boxes will not be carried out. Source: (Leo and Engell, 2021).

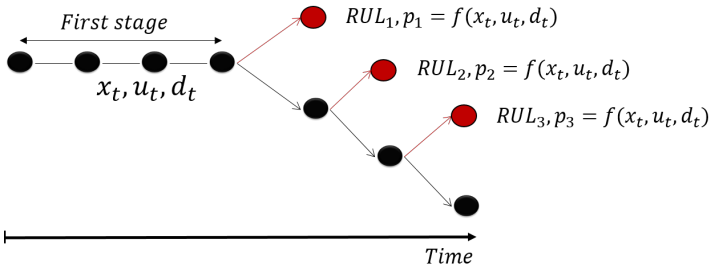

FIGURE 4.3: Scenario tree with a reduced set of uncertainty realizations. The probabilities of the scenarios depend on the first stage variables. Source: (Leo and Engell, 2021).

to the first stage ($t \in \{1, \ldots, 29\}$), and into T^s, the subset of time steps belonging to the remaining stages ($t \in \{30, \ldots, 39\}$). The first-stage decisions are the feed purchasing decisions, the maintenance timing decisions and the plant operating conditions along with the degradation level for the time steps $t \in T^{1stage}$. The recourse variables at each stage are the plant operating conditions for the time related to the corresponding stage ($t \in T^s$) and the amount of products that have to be purchased from external sources to cover the demand. The influencing variable of the Cox model, which defines the hazard function and the probability of the scenarios, is the degradation level at the end of the time horizon of the first-stage T^{1stage} ($t = 29$ and white node in Figure 4.4). It is worth to highlight that the degradation level at the end of the time horizon of the first-stage is defined by the operating conditions of the plant from the beginning of the horizon until the end of time horizon of the first-stage.

4.1.2 MINLP formulation

We describe here the proposed MINLP adopting an NACs formulation to describe the multi-stage nature of the optimization problem.

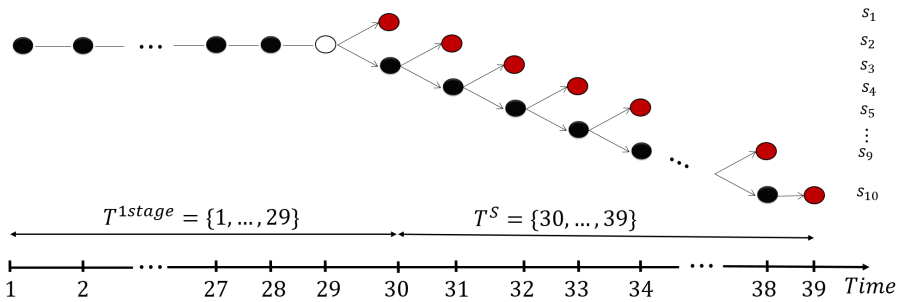

FIGURE 4.4: Scenario tree for the problem under investigation: the red nodes represent the end of the uncertain RUL and the white node the point in time where the degradation level influences the Cox model.

Nomenclature

Indices	
p	products
$t, t\prime$	time periods
$s, s\prime$	scenarios
i	plant inputs
f	feed
Sets	
P	products
T, T^{1stage}, T^s	ordered set of time periods
I	plant input
S	ordered set of scenarios
F	feed
RUL_s	uncertain Remaining Useful Lifetime
Parameters	
D_p	demand of product p
d^0	initial degradation value
IC_f	quality parameter of feed f
d^0, d^{max}, d^{min}	failure and prognosis threshold
UB_f^{feed}	maximum amount of feed f that can be used over the time horizon
$LB_{i,t,s}^{input}, UB_{i,t,s}^{input}$	upper and lower bounds of the plant input i at time period t and scenario s
$UB_{p,t,s}^{y}$	upper bound of production rate of product p at time t and scenario s
$\gamma_{p,i}, r_p$	process parameters
α^i	parameter of the degradation model
M	big-M parameter
$h0_s$	baseline hazard function of scenario s
$price_f^{feed}$	purchasing price of feed f
$price_p^{product}$	production cost or purchasing price of product p to satisfy the demand
$price_i^{input}$	resource price proportional to the input i
c^{CBM}	maintenance cost
β	parameter of the Cox model
Continuous variables	
p_s	probability of scenario s
h_s	hazard function of scenario s
S_s	survival function of scenario s
$cost_s, cost^{feed}$	total cost of scenario s and feed cost
$cost_s^{missing\ \ demand}$	average production cost or product purchasing cost
$cost_s^{input}$	cost of steam and fuel consumption assumed proportional to the plant inputs
$cost_s^{1stage}$	first-stage cost
$y_{p,t,s}$	production of p purchased at time t in scenario s
$u_{i,t,s}$	plant input i at time t in scenario s
$m_{f,t,s}^{feed}$	amount of feed f used at time step t for scenario s
PP_p	amount of product p produced in the next campaign or purchased externally for scenario s
$d_{t,s}$	degradation level at time t and scenario s
Binary variables	
x_t^{CBM}	1 if the maintenance activities are performed at time t
s_t^{CBM}	1 if the maintenance activities start at time t
x_f^{feed}	1 if the feed f is purchased
$y_{f,t}^{feed}$	1 if the feed f is allocated at time t
$s_{f,t}^{feed}$	1 if the allocation of the feed f starts at time t
$x_s^{scenario}$	1 if the degradation level is higher than the threshold d^{min} at $t \in RULs - 1$

Maintenance constraints

The maintenance constraints implement the maintenance policy. A binary variable x_t^{CBM} becomes equal to one when the maintenance activities are performed at time t. Eq. 4.5 ensures that the maintenance activities are started only once over the considered time horizon. Since the goal of this work is to optimize one production campaign, the production of the plant is set to zero after the maintenance activities are performed. For this reason, the binary variable x_t^{CBM} remains equal to one after the maintenance activities are performed (Eq. 4.5) forcing the production of the plant to zero (see Eq. 4.12). The maintenance activities must be performed in a specific time window $\hat{T}$ (in this work between day 30 and 39 corresponding to the set of uncertain RULs) as enforced by Eqs. 4.6-4.7. Eqs. 4.8-4.9 define the starting time of the maintenance activities. The binary variable s_t^{CBM} is equal to one if and only if the maintenance activities start at time t. Note that the maintenance activities can start at time $t = 30$ before any realizations of the end of the uncertain RUL of the plant.

$$x_t^{CBM} \geq x_{t-1}^{CBM} \quad t \in T, t \neq 1 \tag{4.5}$$

$$\sum_{t \in \hat{T}} x_t^{CBM} \geq 1 \tag{4.6}$$

$$\sum_{t \notin \hat{T}} x_t^{CBM} = 0 \tag{4.7}$$

$$s_t^{CBM} \geq x_t^{CBM} - x_{t-1}^{CBM} \quad t \in T, t \neq 1 \tag{4.8}$$

$$s_t^{CBM} \leq x_t^{CBM} \quad t \in T \tag{4.9}$$

Process constraints

The plant produces three products $p \in \{P_1, P_2, P_3\}$ to cover fixed and known product demands D_p. Two plant model inputs ($u_{i,t,s}$) and the degradation level ($d_{t,s}$) determine the production rate according to the plant model (Eq. 4.10). The parameters $\gamma_{p,i}, r_p$ are the result of a linearization procedure to describe the plant behaviour with linear equations. For each time step t and scenario s the production of the plant is computed as a linear combination of the model inputs $u_{i,t,s}$ (weighted by the parameter $\gamma_{p,i}$) minus the loss of performance due to the degradation level $d_{t,s}$ (multiplied by the parameter r_p). The higher is the degradation level the higher is the loss of performance in terms of reduction of the production rate. With respect to the ethylene production plant, the three products represent ethylene, propylene and heavier hydrocarbons. The plant inputs model the plant operating conditions in terms of the naphtha mass flow and the severity of the furnaces. The set S represent the ordered set of scenarios ($S = \{1, \ldots, 10\}$). We consider 10 scenarios to model the uncertain RULs of the plant ($RUL_s = \{30, \ldots, 39\}$). Eq. 4.11 sets the upper and lower bounds of the plant inputs. When the maintenance activities are performed, $x_t^{CBM} = 1$, the input variables are forced to be zero. The maximum production capacity is limited by Eq. 4.12. The upper bound $UB_{p,t,s}^{y}$ is considered to be a function of the time t to model the realization of the uncertainty. In fact, before the end of the RUL the parameter ($UB_{p,t,s}^{y}$) is equal to the maximum production capacity $UB_{p,s}^{y}$. After the realization of the uncertainty, the parameter $UB_{p,t,s}^{y}$ is equal to zero. The demand satisfaction constraint (Eq. 4.13) enforces that the product demand is covered by the

production in the running campaign ($y_{p,t,s}$) or by the production in the next campaign or by purchasing the product from external sources ($PP_{p,s}$). For each scenario s the variables $PP_{p,s}$ identify the amount of product p needed to cover the demand after the failure has occurred.

$$y_{p,t,s} = \sum_{i \in I} \gamma_{p,i} * u_{i,t,s} - r_p * d_{t,s} \quad t \in T, s \in S, p \in P \tag{4.10}$$

$$LB^{input}_{i,t,s} * (1 - x^{CBM}_t) \leq u_{i,t,s} \leq UB^{input}_{i,t,s} * (1 - x^{CBM}_t) \quad t \in T, s \in S, i \in I \tag{4.11}$$

$$y_{p,t,s} \leq UB^{y}_{p,t,s} * (1 - x^{CBM}_t) \quad t \in T, s \in S, p \in P \tag{4.12}$$

$$\sum_{t \in T} y_{p,t,s} + PP_{p,s} = D_p \quad p \in P, s \in S \tag{4.13}$$

Feed purchasing constraints

The following constraints define the feed purchasing options of the plant and the allocation of the feeds over the time horizon. The binary variables x^{feed}_f are set equal to one if the feed f is purchased, and to zero otherwise. An additional binary variable $y^{feed}_{f,t}$ becomes equal to one if the feed f is used at the time step t. Eq. 4.14 ensures that no feed is used if the maintenance activities are performed. When the maintenance activities are not performed ($x^{CBM}_t = 0$), Eq. 4.14 imposes that only one feed can be allocated for each time step t. Eq. 4.15 imposes that the feed f cannot be allocated to any time step t if the feed is not purchased ($x^{feed}_f = 0$). Note that since the binary variable $y^{feed}_{f,t}$ becomes equal to one if the feed f is used at the time step t, the number of time steps of the time horizon T ($|T|$) is a *big-M* parameter for this constraint. Eqs. 4.16-4.17 define the starting time of the feed utilization for each purchased feed. Eq. 4.17 prevents that different feeds are allocated to consecutive time steps by forcing the start of the feed allocation to happen at most once. In other words, each feed f can be used only once for all consecutive time steps. Eq. 4.18 limits the amount of feed f that can be used over the time horizon T if the feed f is purchased ($x^{feed}_f = 1$). The continuous variable $m^{feed}_{f,t,s}$ models the amount of feed f used at time step t for scenario s and the parameter UB^{feed}_f is the maximum amount of feed f that can be used over the time horizon T. If the feed f is not purchased ($x^{feed}_f = 0$) the sum of the feed utilization over the time horizon T is forced to be zero (Eq. 4.18). Note that while the binary variables ($x^{feed}_f, y^{feed}_{f,t}$) that are associated to the purchasing and allocation of the feed are first stage variables, the amount of feed used ($m^{feed}_{f,t,s}$) is a recourse variable. In fact, the amount of feed used is the first input of the plant model ($u_{i=1,t,s}$) as already described in Section 4.1.2 and imposed by Eq. 4.20. If the feed f is not allocated to the time step t, Eq. 4.19 forces the corresponding amount $m^{feed}_{f,t,s}$ to zero.

$$\sum_{f \in F} y^{feed}_{f,t} = 1 - x^{CBM}_t \quad t \in T \tag{4.14}$$

$$\sum_{t \in T} y^{feed}_{f,t} \leq |T| * x^{feed}_{f} \quad f \in F \tag{4.15}$$

$$s^{feed}_{f,t} \geq y^{feed}_{f,t} - y^{feed}_{f,t-1} \quad f \in F, t \in \{2, ..., |T|\} \tag{4.16}$$

$$s^{feed}_{f,t} \leq x^{feed}_{f} \quad f \in F, t \in T \tag{4.17}$$

$$\sum_{t \in T} m^{feed}_{f,t,s} \leq UB^{feed}_{f} * x^{feed}_{f} \quad f \in F, s \in S \tag{4.18}$$

$$m^{feed}_{f,t,s} \leq UB^{feed}_{f} * y^{feed}_{f,t} \quad f \in F, t \in T, s \in S \tag{4.19}$$

$$\sum_{f \in F} m^{feed}_{f,t,s} = u_{i=1,t,s} \quad t \in T, s \in S \tag{4.20}$$

The quality of the feed f (indicated by the parameter IC_f) influences the degradation trajectory. In fact, as described by Eqs. 4.21-4.22, the higher is the quality of the feed the lower is the degradation rate. The degradation reduces the production rate according to the parameter r_p (as described by the plant model Eq. 4.10). Since the parameter r_p varies with the product p the influence of the quality of the feed on the quality of the products (ethylene, propylene and heavier hydrocarbons) is taken into account only in terms of loss of production rate. An extension of the plant model could consider the influence of the feed quality on the product quality also in terms of nominal production rate (if no degradation was generated). In other words, the parameter $\gamma_{p,i}$ in Eq. 4.10 then would vary according to the feed quality.

Degradation model

The following constraints compute the degradation trajectory over the time horizon. The degradation model represents an auto-regressive model with exogenous inputs (ARX) as shown in Eqs. 4.21-4.22: for each scenario s the degradation trajectory $d_{t,s}$ depends on previous degradation value $d_{t-1,s}$, the operating conditions of the plant $u_{i,t}$ and the feed quality described by a feed indicator IC_f. The degradation model parameters (α^i) that describe the influence of the plant operating conditions ($u_{i,t,s}$) on the degradation level must be estimated from process data. The parameter d^0 represent the initial condition of the degradation trajectory. A maximum allowed degradation threshold (d^{max}) is ensured by Eq. 4.23 by forcing the maintenance activities to take place if the degradation level reaches the failure threshold d^{max}. In Eq. 4.24 an indicator Boolean variable $x^{scenario}_{s}$ describes whether the degradation level is higher than the threshold d^{min} (also called prognosis threshold) by the time step before the end of the corresponding RUL ($t \in RUL_s - 1$). The constant ϵ is a small number ($\epsilon = 0.0001$) defining the tolerance for the threshold violation. In case the degradation level is lower than the prognosis threshold d^{min} (or $x^{scenario}_{s} = 0$) no failure scenario can realize in the following time step. This is modelled by setting equal to zero the corresponding scenario probability as imposed by Eq. 4.29. In other words, if the predicted degradation level at time t is too low, we consider not possible that the plant reaches the end of the RUL in the next time steps. Since the degradation

is monotonically increasing, Eq. 4.25 can be formulated to tighten the formulation.

$$d_{t,s} \geq d^0|_{t=1} + d_{t-1,s} + \sum_{i \in I} \alpha^i * u_{i,t,s} + \sum_{f \in F} IC_f * y_{f,t}^{feed} - M * x_t^{CBM} \quad \forall s \in S, t \in T, t < RUL_s \quad (4.21)$$

$$d_{t,s} \leq d^0|_{t=1} + d_{t-1,s} + \sum_{i \in I} \alpha^i * u_{i,t,s} + \sum_{f \in F} IC_f * y_{f,t}^{feed} + M * x_t^{CBM} \quad \forall s \in S, t \in T, t < RUL_s \quad (4.22)$$

$$d_{t,s} \leq d_s^{max}(1 - x_t^{CBM}) \quad \forall s \in S, t \in T \quad (4.23)$$

$$d_{t,s} \leq d^{min} - \epsilon + (M + \epsilon) * x_s^{scenario} \quad \forall s \in S, t \in RUL_s - 1 \quad (4.24)$$

$$x_s^{scenario} \leq x_{s+1}^{scenario} \quad \forall s \in S, t \in T \quad (4.25)$$

Prognosis constraints

The prognosis constraints embed the prognosis model into the production planning optimization. To describe the prognosis constraints, it is worth to remark that each scenario is associated to a time step (identified by the set RUL_s) that defines the point in time when the uncertain RUL is exceeded. In other words each scenario represents an uncertain failure time of the plant. Therefore, the probability of the scenario s represents the probability of realization of the associated RUL of the plant (RUL_s) or, equivalently, the probability that the plant *fails* when the uncertain estimation of the RUL (RUL_s) is exceeded. For scenario s the uncertain failure time RUL_s is associated to a survival function S_s and to a hazard function h_s (Eq. 4.26). The survival function S_s represents the probability of surviving the uncertain RUL (RUL_s). In other words, the survival function of scenario s (S_s) indicates the probability that the failure of the plant does not occur by the point in time identified by the set RUL_s. The hazard function of scenario s (h_s) represents the failure rate of the plant at time t equal to RUL_s, namely when the RUL associated to the scenario s is exceeded. For discrete systems, the hazard function is limited between zero and one (Eq. 4.26) and it can be interpreted as the conditional probability of failure of the plant given that the failure has not occurred before.

Eq. 4.27 ensures that the sum of the probabilities over the scenarios is equal to one. Eq. 4.28 sets to zero the probabilities of those scenarios corresponding to RULs that realize after the maintenance activities start. In other words, these scenarios do not realize. Note that according to Eq. 4.28 the probability of the scenario s is not set to zero if the maintenance activities are performed on the same time step defining the end of the corresponding RUL. Similarly, Eq. 4.29 ensures that the scenarios associated to a degradation level lower than the prognosis threshold d^{min} ($x_s^{scenario} = 0$) do not

realize.

$$0 \leq p_s, S_s, h_s \leq 1 \quad \forall s \in S \tag{4.26}$$

$$\sum_{s \in S} p_s = 1 \tag{4.27}$$

$$p_s \leq 1 - x_t^{CBM} \quad \forall s \in S, t \in RUL_s - 1 \tag{4.28}$$

$$p_s \leq x_s^{scenario} \quad \forall s \in S \tag{4.29}$$

Eqs. 4.30-4.31 link the survival function S_s to the probability p_s. For two consecutive scenarios $s, s+1$ (and therefore $RUL_s < RUL_{s+1}$) Eq. 4.30 defines the probability of failure at time t equal to RUL_s (p_s) as the probability of surviving the time step identified by RUL_s minus the probability of surviving the time step identified by RUL_{s+1}. In other words, the decrease of the probability of surviving a certain point in time is equal to the probability that the failure occurs at that point in time. Similarly, Eq. 4.31 defines the probability of surviving the point in time RUL_s as the sum of the probabilities that the failure occurs at any time later than RUL_s. Eq. 4.31 is redundant but when introduced showed slightly improvements in terms of solution time.

$$p_s = S_s - S_{s+1} \quad \forall s \in S \tag{4.30}$$

$$S_s = \sum_{s\prime > s} p_{s\prime} \quad \forall s \in S \tag{4.31}$$

Eq. 4.32 implements the Cox model determining the hazard function of the earliest uncertain RUL according to the degradation trajectory. The hazard functions of the remaining scenarios are adjusted linearly (Eqs. 4.33-4.34). According to Eq. 4.32, the higher is the predicted degradation level the higher is the hazard associated to the earlier RULs. Note that the covariate of the Cox model is the degradation level at the end of the time interval associated to the first-stage ($|T^{1stage}|$).

$$h_s = h_s^0 * \exp(\beta * (d_t - d^{min})) \quad \forall s = 1, t = |T^{1stage}| \tag{4.32}$$

$$h_s \geq h_{s=1} + \frac{1 - h_{s=1}}{MS - 1} - x_t^{CBM} \quad \forall s \in S, s \neq 1, t \in RUL_s - 1 \tag{4.33}$$

$$h_s \leq h_{s=1} + \frac{1 - h_{s=1}}{MS - 1} - x_t^{CBM} \quad \forall s \in S, s \neq 1, t \in RUL_s - 1 \tag{4.34}$$

The baseline hazard (h_s^0) and the parameter β of the Cox model were estimated from plant data. The parameter β is estimated via the software MATLAB and the function `coxphfit` (*Statistics and Machine Learning Toolbox* 2006) and the parameter MS represents the number of scenarios. The function `coxphfit` estimates the coefficient β by receiving as input the observations on the time-dependent covariate (the degradation level) and the time-to-event data (plant failures). Since the baseline hazard function h_s^0 represents the level of the hazard if no covariates are considered, it can be estimated from the time-to-event data of the plant by using the equations of the survival analysis introduced by Eqs. 4.1-4.3. The probability of failure for a scenario s (i.e. for a given time interval) associated to the baseline hazard function h_s^0 can be computed by dividing the number of failures happened in the given time interval by the total number of observed failures.

Eqs. 4.35-4.36 define the probability of failure for the scenarios that realize ($x_s^{scenario} = 1$) as the product of the failure rate at the point in time equal to RUL_s and the probability of surviving RUL_s. A high failure rate ($h_s \approx 1$) at RUL_s is associated to a high probability of failure ($p_s \approx 1$) at RUL_s only if the probability of surviving until RUL_s is high as well ($S_s \approx 1$).

$$p_s \leq h_s * S_s + (1 - x_s^{scenario}) \quad \forall s \in S \tag{4.35}$$

$$p_s \geq h_s * S_s - (1 - x_s^{scenario}) \quad \forall s \in S \tag{4.36}$$

Figure 4.5 shows an example to illustrate the variables involved in the prognosis constraints along with the associated scenario tree. Each node of the scenario tree represents a time step: the red nodes show the uncertain failure times ($RUL_s = \{4, 5, 6, 7\}$) while the yellow node is associated to the time step of the degradation profile that influences the hazard function according to the Cox model. The first stage of the depicted scenario tree covers the first three time steps ($T^{1stage} = \{1, 2, 3\}$, $|T^{1stage}| = 3$). The maintenance activities are performed at time step six and, therefore, the RUL of the last scenario is associated to a probability equal to zero since it should have realized after the maintenance activities are performed (since $RUL_{s=4} = 7$). The hazard function of the first scenario that is associated to the uncertain RUL equal to four ($RUL_{s=1} = 4$) is computed according to the degradation level at $t = 3$ that defines the end of the time interval modelled by the first stage of the stochastic formulation. Since the degradation model contains an auto-regressive part, the degradation level at $t = 3$ depends on the degradation levels at the previous time steps. The hazard functions of the remaining scenarios are adjusted linearly. Note that the hazard function of the third scenario is almost equal to one: if the failure does not occur before, the failure probability at the point in time equal to six (that defines the RUL of the plant for the third scenario $RUL_{s=3} = 6$) is almost equal to one. However, since the survival function decreases with time (and therefore with the scenarios), the probability of surviving the uncertain RUL associated to the third scenario is relatively low (almost equal to zero) and, consequently, the probability that the corresponding RUL realizes is low as well as shown in Figure 4.5. It is worth to remark that the hazard and the survival functions and the probabilities do not explicitly depend on time but on the scenarios that, however, are associated to consecutive points in time. Moreover, we highlight that the prognosis variables (hazard and survival functions and the probabilities) are not associated to the time steps of the first stage since, by definition, no uncertain parameters (i.e. the RULs or equivalently the failure times) realize in the first stage.

Non-anticipativity constraints

The NACs are introduced to set equal to each other all the variables belonging to the same stage. Defining with $x_{t,s}$ a generic decision variable, the NACs have the following form

$$x_{t,s} = x_{t,s\prime} \quad \forall (s, s\prime) \in S, s\prime = s + 1, t \in \{1, \ldots, RUL_s - 1\} \tag{4.37}$$

The NACs do not apply for the prognosis variables defining the probability, the hazard and the survival functions of the scenarios.

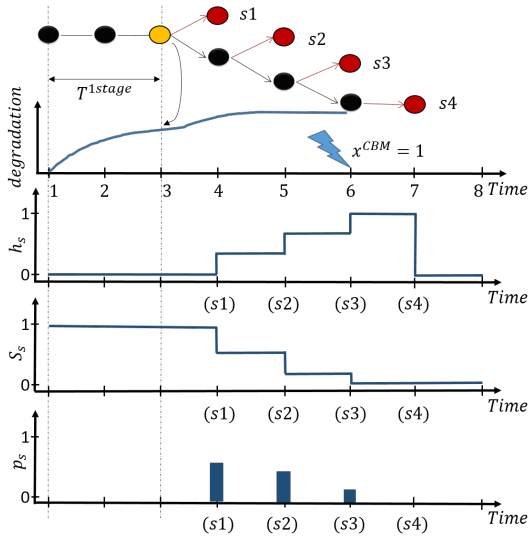

FIGURE 4.5: Illustrative explanation of the variables involved in the prognosis constraints (degradation, hazard and survival functions and probabilities of the scenarios) and the associated scenario tree. Source: (Leo and Engell, 2021).

Objective function

The following constraints compute the total plant cost and define the objective function (Eq. 4.38) of the stochastic program as the sum of the first-stage cost ($cost^{1stage}$) and the expected cost over the scenarios s. The first-stage cost is computed by Eq. 4.39 as the sum of the cost of purchasing the feed, defined by Eq. 4.40, the cost of performing the maintenance activities and the cost of the resource utilization (steam and fuel gas) for the time interval associated to the first-stage. The cost of the maintenance is considered only if the maintenance activities are started in the time horizon T. The cost of the resource utilization (steam and fuel gas) is assumed proportional to the inputs of the plant $u_{i,t,s}$ according to the parameter $price_i^{input}$. In fact, with respect to the ethylene production plant the amount of steam consumed depends on the mass flow of the feed according to the steam-to-hydrocarbon ratio, and the severity of the furnaces (i.e. the cracking temperature of the furnaces) is linked to the amount of fuels that are burned. The first-stage variables $u_{i,t,s}$ have a subscript s because a NAC formulation is described here (the first stage variables related to the feed are introduced without the subscript s). All the first-stage variables are equated to each other by the NACs according to Eq. 4.37.

$$\min z = cost^{1stage} + \sum_{s \in S} p_s * cost_s \tag{4.38}$$

$$cost^{1stage} = cost^{feed} + c^{CBM} * \sum_{t \in T} s_t^{CBM} + \sum_{t \in T^{1stage}} \sum_{i \in I} price_i^{input} * u_{i,t,s=1} \tag{4.39}$$

$$cost^{feed} = \sum_{f \in F} price_f^{feed} * x_f^{feed} \tag{4.40}$$

The scenario costs ($cost_s$) are defined by Eq. 4.41 as the sum of resource consumption cost (i.e. the cost of steam and fuel consumption assumed proportional to the plant inputs) for the time steps belonging to the corresponding stages and scenarios (Eq.

4.42) and the cost of producing the products in the next campaign or purchasing them from external sources (Eq. 4.43).

$$cost_s = cost_s^{missing\ demand} + cost_s^{input} \quad \forall s \in S \tag{4.41}$$

$$cost_s^{input} = \sum_{t \in T^s} \sum_{i \in I} price_i^{input} * u_{i,t,s} \quad \forall s \in S \tag{4.42}$$

$$cost_s^{missing\ demand} = \sum_{p \in P} price_p^{product} * PP_p \quad \forall s \in S \tag{4.43}$$

The variables $cost_s^{missing\ demand}$ represent the terminal cost that has to be paid for considering a finite time horizon and for introducing scenarios that are associated to different durations of the campaign and, therefore, different production costs and amounts. It represents a fictitious cost that we introduce to take into account the production cost of the beginning of following campaign (that is not modelled) or the amount of product to be purchased from external sources to satisfy the demand. This cost term is necessary to compare the production costs of the different scenarios that present different durations of the campaign and, therefore, different satisfaction of the demand (that obviously does not depend on the uncertain duration of the production campaign). To reiterate, the cost of the missing demand $cost_s^{missing\ demand}$ is identified to take into account the influence of the following production campaign on the current one according to the decisions that are made in the current one (i.e. the duration of the campaign) without introducing the production decisions of the beginning of the following campaign that impact the degradation trajectory and, therefore, the timing of the maintenance activities of the following campaign. As a side effect, this modelling strategy reduces the size of the problem since some variables (that model the production after the failure) are set to zero and, therefore, are eliminated from the optimization problem. It is also worth to highlight that extending the formulation to a second campaign would not solve this issue. In fact, the same relation between the second and the third campaigns has to be modelled.

4.1.3 Value of the stochastic solution

The value of the stochastic solution (VSS) measures the advantage of using a stochastic programming formulation over its deterministic counterpart where the stochastic parameters have been replaced by their mean values. The second problem is also called the Expected Value Problem (EVP). The EVP for the proposed formulation considers the mean value of the uncertain RULs and therefore a fixed and not optimized duration of the production campaign. Consequently, the timing of the maintenance activities that define the duration of the production campaign are also fixed and not dependent on the degradation level. To avoid this issue, for the calculation of the VSS we here replace the EVP in the comparison with a deterministic condition-based optimization where a perfectly known degradation model is embedded into the optimization problem to define the RUL according to the operating strategy of the plant, as proposed in many works on CBM optimization (Jain and Grossmann, 1998), (Xenos et al., 2015), (Leo and Engell, 2017). We call this problem Deterministic CBM problem (DCBM). The DCBM problem defines the optimal duration of the production campaign according to the operating conditions of the plant and the certain degradation model. Since the DCBM problem contains additional degrees of freedom

compared to the EVP, the optimal objective function value of the EVP can only be greater or equal (for a minimization problem) than the optimal objective function value of the DCBM problem (Eq. 4.44).

$$z^*_{DCBM} \leq z^*_{EVP} \tag{4.44}$$

Therefore, in this work, the VSS is defined as the difference between the optimal objective function of the stochastic problem with endogenous uncertainty (MSSP), z^*_{MSSP}, and the optimal solution of the recourse problem (RP), z^*_{RP}, obtained by solving the stochastic problem with endogenous uncertainty with the first stage variables fixed to the deterministic solution of the Deterministic CBM problem (DCBM). The definition of the VSS is given in Eq. 4.45.

$$VSS = \frac{z^*_{RP} - z^*_{MSSP}}{z^*_{RP}} \tag{4.45}$$

If we define as VSS^{EVP} the VSS obtained with the deterministic solution of the Expected Value Problem (EVP), the following relation holds

$$VSS \leq VSS^{EVP} \tag{4.46}$$

and therefore the proposed definition of the VSS represents a *lower bound* of the improvement that is achievable by using a stochastic formulation over the deterministic counterpart. For a multi-stage stochastic program it is possible to compute a VSS for each stage (Escudero et al., 2007) by fixing in the recourse problem to the deterministic solution all the variables belonging to the first stage until the corresponding stage. In this work we will focus on the VSS of the first-stage that represents the lowest VSS.

4.1.4 Solution methods

It is a well known fact that stochastic programming formulations give rise to large-scale optimization problems. Endogenous uncertainty formulations further complicate the solution due to the introduction of non-linear non-convex bi-linear terms since the probabilities of the scenarios become decision variables. Therefore, from the solution perspective the challenge for this class of problems lies not only on the computational time but also on the global optimality of the solution. In this work we apply three different solution methods:

- we solve the deterministic equivalent problem with the global solver BARON enhanced with a branching priority strategy
- we apply the generalized Benders decomposition algorithm (GBD) (Geoffrion, 1972) proposing a judicious partition of the variables
- we adapt the Global Optimization Algorithm (GOP) proposed in (Floudas and Visweswaran, 1990) to the class of stochastic programs with decision-dependent uncertainty.

The GOP can be seen as a variant of the GBD to guarantee global optimality for bi-linear non-convex programs. In fact, the GBD might terminate to a local solution

in case of non-convex formulations. We applied the proposed variables partition to both decomposition algorithms as described below.

The problem decomposition

Both the GBD and the GOP belong to the class of primal decomposition methods. We describe here the two decomposition algorithms as they are implemented in this work. The general formulation of the stochastic program with decision-dependent uncertainty is presented in (4.47):

$$\min_{x,y_s,p_s} \quad c^T x + \sum_s p_s * f_s * y_s \tag{4.47a}$$

$$\text{s.t.} \quad g(x, y_s, p_s) \leq 0 \tag{4.47b}$$

$$x \in X, y_s \in Y, p_s \in P \tag{4.47c}$$

$$y_s \in R^n, p_s \in R^n, x \in R^n, x\prime \in \{0,1\}, \tag{4.47d}$$

where $x, x\prime$ represent the continuous and binary first-stage variables, y_s the continuous recourse variables, p_s the probability of the scenarios. Eq. 4.47a models the objective function of the problem as the sum of the first-stage cost and the expected cost over the possible scenarios. Since the the probabilities of the scenarios are decision variables, the objective function introduces non-convexities in the optimization problem. Eq. 4.47b represents the problem constraints that couple the first-stage variables, the recourse variables and the probabilities of the scenarios. Eq. 4.47c describes additional constraints involving separately the first-stage variables, the recourse variables and the scenario probabilities. Both applied decomposition algorithms classify the variables as complicating variables and non-complicating variables in order to generate a relaxed master problem (4.48) that is obtained by projecting the original problem (4.47) into the space of the complicating variables, and a primal problem (4.49), obtained by optimizing only over the non-complicating variables (Laporte and Louveaux, 1993b), (Geoffrion, 1972).

$$\min_{\eta,x,p_s} \quad \eta \tag{4.48a}$$

$$\text{s.t.} \quad \eta \geq c^T x + \sum_s p_s * f_s * \hat{y}_s^k + \hat{\lambda}^{k^T} g(x, \hat{y}_s^k, p_s) \tag{4.48b}$$

$$x \in X, p_s \in P \tag{4.48c}$$

Eq. 4.48b models in the relaxed master problem the Lagrange function where the Lagrange multipliers $\hat{\lambda}^k$ are obtained from the solution of the primal problem (or sub-problem) (4.49) at iteration k. Eq. 4.48b is also called Benders cut or optimality cut.

$$\min_{y_s} \quad c^T \hat{x} + \sum_s \hat{p}_s * f_s * y_s \tag{4.49a}$$

$$\text{s.t.} \quad g(\hat{x}, y_s, \hat{p}_s) \leq 0 \tag{4.49b}$$

$$y_s \in Y \tag{4.49c}$$

The complicating variables appearing in the primal problem (Eqs. 4.49a-4.49b) are fixed to the solution of the relaxed master problem at the previous iteration (or to an

initial value for the first iteration).

We propose to decompose the problem into an MINLP relaxed master problem and an LP primal problem (or sub-problem). The MINLP relaxed master problem includes the following equations for $t \in T^{1stage}$:

- maintenance constraints Eqs. 4.5-4.9
- process constraints Eqs. 4.10-4.13
- feed purchasing constraints Eqs. 4.14-4.20
- degradation constraints Eqs. 4.21-4.25
- prognosis constraints Eqs. 4.26-4.36

The LP primal problem includes the following equations for $t \in T^s$:

- process constraints Eqs. 4.10-4.13
- degradation constraints Eqs. 4.21-4.25

Figure 4.6 shows the decomposed scenario tree. The key idea of the proposed partitions is to consider the probabilities of the scenarios, p_s, as complicating variables in order to render the objective function (Eq. 4.47a) convex for every fixed $p_s = \hat{p}_s$ and $y_s = \hat{y}_s$. Algorithms 2 and 3 describe the implementation of the two decomposition methods. For the GBD (Algorithm 2), we introduce the additional step 4 to adjust the solution of the primal problem for the scenarios with probability p_s^k equal to zero (defined by the solution of the relaxed master). In fact, in the primal problem the scenarios with fixed null probabilities generate null Lagrange multipliers (since the objective function is not sensitive to the right-hand side of the complicating constraints due to the null probability) but they might provide non-zero scenario costs (due to the NACs). This can also be avoided by introducing conditional NACs that, however, would complicate the formulation because of additional binary variables.

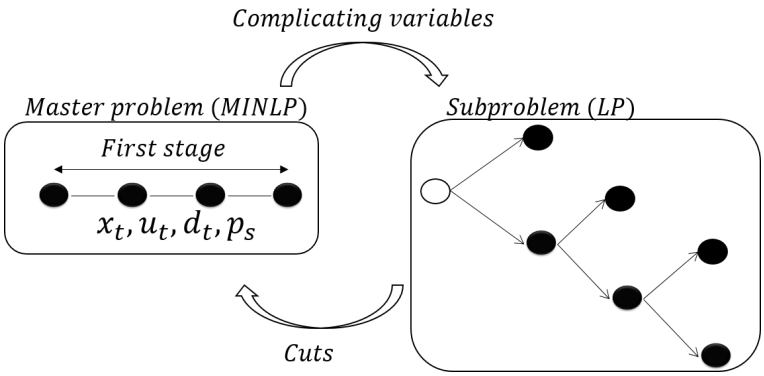

FIGURE 4.6: Decomposed scenario tree. Source: (Leo and Engell, 2021).

Difference between the GBD and the GOP

For a primal decomposition algorithm, the solutions of the primal problem (4.49) and the relaxed master problem (4.48) provide an upper- and a lower-bound of the original

problem (4.47) respectively. As described in Algorithm 2 for the GBD decomposition, at each iteration k the Lagrange function in the relaxed master problem is computed using the solution of the primal problem, namely the optimal Lagrange multipliers and the decision variables involved in the complicating constraints. In the case of bi-linear terms (and in general non-convex constraints) such procedure does not ensure that the relaxed master problem represents a valid under-estimator of the original problem. In other words, the solution is not guaranteed to converge to the global optimum (Sahinidis and Grossmann, 1991). To overcome this issue and to guarantee global optimality, as described in Algorithm 3, the GOP decomposition solves the relaxed master problem for each combination of the bounds of the variables of the relaxed master problem that are involved in the bi-linear terms (instead of fixing them to the solution of the primal problem). These variables are called connected variables and in the proposed formulation they model the cost of the uncertain scenarios. Moreover, the Lagrange function at each iteration is added to the master problem only if the solution of the primal problem satisfies the qualifying constraints. The qualifying constraints for the proposed formulation are defined in Eq. 4.50

$$\begin{aligned} p_s - p_s^k \geq \epsilon \quad if \;\; x_s = x_s^{LB} \quad \forall s \in S \\ p_s - p_s^k \leq -\epsilon \quad if \;\; x_s = x_s^{UB} \quad \forall s \in S \end{aligned} \tag{4.50}$$

where p_s^k represent the value of the probability of the scenarios obtained in the previous iteration $k \in 1, ..., K$ and x_s the connected variables (i.e. the cost of the uncertain scenarios in the proposed formulation) of the Lagrange function for the relaxed master problems. The parameter ϵ is a very small positive number to avoid that both the qualifying constraints in Eq. 4.50 are simultaneously satisfied.
To guarantee global optimality, the GOP at each iteration does not solve the relaxed master problem only once as the GBD but a number of times equal to all the combinations of the upper and lower bounds of the second-stage variables involved in the bi-linear terms. Obviously, this additional step increases the computational time.

Algorithm 2 Benders Decomposition algorithm.

1: **Initialization**: Let $k \leftarrow 0$ and $(x^k, p_s^k) = (x^0, p_s^0)$ the initial values of the complicating variables. Set Upper and Lower bounds $UB = +\inf, LB = -\inf$ and $\epsilon = 0.001$
2: **Iteration Update**: $k \leftarrow k + 1$
3: **Primal problem**: Solve the LP primal problem (4.49) with the complicating variables $(x^k, p_s^k) = (x^{k-1}, p_s^{k-1})$. Obtain solution y_s^*, z_{SP}^*
4: **Adjust scenario costs**: set to zero the scenario costs $\hat{y}_s^k$ associated to a probability p_s^{k-1} equal to zero
5: **Relaxed master Problem**: Solve the relaxed master problem (4.48). Obtain solution x^*, p_s^*, z_{MP}^*
6: **Bounds update**: Update Upper and Lower bounds according to $LB^k = \eta^*, UB^k = min\{UB^{k-1}, z^{SP*}\}$
7: **Convergence test**: If Upper and lower bounds are sufficiently close ($UB^k - LB^k < \epsilon$), stop. Else, go to step 3.

Algorithm 3 GOP algorithm.

1: **Initialization**: Let $k \leftarrow 0$ and $(x^k, p_s^k) = (x^0, p_s^0)$ the initial values of the complicating variables. Set Upper and Lower bounds $UB = +\inf, LB = -\inf$ and $\epsilon = 0.001$
2: **Iteration Update**: $k \leftarrow k + 1$
3: **Sub-problem**: Solve the LP sub-problem (4.49) with the complicating variables $(x^k, p_s^k) = (x^{k-1}, p_s^{k-1})$ obtaining the optimal Lagrange multiplier λ^k
4: **Master Problem**: Add the Lagrange function to the relaxed master problem (4.48) from all the previous iteration $k\prime \in 1, \ldots, k$ if the qualifying constraints (Eq. 4.50) are satisfied.
5: **Master Problem**: Solve the relaxed master problem (4.48) for each combination of the bounds of the variables $cost_s$ and store the solution in z^*_{MP}
6: **Bounds update**: Update Upper and Lower bounds according to $LB^k = min\{z^*_{MP}\}, UB^k = min\{UB^{k-1}, z^{SP*}\}$
7: **Convergence test**: If Upper and lower bounds are sufficiently close ($UB^k - LB^k < \epsilon$), stop. Else, go to step 3.

Generation of the qualifying constraints for the GOP method

The connected variables of the Lagrange function L of the primal sub-problem for the proposed formulation are the variables $cost_s$ that identify the cost of the uncertain scenarios (see Section 2.3.4). Given the gradient of the Lagrange function with respect to the connected variables (Eq. 4.51), the qualifying constraints are shown by Eq. 4.52.

$$\nabla_{cost_s} L = p_s + \lambda_s^k \quad \forall s \in S \tag{4.51}$$

$$\begin{aligned} \nabla_{cost_s} L = p_s + \lambda_s^k \geq 0 \quad if \;\; x_s = x_s^{LB} \quad \forall s \in S \\ \nabla_{cost_s} L = p_s + \lambda_s^k \leq 0 \quad if \;\; x_s = x_s^{UB} \quad \forall s \in S \end{aligned} \tag{4.52}$$

Using the KKT condition of the proposed formulation that is expressed in Eq. 4.53, the qualifying constraints at iteration k can be simplified as shown by Eq. 4.54.

$$\nabla_{cost_s} L = p_s^k + \lambda_s = 0 \quad \forall s \in S \tag{4.53}$$

$$\begin{aligned} \nabla_{cost_s} L = p_s - p_s^k \geq 0 \quad if \;\; x_s = x_s^{LB} \quad \forall s \in S \\ \nabla_{cost_s} L = p_s - p_s^k \leq 0 \quad if \;\; x_s = x_s^{UB} \quad \forall s \in S \end{aligned} \tag{4.54}$$

The gradient of the Lagrange function with respect to the connected variables $\nabla_{cost_s} L$ is set to be greater (lower) than zero when the connected variables are fixed to the lower (upper) bounds (Floudas and Visweswaran, 1990).

Constraint propagation and feasibility cuts

As described in section 4.1.4, the complicating variables appearing in the primal problem are fixed to the solution of the relaxed master problem. Since the formulation described so far does not present full recourse, this might generate an infeasible primal problem. For instance, the optimal solution of the master problem might generate a degradation level close to the maximum threshold by the end of the time

horizon that belong to the first-stage ($t = 29$) and postpone the maintenance activities to the end of the entire planning horizon. This solution would obviously be infeasible for the sub-problem, since the degradation level would overcome the maximum threshold even with the plant input at the lower bounds. To handle this issues, feasibility cuts can be added to the master problem to cut off the solution generating infeasibility. However, since feasibility cuts increase the size of the master problem without improving the bounds, we exploit the dynamic degradation model adding to the master problem a redundant constraint (Eq. 4.55) that enhances the formulation with the feature of full recourse.

$$d_{t=|T^{1stage}|,s} + \sum_{t\prime=30}^{t} \sum_{i \in I} \alpha^i * LB^{inputs}_{i,t\prime,s} + \sum_f IC_f * y^{feed}_{f,t} \leq d^{max} + M * x^{CBM}_t$$
$$\forall s \in S, t \in T^s \quad (4.55)$$

In particular, Eq. 4.55 propagates the computation of the degradation level in the time set of the primal problem with the lower bound of the plant inputs ensuring that for any master problem decisions the degradation level of the primal problem would be under the maximum threshold d^{max}.

Computational Environment

The GBD and the GOP algorithms were implemented within the algebraic modelling language Julia/JuMP. The LP models were solved using the commercial solver CPLEX, and the MINLP models were solved using the global solver BARON version 18.12.26. All problems were solved on an Intel Core i7-2600 machine at 3.40 GHz with 8 processors and 8 GB RAM running Windows 7 Professional.

4.1.5 Results

Computational results

The proposed endogenous uncertainty formulation gives rise to a non-convex MINLP due to the bi-linear terms in the prognosis constraints (Eqs. 4.35-4.36-4.32) and in the objective function (Eq. 4.38). We provide computational results solving the deterministic equivalent with the global solver BARON (Kilinc and Sahinidis, 2018) enhanced with a custom branching priority strategy. We prioritize the variable influencing the probabilities of the scenarios (degradation variable) along the spatial branch-and-bound algorithm. Additionally, we show the performance of the decomposition methods described in section 4.1.4. Tables 4.1-4.2 present the objective functions and computational results obtained adopting the different solution strategies for two and ten scenarios. The results are expressed in terms of objective function value z^*, upper- and lower- bounds of the solution UB/LB and solution time $CPU[s]$. We also provide for the solver BARON the time the incumbent solution was found (t^{inc}) and the number of iterations performed by the decomposition algorithms. The performance of the decompositions algorithms are presented for the two different initial points x^1_0 and x^2_0.
Table 4.1 shows that for small instances the BARON solver reaches the global optimum (since $UB = LB$) in a reasonable amount of time and it is faster than the

decomposition methods. The GBD shows to be faster than the GOP but with performances depending on the initial point. In fact, when the GBD starts from the initial point x_0^1, it reaches the global optimum performing 8 iterations. However, the second initial point x_0^2 leads to a solution with 29 % optimality gap. On the other hand, the performance of the GOP algorithm does not depend on the initial point but the computational time is drastically larger than for the solver BARON.

TABLE 4.1: Computational results with 2 scenarios $RUL_s = \{30, 39\}$. Source: (Leo and Engell, 2021).

$\|RUL_s\| = 2$	z^*	UB/LB	CPU [s]	t^{inc} / it
DE-BARON	2 610,2	2 610,2 / 2 610,2	159	$t^{inc} = 159$
GBD (x_0^1)	2 610,2	2 610,2 / 2 610,2	427	$it = 7$
GBD (x_0^2)	3 703,6	3 703,6 / 3 703,6	165	$it = 3$
GOP (x_0^1)	2 610,2	2 610,2 / 2 610,2	1 059	$it = 7$
GOP (x_0^2)	2 610,2	2 610,2 / 2 610,2	1 299	$it = 12$

Figure 4.7 compares the GBD and the GOP for the small-size case-study (two scenarios) in terms of upper and lower bounds for the two considered initial points x_0^1 and x_0^2. The initial point x_0^1 (top graphs of Figure 4.7) leads both the algorithms to the global optimum and the probabilities of the scenarios (p_1, p_2) to the same optimal solution $(p_1^* = 0, p_2^* = 1)$. The upper and lower bounds of the two algorithms are almost identical: this means the intermediate solutions of the GBD always satisfy the strong duality theory and therefore the qualifying constraints of the Lagrange function do not need to be enforced. The influence of the qualifying constraints can be seen in the bottom graphs of Figure 4.7 obtained starting from the initial point x_0^2. Even though the GBD does not converge to the global optimum, the probabilities of the scenarios converge to the same solution as the GOP $(p_1^* = 0, p_2^* = 1)$.
Table 4.2 shows the computational results obtained with 10 scenarios. The solver BARON enhanced with the custom branching priorities does not terminate after more than 15 days of computation even though the incumbent solution is found after circa 12 hours. Without the branching priorities, the solver BARON with a time limit of circa two days (CPU = 150268 [s]) finds an intermediate solution ($UB = 28154.5$ with time of the incumbent solution equal to $t^{inc} = 56969$) which is significantly worse compared to the case with the priority strategy. The incumbent solution, when the branching priorities are implemented, presents an optimality loss of 15.9% compared to the GBD solution. In fact, the GBD reaches the global optimum independently on the initial point and it does not require more than 5100 [s] to terminate. The GOP method reaches the global optimum only after circa 3 days of computation. The increase of the problem dimension reduces the optimality gap for GBD and drastically increases the solution time for the GOP. In fact, as described in section 4.1.4, the relaxed master problem in the GOP must be solved for each combination of the upper- and lower-bounds of the costs of the scenarios. Obviously, increasing the number of scenarios the number of times the relaxed master problem has to be solved increases exponentially. Moreover, it is worth to highlight that the GOP requires the upper- and lower-bounds of the cost of the scenarios appearing in the bi-linear objective function. Due to the nature of these variables it is not straightforward to obtain these bounds and it might require the solution of additional optimization problems.
Since the GBD for the 10-scenario instance represents the best solution method, the following results discussion is performed only on those obtained with the GBD. Table 4.3 evaluates the proposed stochastic formulation in terms of the VSS as described

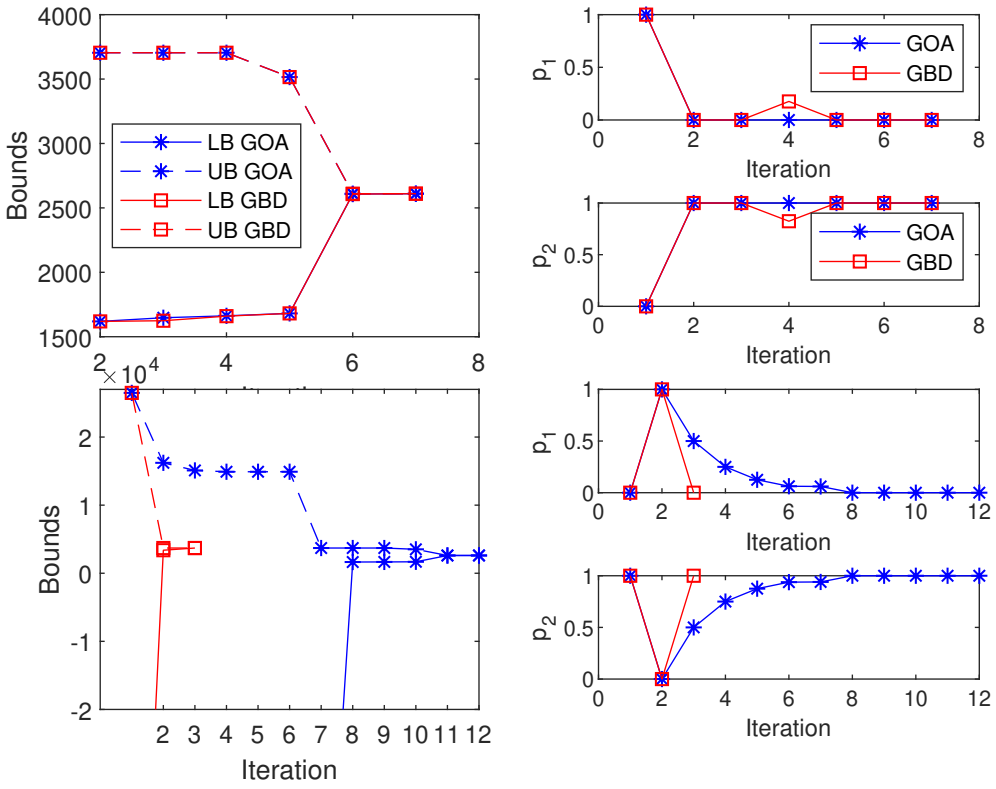

FIGURE 4.7: Upper- and lower-bounds for the GBD and GOP algorithms for the initial points x_0^1 (top) and x_0^2 (bottom). Source: (Leo and Engell, 2021).

TABLE 4.2: Computational results with 10 scenarios $RUL_s = \{30 \dots 39\}$. Source: (Leo and Engell, 2021).

$\lvert RUL_s \rvert = 10$	z^*	UB/LB	CPU [s]	t^{inc} / it
DE-BARON	14 259,4	14 259,4 / 0,0	1 555 200	$t^{inc} = 45964$
GBD (x_0^1)	12 295,0	12 295,0 / 12 295,0	5 100	$it = 15$
GBD (x_0^2)	12 295,0	12 295,0 / 12 295,0	593	$it = 8$
GOP (x_0^1)	12 295,0	12 295,0 / 12 295,0	272 469	$it = 7$
GOP (x_0^2)	12 295,0	12 295,0 / 12 295,0	295 128	$it = 9$

in section 4.1.3. The optimal objective function of the deterministic formulation (z^*_{DCBM}), the corresponding recourse problem (z^*_{RP}) and the stochastic programming counterpart with endogenous uncertainty (z^*_{MSSP}) are listed. We compute the VSS for different values of the prognosis threshold d^{min}: a nominal value ($d^{min} = 1220$), a low value ($d^{min} = 1215$) and a high value ($d^{min} = 1230$). The prognosis threshold d^{min} defines the minimum degradation level such that a failure scenario can realize in the following time step. In case the degradation level is lower than the prognosis threshold d^{min} no failure scenario can realize in the following time step. We also report the computational time and the number of iterations of the GBD algorithm. For all the instances the stochastic programming clearly outperforms the deterministic counterpart and the VSS can be quite significant. Reducing the value of the prognosis threshold means reducing the synergies between the plant operating conditions and the probability of the uncertain RULs that can be exploited by the optimizer. Even

though the VSS for the case with lower prognosis threshold ($d^{min} = 1215$) is still largely greater than zero, it is lower than in the other two cases.
Table 4.4 performs the same analysis with modified product demands: a low demand (reduction of 10 %) and a high demand (increase of 30 %). A reduction of the product demand generates production flexibility that can be exploited by the optimizer. The VSS for all the cases is significantly greater than zero.

TABLE 4.3: Value of the Stochastic solution for different values of the prognosis threshold. Source: (Leo and Engell, 2021).

	$d^{min} = 1215$	$d^{min} = 1220$	$d^{min} = 1230$
z^*_{DCBM}	1 691,8	1 691,8	1 691,8
z^*_{RP}	15 478,5	14 508,5	12 970,6
z^*_{MSSP}	14 440,8	12 295,0	8 004,87
VSS	6,7 %	15,2 %	38,2 %
CPU/it	9 745 / 8	477 /6	1 361 /14

TABLE 4.4: Value of the Stochastic solution for different values of the product demand. Source: (Leo and Engell, 2021).

	$\Delta D = -10\%$	$\Delta = +30\%$
z^*_{DCBM}	1 188,9	45 135,8
z^*_{RP}	2 346,8	88 784,5
z^*_{MSSP}	2 035,9	86 760,9
VSS	13,3 %	2,2 %
CPU/it	210 / 8	1 990 /19

Discussion

In this section we investigate how the stochastic and deterministic formulations impact the optimal production strategy. Figure 4.8a shows the degradation trajectories and the maintenance timing obtained by solving the proposed multi-stage endogenous formulation (MSSP) and the deterministic counterpart (DCBM). The degradation profiles are determined by the plant production and the purchased feed shown in Figures 4.8b-4.8c. Note that the production rate of the plant (Figure 4.8c) decreases over time due to the increase of the degradation level (as described by the plant model by Eq. 4.10). To improve the readability of the figure, the continuous line shows the results of the scenario associated to the longest RUL, while the dashed lines represent the remaining scenarios. Figure 4.8d shows the amount of products to be produced in the next campaign or to be purchased from external sources to cover the demand for the recourse problem and the stochastic formulation. It is interesting to notice that the stochastic formulation proposes a different operating strategy compared to the deterministic counterpart. In fact, as shown in Figure 4.8a, the stochastic solution postpones the maintenance activities compared to the deterministic solution by generating a less steep degradation profile. This is mainly achieved by purchasing higher quality and more expensive feeds (Figure 4.8b). In fact, the feeds of type 8-9-10, purchased only by the stochastic solution and not by the deterministic one, are associated to a low feed degradation index (IC_f) and therefore

a high price. Additionally, the stochastic feed purchasing strategy allows the plant to increase the throughput (see Figure 4.8c) compared to the deterministic production strategy. This results into a reduction of the amount of products needed to cover the demand after the failure has occurred for the uncertain RULs of the plant that are associated to the higher probabilities of realization. In fact, as shown in Figure 4.8d, even though the deterministic solution plans to cover the entire demand only by the production (without producing in the next campaign or purchasing products externally), the introduction of the uncertainty (Recourse Problem) forces the plant to satisfy the demand only in the next campaign or to drastically purchase products from external sources. The stochastic formulation (MSSP), being aware of the uncertainty, reduces the production shift to the following campaign or the amount of products that are purchased from external sources for the uncertain scenarios associated to higher probabilities. Additionally, analysing the optimal prognosis variables shown in Figure 4.9, it is interesting to highlight that the stochastic formulation sets to zero the probability of the first scenario (earliest RUL) since the degradation level at time $t = 29$ (equal to 1219 $^{\circ}C$) is lower than the prognosis threshold (1220 $^{\circ}C$). This means that the scenario corresponding to the earliest RUL does not realize along with the associated costs. Figure 4.9 compares the optimal values of the prognosis variables to the baseline values that represent the hazard and survival functions and the probabilities of the scenarios if the covariates of the Cox model (the degradation level in this work) are equal to zero. The comparison shows the important effect that the degradation level has on the probabilities of the uncertain RULs.

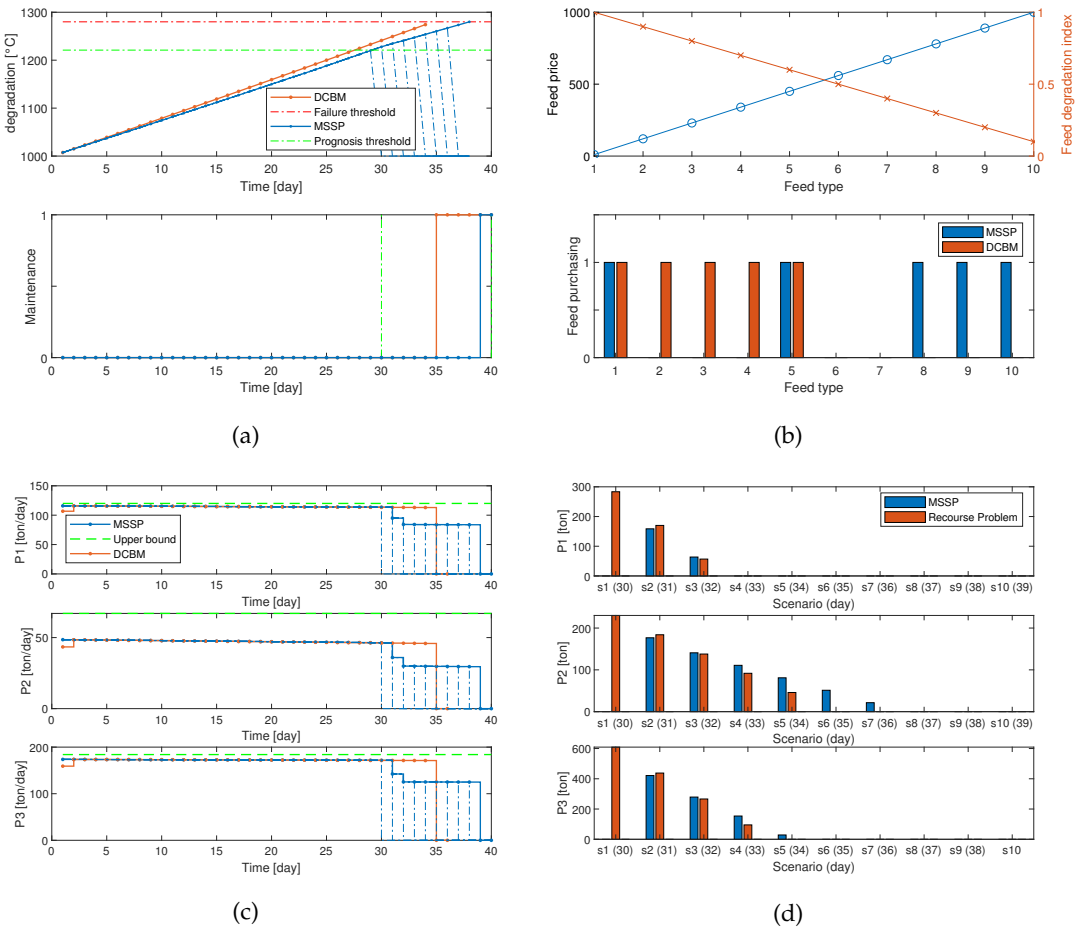

FIGURE 4.8: Results of the deterministic and stochastic optimizations: (a) degradation trajectories and timing of the maintenance, (b) feed parameters and feed purchasing strategy, (c) production profiles, (d) amount of products to be produced in the next campaign or purchased from external sources. Source: (Leo and Engell, 2021).

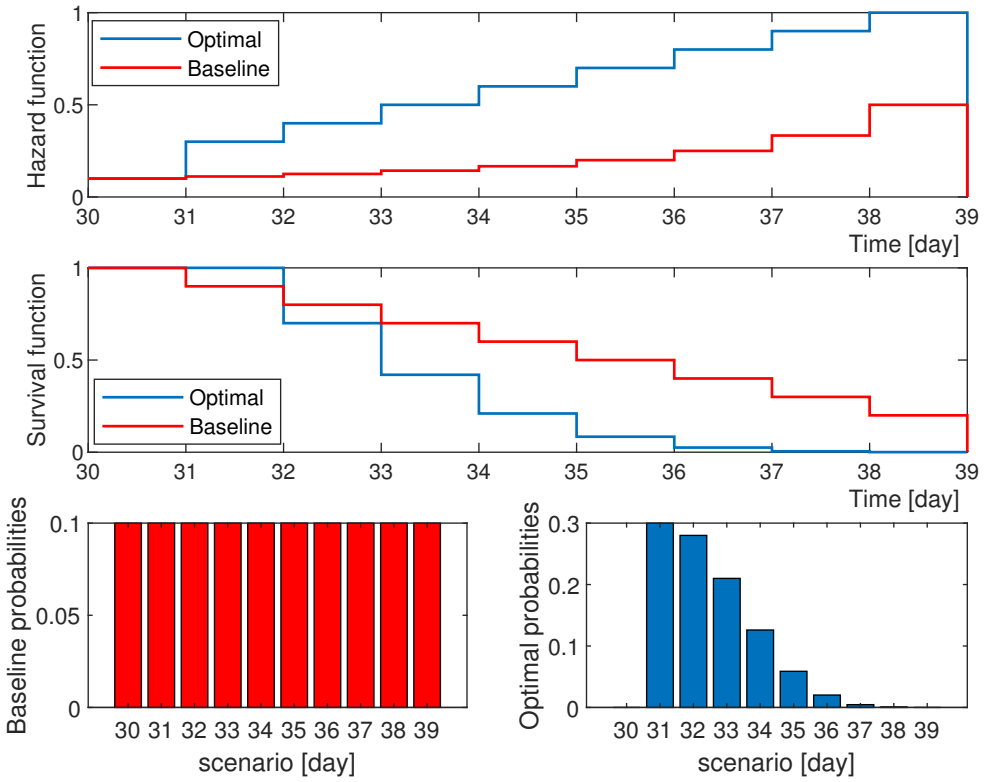

FIGURE 4.9: Optimal prognosis variables over the uncertain RULs: (top) hazard function, (middle) survival function, (bottom left) probabilities of the scenarios associated to the baseline hazard function h_s^0, (bottom right) optimal probabilities of the scenarios. Source: (Leo and Engell, 2021).

Figure 4.10 shows the trajectory of the input that influences the degradation level most (naphtha mass flow) for the stochastic and deterministic solutions and the corresponding optimal probabilities of the scenarios (only for the stochastic solution) for the different values of the product demands already introduced above (nominal, low and high). To improve the readability of this figure the scenarios associated to the uncertain RULs that realize before the maintenance activities are performed are not shown. Figure 4.10 proves the ability of the proposed stochastic formulation to exploit the synergies between plant operation, prognosis and condition-based maintenance. In fact, according to the product demands, the stochastic formulations modify the plant operation (naphtha mass flow) and the associated probabilities of the scenarios. For the case with a reduced demand and, therefore, increased production flexibility (middle in Figure 4.10) the stochastic solution significantly differs from the deterministic solution, since it is aware of the possibility to reduce the degradation level to avoid the realization of the more costly scenarios (with earlier RUL).

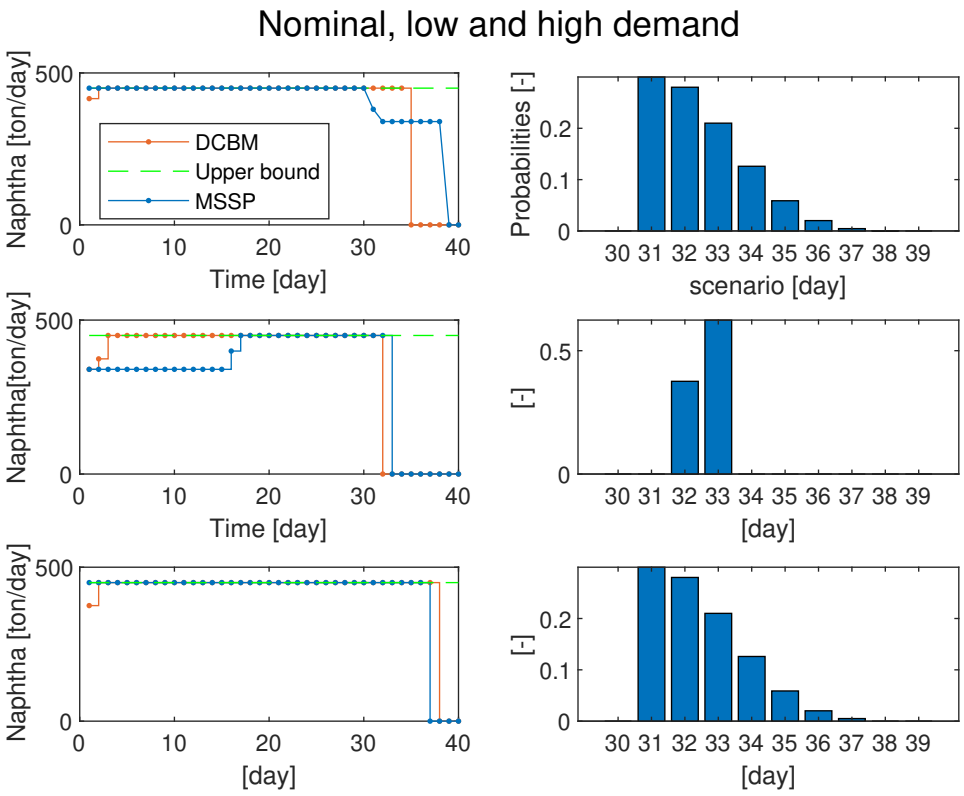

FIGURE 4.10: Stochastic and deterministic solutions for nominal demand (top), low demand (middle) and high demand (down). Source: (Leo and Engell, 2021).

4.2 Combined Type-I and Type-II endogenous uncertainties

This section is based upon

- Leo E. and Engell S., *Handling Type-I and Type-II endogenous uncertainties in simultaneous production planning and condition-based maintenance optimization in continuous production*, Computers & Chemical Engineering, volume 174, June 2023

This section extends the formulation of decision-dependent uncertainty that is presented in Section 4.1 by optimizing two production campaigns (defined as the production time between two consecutive maintenance events). The extension of the formulation to multiple production campaigns is a necessary step to perform medium-long term production planning. Considering multiple production campaigns further complicates the optimization problem not only because of the longer time horizon that must be considered but also because the timing of the realization of the uncertainty is influenced by the decision variables. In fact, according to the timing of the maintenance activities, and therefore the starting time of the production campaigns, the structure of the scenario tree can be altered and some scenarios will never realize. Additionally, as already explained in Section 4.1, the probabilities of the realizing scenarios are influenced by the degradation trajectory and the operating conditions of the plant. To model these problem features, we propose a stochastic programming formulation with endogenous uncertainty where both Type-I and Type-II features are present. A similar formulation has never been presented in the literature.

The figures and tables of this sections are adapted from (Leo and Engell, 2023).

4.2.1 Problem statement

We consider a continuous production plant with a fixed and known product demand over the planning horizon. The goal is to minimize the total production cost that consists of the cost of performing the maintenance activities, the cost of purchasing the feed, the cost of the steam and fuel consumption (also referred as resource consumption cost) and the cost of producing the products in the following campaigns or to purchase them from external sources if the demand is not satisfied by the production during the campaigns considered in this optimization. We consider the following decision variables:

- the feeds to be purchased
- the operating conditions of the plant
- the degradation trajectory of the equipment
- the amount of products to be produced in the future campaigns or to be purchased from external sources
- the starting times of the maintenance activities.

The problem statement is similar to the one described in Section 4.1.1 except for the introduction of multiple production campaigns. This difference is not trivial at all since it introduces the possibility for the decision maker to modify the timing of the realization of the uncertain parameters and, therefore, to modify the structure of the scenario-tree so that also Type-II endogenous uncertainties have to be considered.

4.2.2 Modelling of the uncertainty

In the proposed formulation, as in the one presented in Section 4.1, the discrete scenarios represent possible realizations of the uncertain failure times of the plant, i.e. uncertain predictions of the point in time when the degradation trajectory reaches the failure threshold and maintenance has to take place. Figure 4.11 shows the scenario-tree of the proposed multi-stage stochastic program (MSSP) where two production campaigns are considered and two possible realizations of the failure times for each campaign are modelled. The failure times are marked by the orange nodes, the time steps of the first production campaign by black nodes and the time steps of the second production campaign by green nodes. When the RUL is over (and therefore the degradation trajectory has reached the failure threshold), the plant must be shut down to perform the maintenance activities to restore the production operations. The proposed formulation models the uncertainty by introducing two types of endogenous uncertainties: decision-dependent probabilities (Type-I) and a decision-dependent structure of the tree (Type-II).

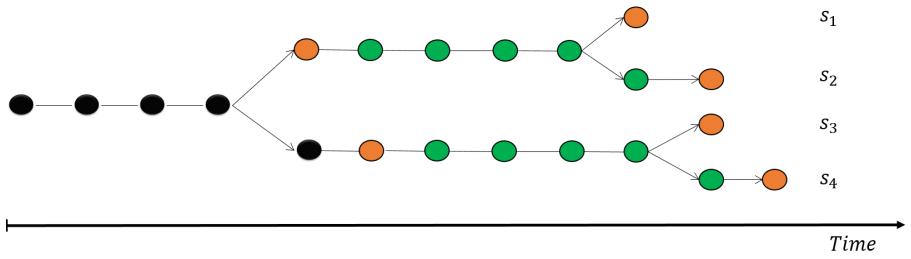

FIGURE 4.11: Multi-stage breakdown scenario-tree for two production campaigns (black and green nodes) and two uncertain failure times and maintenance intervals for each campaign (orange nodes). Source: (Leo and Engell, 2023)

Decision-dependent structure

To explain how the decisions on the timing of the maintenance activities influence the structure of the scenario-tree, Figure 4.12 shows different choices of the timing of the maintenance activities and the resulting scenario-tree. Figure 4.12 shows two production campaigns and for each campaign two uncertain scenarios (that represent the uncertain failure times). The orange nodes represent the realizations of the failures of the plant (i.e. a reactive maintenance activity takes place), while the white nodes identify the timings of the preventive maintenance activities that do not let the failures realize. When both breakdown scenarios of the first and second production campaigns can realize (see Figure 4.12a), the problem gives rise to a multi-stage tree. If the first maintenance activity takes place before the realization of the uncertain failure time of the first campaign (white node), as depicted in Figure 4.12b, the two breakdown scenarios of the first production campaign for the case without preventive maintenance will not realize and the resulting scenario-tree defines a two-stage program where only the realization of the breakdown scenarios of the second campaign can take places. Additionally, the scenarios of the second production campaign realize earlier since the timing of the maintenance activity has shortened the duration of the first production campaign. If the maintenance activity of the second production campaign take place before the realization of the breakdown scenarios of the second campaign (Figure 4.12c), none of the uncertain failures in

Figure 4.12a can realize. Figure 4.12 does not show all the possible scenario-trees but only some possible scenario-trees that realize according to the timing of the preventive maintenance activity. The full scenario-tree that includes all the possible timings for reactive maintenance (orange nodes) and predictive maintenance (white nodes) is represented in Figure 4.13.

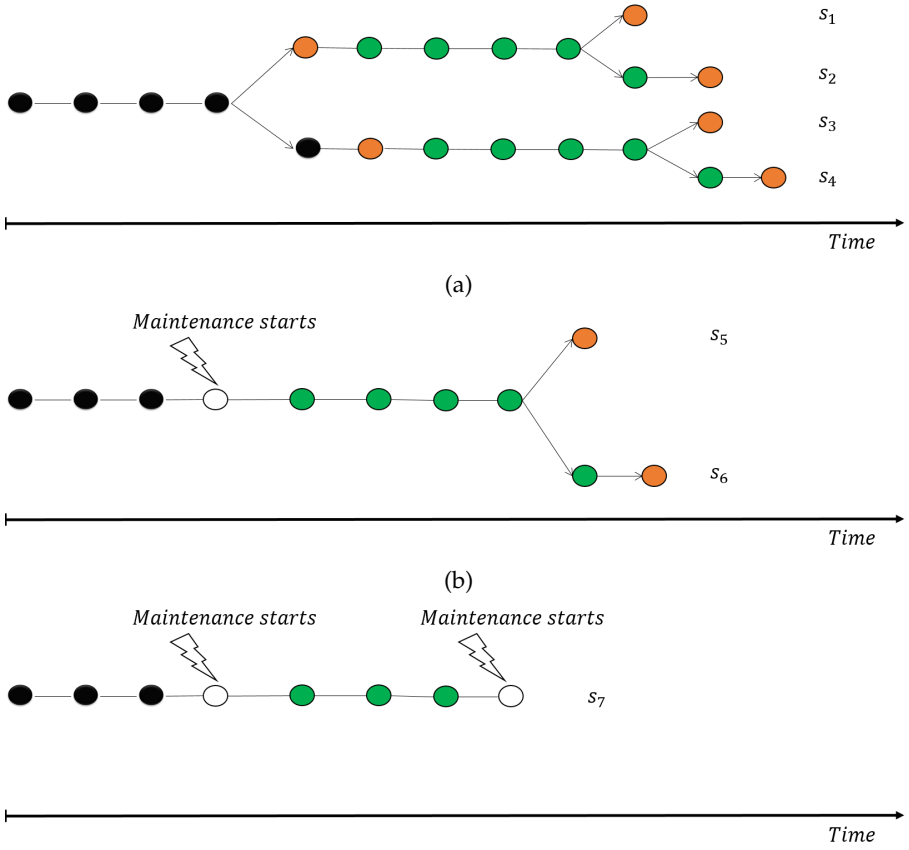

FIGURE 4.12: Influence of the timing of the maintenance activities on the structure of the scenario-tree. (a) A multi-stage tree results if the breakdown scenarios of the first and second production campaigns can realize; (b) a two-stage scenario-tree results if the first maintenance activity takes place before the branching of the scenarios of the first production campaign can realize; (c) a deterministic problem results if both the maintenance activities are performed before the branching of the scenario tree. Source: (Leo and Engell, 2023)

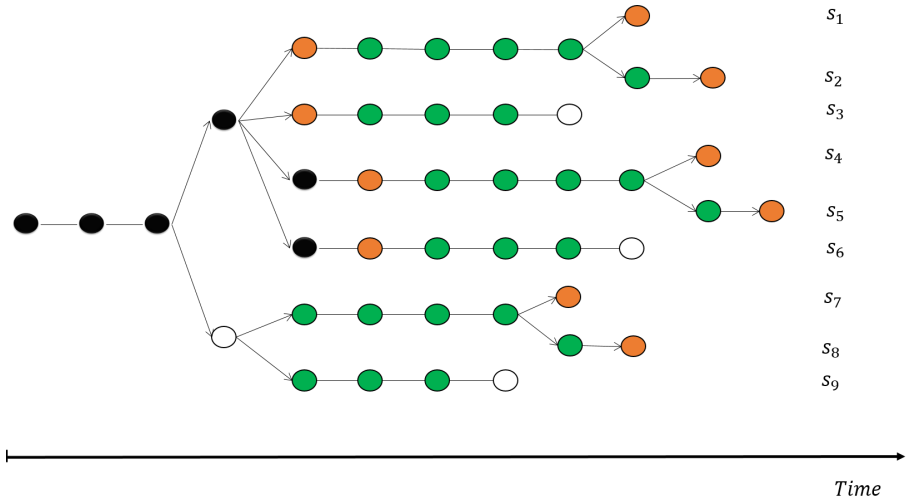

FIGURE 4.13: Full scenario-tree for the example with two production campaigns (black and green nodes) and for each campaign two uncertain scenarios: the orange nodes represent the reactive maintenance activities (i.e. the uncertain failure times realize) and the white nodes represent the predictive maintenance activities that do not let the uncertain failures realize. Source: (Leo and Engell, 2023)

From the example that is depicted in Figures 4.12-4.13, it is clear that the decision maker is able to influence the structure of the scenario-tree by acting on the timing of the maintenance activities (preventive or reactive maintenance).

4.2.3 Modelling approaches for combined Type-I and Type-II endogenous uncertainties

We propose here two modelling approaches to formulate a stochastic program that combines Type-I and Type-II endogenous uncertainties. The goal is to analyse the influence of the mathematical formulation on the computational effort needed to find the global optimum of the resulting non-convex problem.

The modelling of the Type-I endogenous uncertainty features (i.e. the dependency of the probability of the uncertainty on the decision variables) does not differ from the approach described in Section 4.1. The hazard and the survival functions of the uncertain RULs, along with the probabilities, are introduced as decision variables. The relation between the degradation levels, the plant operating conditions and the probabilities of the scenarios is described by the prognosis technique of the Cox model (Cox, 1972).

The modelling of the Type-II endogenous uncertainty features (i.e. the dependency of the structure of the scenario tree on the decision variables) is performed here adopting two approaches. The first approach creates an augmented scenario tree (that is called here superstructure scenario-tree) by combining all the possible states of the system that are defined by possible timings of the maintenance activities. The second approach implements conditional non-anticipativity constraints defined in (Apap and Grossmann, 2017) to model the scenarios that do not realize.

Superstructure scenario-tree approach

This approach builds up a superstructure tree where all the possible structures of the tree are modelled. The different structures of the tree are defined by the timing of the maintenance activities and if a structure cannot realize because of predictive maintenance, the probabilities of the corresponding scenarios are set equal to zero. This approach is, therefore, targeted to the case of combined Type-I and Type-II endogenous uncertainties since the probabilities of the scenarios are decision variables and not parameters. Considering the problem instance with two production campaigns and two uncertain breakdown scenarios per campaign that was introduced in Figures 4.12-4.13, Figure 4.14 shows the corresponding superstructure scenario-tree. Compared to the scenario-tree that is depicted in Figure 4.13, the scenario-tree in Figure 4.14 is equivalent but it does not show the scenarios that end with the (white) nodes that are associated to the preventive maintenance activities. In fact, the starting times of the preventive maintenance activities are identified by the binary variables x^{CBM} that when activated force to zero the production for the remaining time of the campaign. The scenarios $s_1, \ldots, s_4$ model the situation where the breakdown scenarios of the first and of the second production campaign can realize. The scenarios s_5, s_6 describe the case where the maintenance activity of the first production campaign takes place before the realization of the uncertain parameters and, therefore, none of the breakdown scenarios of the first production campaign can realize. As an example, Figure 4.14 shows this second case where the probabilities of the scenarios that cannot realize are set to zero.
In comparison with a standard stochastic formulation with exogenous uncertainty, this approach increases the number of scenarios that are needed to model the problem since all the possible structures of the tree must be considered. While the standard breakdown tree contains four scenarios (see Figure 4.12a), the superstructure scenario-tree needs six scenarios to integrate the features of the endogenous uncertainty.

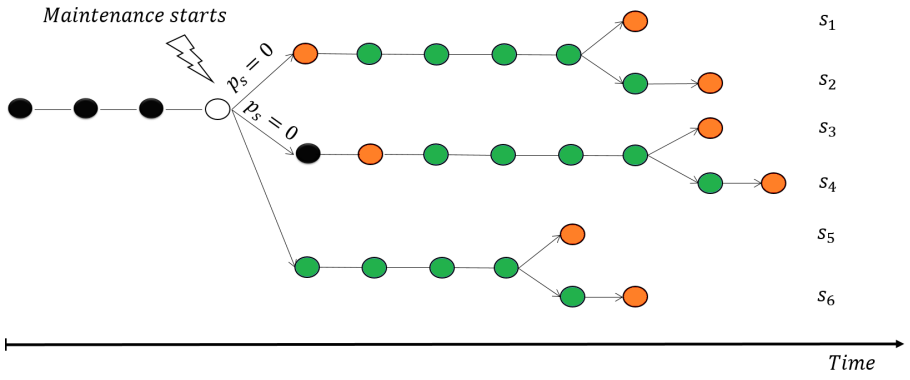

FIGURE 4.14: Superstructure scenario-tree: Subtree of the full scenario tree for the case where preventive maintenance is executed at interval four. The upper four scenarios are deactivated by setting their probabilities to zero. Source: (Leo and Engell, 2023)

Conditional non-anticipativity approach

The conditional non-anticipativity constraints (NACs) are NACs that are activated by the decision variables to render some scenarios indistinguishable by forcing the recourse variables of these scenarios to be equal to each other in case the realization of the uncertain parameters can not take place. Considering the example that was

introduced in Figure 4.12a with four possible scenarios $s_1, \ldots, s_4$, Figure 4.15 depicts the case where the scenarios of the first production campaign do not realize since the maintenance activity takes place before their realization. In this case, the scenarios that do not realize become indistinguishable as shown in Figure 4.15a. Figure 4.15b shows the equivalent scenario tree modelled via NACs. The vertical lines represent the permanent NACs, while the dash green curves the conditional NACs that are activated by the decisions on the maintenance activities. Since the maintenance activities render the two scenarios of the first campaign indistinguishable, the corresponding conditional NACs force the recourse variables of these two scenarios to be identical. In contrast to the approach that creates the superstructure scenario-tree, this method does not increase the number of scenarios to model the endogenous uncertainty in comparison to a standard formulation with exogenous uncertainty but requires a larger number of constraints (i.e. the NACs) and implicit model reformulations to represent the changes in the RUL due to the maintenance decisions.

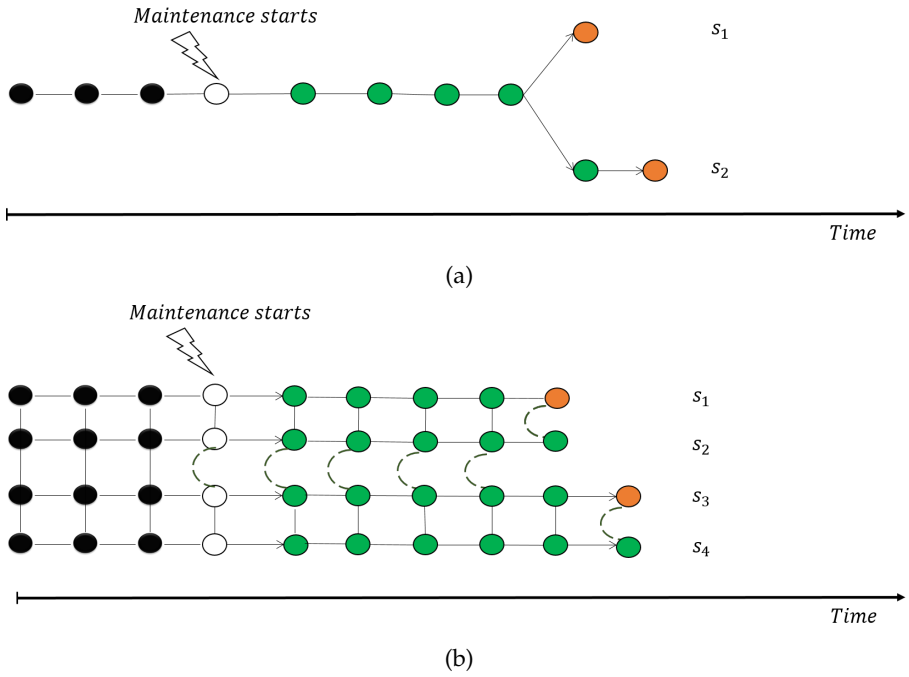

FIGURE 4.15: (a) Representation of the sub-tree that results if preventive maintenance takes place at interval four; (b) scenario-tree of the conditional NACs formulation: the vertical lines represent the permanent NACs, while the dashed green curves the conditional NACs that are activated by the decisions on the maintenance activities. Source: (Leo and Engell, 2023)

Nomenclature

Indices	
p	products
$t, t\prime$	time periods
$s, s\prime$	scenarios
i	plant inputs
f	feed
c	campaign
r	realization of the uncertainty
Sets	
P	products
T, T^{1stage}, T^{s}	time periods
I	plant input
S	scenarios
F	feed
C	campaign
$RUL_{s,c}$	uncertain Remaining Useful life
$ANC_{c,r}$	sub-set of scenarios for campaign c and uncertainty realization r
Parameters	
R_c	number of tree branching for production campaig c
D_p	demand of product p
d^0	initial degradation value
IC_f	quality parameter of feed f
d^0, d^{max}	initial and maximum degradation values
UB_f^{feed}	Maximum amount of feed f
$LB_{i,t,s}^{input}, UB_{i,t,s}^{input}$	upper and lower bounds of the plant input i at time period t and scenario s
UB_p^y	Upper bound of production rate of product p at time t and scenario s
γ_i^p	process parameters
α^i	parameter of the degradation model
M	big-M parameter
d^{CBM}	maintenance duration
$h0_s$	baseline hazard function of scenario s
$price_f^{feed}$	purchasing price of feed f
$price_p^{product}$	average cost of producing product p in the next camapign or purchasing it to satisfy the demand
$price_i^{resource}$	resource price proportional to the input i
β	parameter of the Cox model
$L_{t,c,c\prime,s\prime}^{SST}$	boolean matrix for the permanent NACs for the superstructure tree formulation
$L_{t,c,c\prime,s\prime}^{cNAC}$	boolean matrix for the permanent NACs for the conditional NACs formulation
Continuous variables	
p_s^{MSSP}	probability of scenario s
$p_{c,s}^{RUL}$	probability of scenario s for campaign c
$h_{c,s}$	hazard function of scenario s for campaign c
$S_{c,s}$	survival function of scenario s for campaign c
$cost_s, cost^{feed}$	total cost of scenario s and feed cost
$cost^{missing\ \ demand}$	cost of producing in the next campaign or purchasing products from external sources
$cost_s^{resource}, cost_s^{CBM}$	resource purchasing cost and cost of performing the maintenance activities
$y_{p,t,s,c}$	production of p purchased at time t in scenario s
$u_{i,t,s,c}$	plant input i at time t in scenario s
$PP_{p,s}$	product p to be produced in the following campaign or to be purchased to cover the demand for scenario s
$d_{t,s,c}$	degradation level at time t and scenario s
$m_{f,t,s,c}^{feed}$	amount of feed f used at time t of the campaign c for scenario s
Binary variables	
$x_{t,c,s}^{CBM}$	1 if the maintenance activities are performed at time t of the campaign c for scenario s
x_f^{feed}	1 if the feed f is purchased
$y_{f,t,s,c}^{feed}$	1 if the feed f is allocated at time t of the campaign c for scenario s
$s_{f,t,s,c}^{feed}$	1 if the allocation of the feed f starts at time t of the campaign c for scenario s
$s_{t,s,c}^{campaign}$	1 if the campaign c starts at time t for scenario s
$x_{t,s,c}^{campaign}$	1 if the campaign c is active at time t for scenario s

4.2.4 MINLP formulations

We describe here the two MINLP formulations that are obtained by applying the two proposed modelling approaches. Section 4.2.4 discusses the MINLP model that results from the application of the approach that is based on the superstructure scenario-tree, while Section 4.2.4 presents the MINLP that is generated when using conditional NACs.

MINLP formulation based on the superstructure-tree

Figure 4.16 shows the superstructure tree when two production campaigns and two uncertain failure times for each campaign are considered. The multi-stage tree presents in total six scenarios over the time horizon of 10 time intervals. While Figure 4.16a shows a depiction of the scenario-tree where the branching is visible, Figure 4.16b depicts the representation of the monolithic MINLP with NACs. The scenarios $s_1, \ldots, s_4$ are associated to the condition that the failures of the first production campaign (black nodes) realize (i.e. breakdowns and subsequent reactive maintenance take place in the first campaign), the scenarios s_5, s_6 are associated to the case where preventive maintenance takes place in interval four. Therefore, it must be modelled that the subsets of scenarios $s_1, \ldots, s_4$ and s_5, s_6 cannot both realize. This is handled by adjusting the probabilities of the scenarios depending on the decision on preventive maintenance with the subset of the prognosis constraints in Section 4.2.4. As described before, the scenarios that are associated to the realization of the predictive maintenance activities are not depicted (white scenarios in Figure 4.13) because a binary variable is introduced to define the starting times of the maintenance activities and to set to zero the production amount.

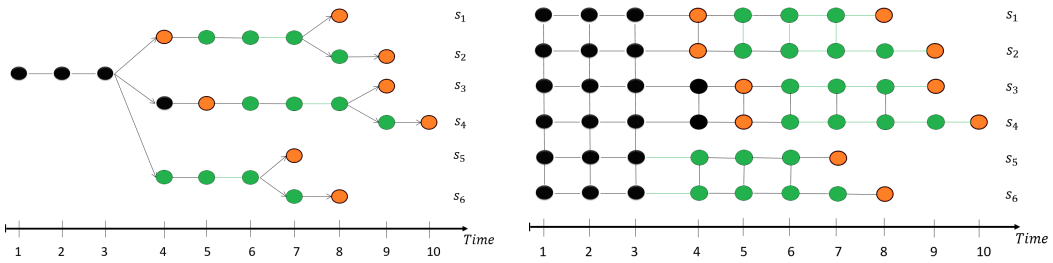

FIGURE 4.16: Two equivalent versions of the superstructure scenario-tree: (a) standard and (b) unfolded representation with NACs of the stochastic problem. Source: (Leo and Engell, 2023)

We first describe the sets and parameters that are needed to model the features of both types of endogenous uncertainties. A standard (permanent) NAC formulation is used and $s \in S$ labels the scenarios of the multi-stage tree (i.e. path of the tree from the origin to the leaf node). In Figure 4.16 the set S is defined as $S = \{s_1, s_2, s_3, s_4, s_5, s_6\}$.

In addition to the standard NAC formulation, a set of parameters that map the stages of the system is needed to adjust the probabilities of the branches of the tree since they depend on a decision variable. The parameter R_c represents the number of branches of the tree that are present in each stage. In terms of production campaign c, the parameter R_c identifies how many times the scenario-tree has a branching point

(e.g. in Figure 4.16 $R_{c=1} = 1$, $R_{c=2} = 3$).

Since for a multi-stage tree as in Figure 4.16 a scenario is defined as the path from the origin node to the leaf node, the set $ANC_{c,r}$ maps the breakdown scenarios of each campaign c to the set of multistage scenarios S according to the campaign c and the scenario r of the previous campaign. In other words, the set $ANC_{c,r}$ maps the (standard) NAC scenario tree (Figure 4.16b) to the standard scenario tree (Figure 4.16a). In Figure 4.16 the following parameters can be identified: $ANC_{c=2,r=1} = \{1, 2\}$, $ANC_{c=2,r=2} = \{3, 4\}$, $ANC_{c=2,r=3} = \{5, 6\}$. The proposed formulation requires these parameters to enforce the constraints on the probabilities of the stages of the scenario tree (e.g. for the first campaign in in Figure 4.16a the sum of the probabilities of the breakdown scenarios and the scenario that is associated to the predictive maintenance activities must be equal to one).

The set $\hat{T}_{c,r}$ identifies the interval after which the tree branches for each campaign c and each breakdown scenario of the previous campaign r (e.g. in Figure 4.16, $\hat{T}_{c=1,r=1} = 3$, $\hat{T}_{c=2,r=2} = 8$. Since the first campaign has not a previous campaign, we assume $r = 1$).

The set $FT_{c,s}$ contains the uncertain failure times of the plant for each production campaign c and breakdown scenario s. For example, the tree that is shown in Figure 4.16 is associated to the following failure times: $FT_{c=1,s=1} = 4$ and $FT_{c=2,s=1} = 8$. Since each scenario represents an uncertain realization of the failure of the plant and is associated to a maximum degradation level, we assumed that the first time steps of each production campaign cannot generate a possible failure since the degradation trajectory cannot reach the maximum threshold in such short amount of time. We assumed that the accumulation of the degradation level needs at least three time intervals to generate a failure.

Maintenance constraints

In this work, we define as production campaign the production time between two consecutive maintenance events. Therefore, the maintenance constraints define the start of the maintenance activities and the starting and ending times of the production campaigns. The binary variable $x^{CBM}_{t,s,c}$ is equal to one if the maintenance activities start at time t for scenario s and campaign c, while the variable $x^{campaign}_{t,s,c}$ is equal to one if the production campaign c is active at time t for scenario s. Eq. 4.56 states that no production campaign is active at time t if the maintenance activities are performed at time t. Eq. 4.57 enforces that the maintenance activities for the campaign c cannot start if the production campaign c has not started before. The binary variable $s^{campaign}_{t,s,c}$ defines the starting time of the production campaigns and is equal to one if the campaign c starts at time t for scenario s.

$$\sum_{c \in C} x^{campaign}_{t,s,c} \leq 1 - \sum_{c \in C} x^{CBM}_{t,s,c} \quad \forall s \in S, t \in T \tag{4.56}$$

$$x^{CBM}_{t,s,c} \leq \sum_{t\prime \in \{1,\dots,t\}} s^{campaign}_{t\prime,s,c} \quad \forall s \in S, c \in C \tag{4.57}$$

Eq. 4.58 imposes that only one production campaign c can be active at time t while Eq. 4.59 ensures that each campaign c can start only once over the time horizon T. According to Eq. 4.60, for each time step t at maximum the maintenance activities of one campaign c can be performed.

$$\sum_{c \in C} x_{t,s,c}^{campaign} \leq 1 \quad \forall t \in T, s \in S \tag{4.58}$$

$$\sum_{t \in T} s_{t,s,c}^{campaign} \leq 1 \quad \forall c \in C, s \in S \tag{4.59}$$

$$\sum_{c \in C} x_{t,s,c}^{CBM} \leq 1 \quad \forall t \in T, s \in S \tag{4.60}$$

The starting times for each campaign c are defined by Eqs. 4.61-4.62.

$$s_{t,s,c}^{campaign} \geq x_{t,s,c}^{campaign} - x_{t-1,s,c}^{campaign} \quad \forall t \in T, t \neq 1, s \in S, c \in C \tag{4.61}$$

$$s_{t,s,c}^{campaign} \leq x_{t,s,c}^{campaign} \quad \forall t \in T, s \in S, c \in C \tag{4.62}$$

Eq. 4.63 determines the initial conditions of the plant by forcing the first production campaign to start at the first time step.

$$s_{t,s,c}^{campaign} = 1 \quad \forall s \in S, t = 1, c = 1 \tag{4.63}$$

Process constraints

The plant produces three products $p \in \{P_1, P_2, P_3\}$ to cover a fixed and known product demand D_p. The plant model that is implemented by Eq. 4.64 is the result of a linearization procedure to describe the influence of the model inputs $u_{i,t,s,c}$ on the production level $y_{p,t,s,c}$ via the parameters $\gamma_{p,i}$. Note that the degradation level $d_{t,s,c}$ influences the production rate according to the parameter r_p. Eqs. 4.65-4.66 impose the upper and lower bounds to the plant inputs for the active production campaign. When the production campaign c is not active (i.e. $x_{t,c,s}^{campaign} = 0$) the input variables are forced to be zero. Eq. 4.67 sets the maximum production capacity, while Eq. 4.68 ensures that the product demand is satisfied by the production in the current campaigns ($y_{p,t,s,c}$) or by producing in the following campaign or purchasing the products from external sources ($PP_{p,s}$).

$$y_{p,t,s,c} = \sum_i \gamma_i^p * u_{i,t,s,c} - r_p * d_{t,s,c} \quad \forall t \in T, s \in S, p \in P, c \in C \tag{4.64}$$

$$u_{i,t,s,c} \leq UB_{i,t,s}^{input} * x_{t,s,c}^{campaign} \quad \forall t \in T, s \in S, i \in I, c \in C \tag{4.65}$$

$$LB_{i,t,s}^{input} * x_{t,s,c}^{campaign} \leq u_{i,t,s,c} \quad \forall t \in T, s \in S, i \in I, c \in C \tag{4.66}$$

$$y_{p,t,s,c} \leq UB_p^y * x_{t,s,c}^{campaign} \quad \forall t \in T, s \in S, p \in P, c \in C \tag{4.67}$$

$$\sum_{c\in C}\sum_{t\in T} y_{p,t,s,c} + PP_{p,s} \geq D_p \quad \forall p \in P, s \in S \tag{4.68}$$

Feed purchasing constraints

The following constraints define the feed purchasing strategy of the plant and the allocation of the feeds over the time horizon. The binary variables $x^{feed}_{f,s,c}$ are set equal to one if the feed f is purchased for scenario s in campaign c and to zero otherwise. An additional binary variable $y^{feed}_{f,t,s,c}$ becomes equal to one is the feed f is used at the time step t during the production campaign c for scenario s. Eq. 4.69 ensures that no feed is used if the maintenance activities are performed. Eqs. 4.70-4.71 define the starting time (that is identified by the binary variable $s^{feed}_{f,t,s,c}$) of the feed utilization for each feed that is purchased. The quality of the feed f (that is indicated by the parameter IC_f) influences the degradation trajectory (see Eqs. 4.75-4.76). Eq. 4.72 limits the amount of feed f that can be used over the time horizon T if the feed f is purchased ($x^{feed}_f = 1$). The continuous variable $m^{feed}_{f,t,s,c}$ models the amount of feed f used at time step t for scenario s and campaign c and the parameter UB^{feed}_f is the maximum amount of feed f that can be used over the time horizon T. If the feed f is not purchased ($x^{feed}_f = 0$), its allocation over the time horizon T is forced to be zero (Eq. 4.72). Similarly, if the feed f is not allocated to the time step t, the amount of feed used at time t is forced to be zero (Eq. 4.73). Eq. 4.74 imposes that the amount of feed used at time t is the first input of the plant model ($u_{i=1,t,s,c}$) as already described for the process constraints.

From the computational perspective It is important to highlight that the variables $y^{feed}_{f,t,s,c}$, $s^{feed}_{f,t,s,c}$, $x^{CBM}_{t,s,c}$ represent integer recourse variables.

$$\sum_{f\in F} y^{feed}_{f,t,s,c} = 1 - x^{CBM}_{t,s,c} \quad \forall t \in T, s \in S, c \in C \tag{4.69}$$

$$s^{feed}_{f,t,s,c} \geq y^{feed}_{f,t,s,c} - y^{feed}_{f,t-1,s,c} \quad \forall f \in F, s \in S, c \in C, t \in \{2,\ldots,|T|\} \tag{4.70}$$

$$s^{feed}_{f,t,s,c} \leq x^{feed}_f \quad f \in F, s \in S, c \in C, t \in T \tag{4.71}$$

$$\sum_{t\in T} m^{feed}_{f,t,s,c} \leq UB^{feed}_f * x^{feed}_f \quad f \in F, s \in S, c \in C \tag{4.72}$$

$$m^{feed}_{f,t,s,c} \leq UB^{feed}_f * y^{feed}_{f,t,s,c} \quad f \in F, t \in T, s \in S, c \in C \tag{4.73}$$

$$\sum_{f\in F} m^{feed}_{f,t,s,c} = u_{i=1,t,s,c} \quad t \in T, s \in S, c \in C \tag{4.74}$$

Degradation model

The degradation constraints implement the degradation model to predict the degradation evolution over the time horizon T. Eqs. 4.75-4.76 predict the degradation level $d_{t,s,c}$ for each scenario s and campaign c according to the previous degradation value $d_{t-1,s,c}$, the operating conditions of the plant $u_{i,t,c}$ and the feed quality that is described by the feed indicator IC_f. It is worth to highlight that the degradation prediction is extended until the RUL is over ($t < FT_{c,s}$). The degradation model parameters (α^i) that describe the influence of the plant operating conditions ($u_{i,t,s,c}$) on the degradation level must be estimated from process data. The parameter d^0 represents the initial degradation level and the threshold d^{max} represents the maximum degradation value before the failure happens (Eq. 4.77).

$$d_{t,s,c} \geq d^0 * s^{campaign}_{t,s,c} + d_{t-1,s,c} + \sum_{i \in I} \alpha^i * u_{i,t,s,c} + \sum_{f \in F} IC_f * y^{feed}_{f,t,s,c} - M * x^{campaign}_{t,s,c} \quad \forall c \in C, s \in S, t \in T, t < FT_{c,s} \tag{4.75}$$

$$d_{t,s,c} \leq d^0 * s^{campaign}_{t,s,c} + d_{t-1,s,c} + \sum_{i \in I} \alpha^i * u_{i,t,s,c} + \sum_{f \in F} IC_f * y^{feed}_{f,t,s,c} + M * x^{campaign}_{t,s,c} \quad \forall c \in C, s \in S, t \in T, t < FT_{c,s} \tag{4.76}$$

where M represent a *big-M* parameter that is set equal to the maximum degradation threshold d^{max}.

$$d_{t,s,c} \leq d^{max}(1 - x^{CBM}_{t,s,c}) \quad \forall c \in C, s \in S, t \in T \tag{4.77}$$

Non-anticipativity constraints

The NACs are the main difference between the two formulations that are proposed in this work. In fact, while the formulation that is based on the superstructure scenario-tree presents only the (standard) permanent NACs, the formulation that is based on the conditional NACs presents, in addition, the NACs that are activated by the decision variables (i.e. the conditional NACs).

For the superstructure tree formulation, Eq. 4.78 describes the permanent NACs for the continuous variables that model the production of the plant ($y_{p,t,s,c}$).

$$y_{p,t,s,c} = y_{p,t,s\prime,c} \quad \forall p \in P, (t, c, s, s\prime) \in L^{SST}_{t,c,s,s\prime} \tag{4.78}$$

The matrix $L^{SST}_{t,c,s,s\prime}$ is an appropriate matrix of Boolean parameters that describe the structure of the scenario-tree. For example, in Figure 4.16 the first three time step of the first production campaign ($c = 1$) must be identical for all the scenarios and therefore $L^{SST}_{t=\{1,2,3\},c=1,s,s\prime} = 1 \ \ \forall (s, s\prime) \in S$.

Realization of the uncertainty

The equations that model the realization of the uncertain parameters describe that the RUL of the plant is over ($t \geq FT_{c,s}$) by forcing to zero the production of the plant (Eq. 4.79). As already discussed, the set $FT_{c,s}$ represents a set of uncertain failure times of the plant for each campaign c. Since the superstructure scenario-tree formulation associates a branch of the scenario-tree to each possible branching of the tree (i.e. if the scenario s realizes or not), the modelling of the realization of the uncertain parameters results straightforwardly by forcing to zero the production of the structures of the scenario-tree that do not realize.

$$y_{p,t,s,c} = 0 \quad \forall c \in C, s \in S, p \in P, t \in T, t \geq FT_{c,s} \tag{4.79}$$

Prognosis constraints

The prognosis constraints are key for both the proposed formulations since they integrate the prognosis model within the production planning optimization. The probabilities of the failures (probabilities of the stages) $p^{FT}_{s,c}$, the hazard function $h_{s,c}$ and the survival function $S_{s,c}$ for each scenario s and campaign c are modelled as decision variables by Eq. 4.80 to integrate the Cox model. While the variables $p^{FT}_{s,c}$ represent the probability of the failure for the campaign c and scenario s (i.e. the probability of a single branch of the tree), the variables p^{MSSP}_{s} that are introduced by Eq. 4.82 identify the conditional probability of the entire path of the multi-stage tree (from the origin node to the leaf node). The conditional probabilities of the scenario s of the multi-stage tree (p^{MSSP}_{s}) are computed by Eq. 4.81 by multiplying the probabilities of the failures ($p^{FT}_{s,c}$) that belong to the same path of the scenario-tree. Eq. 4.83 forces the sum of the probabilities over the scenarios to one.

$$0 \leq p^{FT}_{s,c}, S_{c,s}, h_{c,s} \leq 1 \quad \forall c \in C, s \in S \tag{4.80}$$

$$p^{MSSP}_{s} = \prod_{c \in C} p^{FT}_{s,c} \quad \forall s \in S \tag{4.81}$$

$$0 \leq p^{MSSP}_{s} \leq 1 \quad \forall s \in S \tag{4.82}$$

$$\sum_{s \in S} p^{MSSP}_{s} = 1 \tag{4.83}$$

Eqs. 4.84-4.85 implement the relations between the probabilities of the uncertain failures and the survival variables by defining the probability of failure at time t ($p^{FT}_{s,c}$) as the change of the probability of surviving time t ($S_{s,c} - S_{s+1,c}$). Similarly, the probability of surviving time t ($S_{s,c}$) must be equal to the sum of the probabilities of failing in the future time steps.

$$p^{FT}_{s,c} = S_{s,c} - S_{s+1,c} \quad \forall c \in C, r \in R_c, s \in ANC_{c,r}, s <| \, ANC_{c,r} \, | \tag{4.84}$$

$$S_{s,c} = \sum_{s\prime > s} p^{RUL}_{s\prime,c} \quad \forall c \in C, r \in R_c, (s, s\prime) \in ANC_{c,r} \tag{4.85}$$

To balance computational complexity and model accuracy, a linearized Cox model is implemented by Eqs. 4.87-4.88. The Cox model adjusts the hazard function of the earliest uncertain failures for each production campaign according to the degradation

level reached at the time step where the tree branches ($t \in \hat{T}_{c,r}$). The earliest uncertain failure time is identified as the first element of the set $ANC_{c,r}$ ($ANC_{c,r}(1)$).
To identify the scenarios that realize we introduce a binary variables $Z_{c,s}$ that is equal to one if the failure (breakdown scenario) s of the production campaign c realizes (Eq. 4.86) or, in other words, if the production campaign c is active at the time step t when the uncertain parameters realize ($t = FT_{c,s}$) since the maintenance activities have not started earlier. It is worth to highlight that the hazard function is computed only for the scenarios that realize by implementing the big-M constraints in Eqs. 4.87-4.88.

$$Z_{c,s} = x^{campaign}_{s,c,t} \quad \forall c \in C, s \in S, t = FT_{c,s} \tag{4.86}$$

$$h_{s,c} \geq h^0_{s,c} * \beta * (d_{t,s,c} - d^{min}) - (1 - Z_{c,s}) \quad \forall c \in C, r \in R_c, s \in ANC_{c,r}(1), t \in \hat{T}_{c,r} \tag{4.87}$$

$$h_{s,c} \leq h^0_{s,c} * \beta * (d_{t,s,c} - d^{min}) + (1 - Z_{c,s}) \quad \forall c \in C, r \in R_c, s \in ANC_{c,r}(1), t \in \hat{T}_{c,r} \tag{4.88}$$

Eq. 4.89 tightens the formulation by imposing that if the scenarios of the first production campaign do not realize, the following scenarios on the same path of the multi-stage tree cannot realize.

$$Z_{c+1,s} \leq Z_{c,s} \quad \forall c = 1, s \in S \tag{4.89}$$

While the hazard function of the first scenario for each campaign is computed according to the relations in Eqs. 4.87-4.88, the hazard functions of the remaining scenarios are adjusted linearly if the scenarios realize according to Eqs. 4.90-4.91. The higher is the predicted degradation level the higher is the probability of the earlier failure time. The nominal hazard function h^0_s and the parameters β of the Cox model must be estimated from plant data (e.g. using the software MATLAB and the function `coxphfit` (*Statistics and Machine Learning Toolbox* 2006)).

$$h_{s,c} \geq h_{\bar{s},c} + \frac{1 - h_{\bar{s},c}}{N_c - 1} - (1 - Z_{c,s}) \quad \forall c \in C, r \in R_c, \bar{s} = ANC_{c,r}(1), s > \bar{s}, t \in \hat{T}_{c,r} \tag{4.90}$$

$$h_{s,c} \leq h_{\bar{s},c} + \frac{1 - h_{\bar{s},c}}{N_c - 1} + (1 - Z_{c,s}) \quad \forall c \in C, r \in R_c, , \bar{s} = ANC_{c,r}(1), s > \bar{s}, t \in \hat{T}_{c,r}, \tag{4.91}$$

The parameter N_c represents the number of breakdown scenarios for production campaign c.

Eqs. 4.92-4.93 compute the probability of the uncertain failure times that realize according to the non-linear survival relations with the hazard and survival functions.

$$p^{FT}_{s,c} \leq h_{s,c} * S_{s,c} + (1 - Z_{c,s}) \quad \forall c \in C, s \in S \tag{4.92}$$

$$p^{FT}_{s,c} \geq h_{s,c} * S_{s,c} - (1 - Z_{c,s}) \quad \forall c \in C, s \in S \tag{4.93}$$

For each production campaign c, Eqs. 4.94-4.95 impose that the sum of the probabilities of the uncertain failure times must be equal to one if the scenarios realize (i.e. if the production campaign is active at the branching time of the scenario-tree).

$$\sum_{s \in ANC_{c,r}} p^{FT}_{s,c} \geq 1 - M * (1 - x^{campaign}_{t,s\prime,c}) \quad \forall c \in C, r \in R_c, t \in \hat{T}_{c,r}, s\prime \in ANC_{c,r}(1) \tag{4.94}$$

$$\sum_{s \in ANC_{c,r}} p^{FT}_{s,c} \leq 1 + M * (1 - x^{campaign}_{t,s\prime,c}) \quad \forall c \in C, r \in R_c, t \in \hat{T}_{c,r}, s\prime \in ANC_{c,r}(1) \tag{4.95}$$

For the superstructure tree formulation, the probabilities of the scenarios that do not realize must be set to zero (Eqs. 4.96-4.97). The subset of scenarios $\hat{S} = \{s_1, s_2, s_3, s_4\}$ are associated to the condition that the scenarios of the first production campaign realize (i.e. if the first production campaign is active at the time step when the tree branches). The subset $\tilde{S} = \{s_5, s_6\}$ represents the structure of the scenario-tree that is associated to the opposite condition. For Eq. 4.96, if the variable $Z_{c,s}$ is equal to zero for the breakdown scenario s in campaign c (i.e. the breakdown scenario does not realize), the probability of the breakdown scenario s in campaign c is set to zero. The opposite condition is implemented in Eq. 4.97.

$$p^{FT}_{s,c} \leq Z_{c,s} \quad \forall c \in C, s \in \hat{S} \tag{4.96}$$

$$p^{FT}_{s,c} \leq 1 - Z_{c,s} \quad \forall c = 2, s \in \tilde{S} \tag{4.97}$$

A special consideration must be reserved to the scenarios of the last campaign (second in this example, but it would be valid for an arbitrary number of production campaigns). In fact, if all the scenarios of the last campaign do not realize, setting to zero their probabilities ($p^{FT}_{s,c}$) implies that the conditional probability of the entire path of the tree (p^{MSSP}_s) becomes zero erroneously computing an expected cost equal to zero (see definition of the expected cost in Eq. 4.103 that multiplies the cost of scenario $cost_s$ and the probability of the path of the tree p^{MSSP}_s). To avoid this issue, if all the scenarios of the last campaign do not realize, we impose that the probability of the first of these scenarios is equal to one and all the remaining probabilities are set to zero (Eqs. 4.98-4.99). Eqs. 4.98-4.99 implement this condition for the last production campaign ($c = 2$) according to the value of the binary variable $x^{campaign}_{t,s,c}$ at the time step where the tree branches ($t \in \hat{T}_{c,r}$): if the production campaign is not active when the tree branches, none of the scenarios will realize.

$$p^{FT}_{s,c} \geq 1 - x^{campaign}_{t,s,c} \quad \forall c = 2, r \in R_c, s = ANC_{c,r}(1), t \in \hat{T}_{c,r} \tag{4.98}$$

$$p^{FT}_{s,c} \leq x^{campaign}_{t,s,c} \quad \forall c = 2, r \in R_c, s \in ANC_{s,r}, s \neq ANC_{c,r}(1), t \in \hat{T}_{c,r} \tag{4.99}$$

Note that since the probabilities of the failure times are dependent on decision variables they are subject to the (standard) NACs. For the scenario-tree in Figure 4.16, the NACs in Eqs. 4.100-4.102 must be introduced for the probabilities of the RULs. Similar equations must be enforced for the hazard and survival variables.

$$p^{FT}_{s,c} = p^{FT}_{s\prime,c} \quad \forall s = 1, s\prime = 2, c = 1 \tag{4.100}$$

$$p^{FT}_{s,c} = p^{FT}_{s\prime,c} \quad \forall s = 3, s\prime = 4, c = 1 \tag{4.101}$$

$$p^{FT}_{s,c} = p^{FT}_{s\prime,c} \quad \forall s = 5, s\prime = 6, c = 1 \tag{4.102}$$

Objective function

The objective function computes the total plant cost that is defined by Eq. 4.103 as the sum of the first-stage cost, i.e. the cost of purchasing the feed ($cost^{1stage}$), and the expected cost over the scenarios s. The first-stage cost is determined by Eq. 4.104.

$$\min z = cost^{1stage} + \sum_{s \in S} p_s^{MSSP} * cost_s \tag{4.103}$$

$$cost^{1stage} = \sum_{f \in F} price_f^{feed} * x_f^{feed} \tag{4.104}$$

According to Eq. 4.105, the costs of the scenarios ($cost_s$) consist of the cost of the resource utilization ($cost_s^{resource}$), the cost of performing the maintenance activities ($cost_s^{CBM}$), and the cost of producing the products in the following campaigns or purchasing them from external sources ($cost_s^{missing\ demand}$) to cover the demand (Eq. 4.107). The cost of the resource utilization (e.g. steam and fuel gas) is defined by Eq. 4.106 and is assumed proportional to the inputs of the plant $u_{i,t,s,c}$ according to the parameter $price_i^{resource}$.

$$cost_s = cost_s^{missing\ demand} + cost_s^{resource} + cost_s^{CBM} \quad \forall s \in S \tag{4.105}$$

$$cost_s^{resource} = \sum_{c \in C} \sum_{t \in T} \sum_{i \in I} price_i^{resource} * u_{i,t,s,c} \quad \forall s \in S \tag{4.106}$$

$$cost_s^{missing\ demand} = \sum_{p \in P} price_p^{product} * PP_{p,s} \quad \forall s \in S \tag{4.107}$$

$$cost_s^{CBM} = c^{CBM} * \sum_{c \in C} \sum_{t \in T} x_{t,s,c}^{CBM} \quad \forall s \in S \tag{4.108}$$

MINLP formulation based on conditional NACs

The formulation that is based on the conditional NACs needs a smaller number of scenarios in comparison to the formulation that is based on the superstructure scenario-tree. Considering the problem instance with two uncertain failure times for each production campaign, the superstructure scenario-tree consists of six scenarios (Figure 4.16) while the scenario-tree with conditional NACs needs only four scenarios (Figure 4.17).

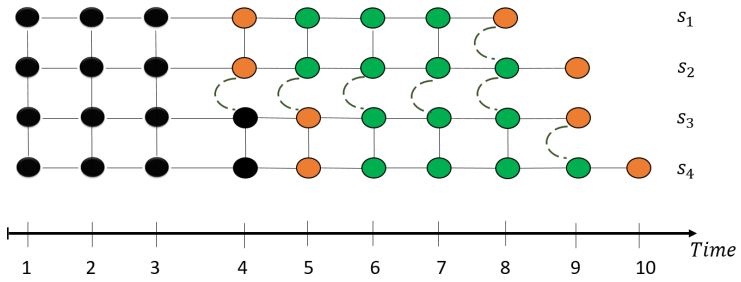

FIGURE 4.17: Scenario-tree of the formulation based on the conditional NACs for the example with two uncertain failure times for each of the two production campaigns: non-anticipativity representations of the stochastic program. Source: (Leo and Engell, 2023)

The vertical lines in Figure 4.17 represent the permanent NACs while the dashed ones identify the conditional NACs that are activated by the variables that identify the maintenance activities. The activation of the conditional NACs enforces that the scenarios that are linked by the conditional NACs are indistinguishable since the associated recourse variables are forced to be identical. As an example, in Figure 4.17 if the maintenance activities of the second production campaign for the scenarios s_1 and s_2 are started before the realization of the uncertain failures, the conditional NACs are activated to render indistinguishable the two scenarios since the uncertain failures cannot happen. Similarly, for the first production campaign the binary variable $x^{campaign}_{t=3,s,c=1}$ defines whether the first production campaign ($c = 1$) is active at the point in time when the tree branches ($t = 3$). In fact, if the first production campaign is not active at the branching time, the conditional NACs must be activated since the first two uncertain failures (orange nodes at time $t = 4$ and $t = 5$) cannot realize. Moreover, in this formulation the activation of the conditional NACs shifts the realization of the uncertainties of the following campaigns to earlier points in time.
The degradation level influences the probabilities of the realizations of the failures according to the Cox Model. For the sake of readability, we define with K the variable that identifies if the first production campaign is active when the tree branches (Eq. 4.109). Note that this is a first stage variable and therefore equal for all the scenarios.

$$K = x^{campaign}_{t,s,c} \quad s \in S, t = 3, c = 1 \tag{4.109}$$

It is worth to highlight that when the second campaign is not active at the branching time, the corresponding recourse variables are set to zero and, therefore, equal to each other, since no further production campaign is considered.

The sets and parameters that were introduced for the formulation based on the superstructure tree to model the features of both types of endogenous uncertainties are adopted also for the formulation based on the conditional NACs. In Figure 4.17 the set of scenarios S is defined as $S = \{s_1, s_2, s_3, s_4\}$. The set $FT_{c,s}$ contains the uncertain failure times of the plant for each production campaign c and breakdown scenario s. For example, the tree shown in Figure 4.17 is associated to the following failure times for the first scenario: $FT_{c=1,s=1} = 4$ and $FT_{c=2,s=1} = 8$. To keep track of the stages, the parameter R_c represents the number of times the scenario tree branches for production campaign c ($R_{c=1} = 1$, $R_{c=2} = 2$) and the set $ANC_{c,r}$ associates the multistage scenario set S to the breakdown scenarios of campaign c and

scenario r of the previous campaign ($ANC_{c=2,r=1} = \{1,2\}$, $ANC_{c=2,r=2} = \{3,4\}$). The set $\hat{T}_{c,r}$ identifies the point in time where the tree branches ($\hat{T}_{c=1,r=1} = 3$, $\hat{T}_{c=2,r=2} = 8$).

The maintenance constraints (Eqs. 4.56-4.63), the process constraints (Eqs. 4.64-4.68), the feed purchasing constraints (Eqs. 4.69-4.71), and the definition of the objective function (Eqs. 4.103-4.107) of the conditional NACs formulation are in common with the superstructure tree model that is described in Section 4.2.4.

Realization of the uncertainty

As previously described, the uncertain failures realize if the production campaign is active when the scenario-tree branches. If the scenarios realize, the uncertain failures realize and the production rate of the plant (that is identified by the continuous variables $y_{p,t,s,c}$) is set to zero (see Eqs. 4.110-4.111). The binary variables $x^{campaign}_{t,s,c}$ identify if the production campaign c is active at the branching time $t \in \hat{T}_{c,r}$.

$$y_{p,t,s,c} \geq -UB^{y}_{p} * (1 - x^{campaign}_{t\prime,s,c}) \quad s \in S, p \in P, c \in C, t \geq FT_{c,s}, r \in R_c, t\prime \in \hat{T}_{c,r} \tag{4.110}$$

$$y_{p,t,s,c} \leq +UB^{y}_{p} * (1 - x^{campaign}_{t\prime,s,c}) \quad s \in S, p \in P, c \in C, t \geq FT_{c,s}, r \in R_c, t\prime \in \hat{T}_{c,r} \tag{4.111}$$

The parameter UB^{y}_{p} represents the big-M parameter that is set equal to the maximum production capacity for the product p.
If the maintenance activities of the first production campaign c start before the realization of the uncertain failures (in other words if the production campaign is not active when the tree branches), the timing of the realizations of the uncertain failures of the following campaign $c+1$ must be modified. Since the time is not a decision variable in a discrete-time formulation, a shifted set of uncertain failures ($\overline{FT}_{c,s}$) is used to implement this feature. Eqs. 4.112-4.113 impose the shifted realizations of the uncertainties. In this work, because of the nature of the source of the uncertainty, the realization of the uncertain parameters can only be shifted to the left and not postponed.

$$y_{p,t,s,c} \geq -UB^{y}_{p} * K \quad \forall s \in S, c = 2, p \in P, t \geq \overline{FT}_{c,s} \tag{4.112}$$

$$y_{p,t,s,c} \leq +UB^{y}_{p} * K \quad \forall s \in S, c = 2, p \in P, t \geq \overline{FT}_{c,s} \tag{4.113}$$

Degradation model

The idea of the degradation model does not change compared to the one that is implemented for the formulation that is based on the superstructure scenario-tree. However, its implementation must consider the possible shift of the realization of the uncertain parameters. Eqs. 4.114-4.115 implement the degradation model (that is already described in the previous section) if the first production campaign is active at the branching time of the scenario-tree ($K = 1$). This condition is implemented with a big-M formulation and the big-M parameter d^{max} that represents the maximum

degradation level.

$$d_{t,s,c} \geq d^0 * s^{campaign}_{t,s,c} + d_{t-1,s,c} + \sum_{i \in I} \alpha^i * u_{i,t,s} + \sum_{f \in F} IC_f * y^{feed}_{f,t,s,c} - d^{max} * (2 - x^{campaign}_{t,s,c} - K) \quad \forall c \in C, s \in S, t \in T, t < FT_{s,c} \quad (4.114)$$

$$d_{t,s,c} \leq d^0 * s^{campaign}_{t,s,c} + d_{t-1,s,c} + \sum_{i \in I} \alpha^i * u_{i,t,s} + \sum_{f \in F} IC_f * y^{feed}_{f,t,s,c} + d^{max} * (2 - x^{campaign}_{t,s,c} - K) \quad \forall c \in C, s \in S, t \in T, t < FT_{s,c} \quad (4.115)$$

Eqs. 4.116-4.117 compute the degradation trajectories if the first production campaign is not active at the branching time of the scenario-tree ($K = 0$) and, therefore, considering a shifted set of uncertain failures ($\overline{FT}_{c,s}$). Note that the set of constraints is enforced only for the second production campaign ($c = 2$) where the scenarios might be shifted, in contrast to the scenarios of the first production campaign.

$$d_{t,s,c} \geq d^0 * s^{campaign}_{t,s,c} + d_{t-1,s,c} + \sum_{i \in I} \alpha^i * u_{i,t,s} + \sum_{f \in F} IC_f * y^{feed}_{f,t,s,c} - d^{max} * (1 - x^{campaign}_{t,s,c} + K) \quad \forall c = 2, s \in S, t \in T, t < \overline{FT}_{s,c} \quad (4.116)$$

$$d_{t,s,c} \leq d^0 * s^{campaign}_{t,s,c} + d_{t-1,s,c} + \sum_{i \in I} \alpha^i * u_{i,t,s} + \sum_{f \in F} IC_f * y^{feed}_{f,t,s,c} + d^{max} * (1 - x^{campaign}_{t,s,c} + K) \quad \forall c = 2, s \in S, t \in T, t < \overline{FT}_{s,c} \quad (4.117)$$

Eq. 4.77 that is already introduced in Section 4.2.4 to impose the maximum degradation level must also be enforced for the formulation that is based on the conditional NACs.

Non-anticipativity constraints

The permanent NACs for the formulation that is based on the conditional NACs are described by Eq. 4.118. The matrix $L^{cNAC}_{t,c,c\prime,s\prime}$ describes the scenario-tree that is shown in Figure 4.17.

$$y_{p,t,s,c} = y_{p,t,s\prime,c} \quad \forall p \in P, (t, c, s, s\prime) \in L^{cNACs}_{t,c,s,s\prime} \quad (4.118)$$

Additionally, this formulation has to include the NACs that are activated by the decision variables to render some scenarios indistinguishable. The conditional NACs are described by Eqs. 4.119-4.120 for the variables $y_{p,t,c,s}$ (that model the production levels of the plant).

$$y_{p,t,s,c} \leq y_{p,t,s\prime,c} + UB^y_p * K \quad \forall p \in P, c = 2, (s, s\prime) \in L^{cNACs}_{t,c,s,s\prime}, s\prime > s \quad (4.119)$$

$$y_{p,t,s,c} \geq y_{p,t,s\prime,c} - UB^y_p * K \quad \forall p \in P, c = 2, (s, s\prime) \in L^{cNACs}_{t,c,s,s\prime}, s\prime > s \quad (4.120)$$

The parameter UB_p^y represents a *big-M* parameter to render the constraints redundant in case the condition that is expressed by the binary variable K is not fulfilled. The idea behind the conditional NACs is to force the recourse variables of the scenarios that do not realize ($K = 0$) to be identical. For example, if the first production campaign is not active at the point in time when the realizations of the failures take place since the maintenance activities have started before the bifurcation of the scenario-tree ($x^{campaign}_{t=3,s\in\{1,2,3,4\},c=1} = 0$ and $K = 0$), the recourse variables of the following campaign are forced to be identical, since the uncertain RULs do not realize. The conditional NACs are not applied to the prognosis variables (hazard, survival and probabilities of the uncertain RULs).

Prognosis constraints

Eqs. 4.80, 4.82, 4.83, 4.84, 4.85 that were described in Section 4.2.4 are enforced also for the this formulation. They introduce the probabilities of the scenarios, the hazard functions and the survival functions as decision variables. Eqs. 4.121-4.122 implement the Cox model computing the hazard variables of the earlier failure times of each campaign if both the campaigns are active at their branching times. The earliest uncertain failure time for the campaign c is identified as the first element of the set $ANC_{c,r}$ ($ANC_{c,r}(1)$). The term $(c - \sum_{c\prime\in\{1,\dots,c\}} x^{campaign}_{t,s,c\prime})$ implements the condition that all the campaigns from the first one until campaign c are active at their branching times to enforce the constraints. In fact, if the first production campaign is not active at the branching time of the scenario-tree, the failures of the second campaign are shifted and computed according to the degradation level that is reached at a shifted point in time.

$$h_{s,c} \geq h^0_{s,c} * \beta * (d_{t,s,c} - d^{min}) - (c - \sum_{c\prime\in\{1,\dots,c\}} x^{campaign}_{t,s,c\prime}) \quad \forall c \in C, r \in R_c, s \in ANC_{c,r}(1), t \in \hat{T}_{c,r} \tag{4.121}$$

$$h_{s,c} \leq h^0_{s,c} * \beta * (d_{t,s,c} - d^{min}) + (c - \sum_{c\prime\in\{1,\dots,c\}} x^{campaign}_{t,s,c\prime}) \quad \forall c \in C, r \in R_c, s \in ANC_{c,r}(1), t \in \hat{T}_{c,r} \tag{4.122}$$

Eqs. 4.123-4.124 adjust linearly the hazard functions of the remaining scenarios. The parameter N_c indicates the number of scenarios for production campaign c.

$$h_{s,c} \geq h_{s=1,c} + \frac{1 - h_{s=1,c}}{N_c - 1} - (c - \sum_{c\prime\in\{1,\dots,c\}} x^{campaign}_{t,s,c\prime}) \quad \forall c \in C, r \in R_c, s \notin ANC_{c,r}(1), t \in \hat{T}_{c,r} \tag{4.123}$$

$$h_{s,c} \leq h_{s=1,c} + \frac{1 - h_{s=1,c}}{N_c - 1} + (c - \sum_{c\prime \in \{1,\ldots,c\}} x^{campaign}_{t,s,c\prime}) \quad \forall c \in C, r \in R_c, \notin ANC_{c,r}(1), t \in \hat{T}_{c,r} \quad (4.124)$$

If the first production campaign is not active at the branching time ($K = 0$), Eqs. 4.125-4.128 implement the Cox model for the shifted uncertain failure times of the second production campaign ($c = 2$) if the production campaign is active (by using the shifted sets $\overline{ANC}_{c,r}$ and $\overline{\hat{T}}_{c,r}$). Eqs. 4.121-4.124 and 4.125-4.128 implement the same constraints for two different sets of uncertain failure times.

$$h_{s,c} \geq h^0_{s,c} * \beta * (d_{t,s,c} - d^{min}) - (1 - x^{campaign}_{t,s\prime,c} + K) \quad \forall c = 2, r \in R_c, s \in \overline{ANC}_{c,r}(1), t \in \overline{\hat{T}}_{c,r} \quad (4.125)$$

$$h_{s,c} \leq h^0_{s,c} * \beta * (d_{t,s,c} - d^{min}) + (1 - x^{campaign}_{t,s\prime,c} + K) \quad \forall c = 2, r \in R_c, s \in \overline{ANC}_{c,r}(1), t \in \overline{\hat{T}}_{c,r} \quad (4.126)$$

$$h_{s,c} \geq h_{s=1,c} + \frac{1 - h_{s=1,c}}{N_c - 1} - (1 - x^{campaign}_{t,s\prime,c} + K) \quad \forall c = 2, r \in R_c, s \notin \overline{ANC}_{c,r}(1), t \in \overline{\hat{T}}_{c,r} \quad (4.127)$$

$$h_{s,c} \leq h_{s=1,c} + \frac{1 - h_{s=1,c}}{N_c - 1} + (1 - x^{campaign}_{t,s\prime,c} + K) \quad \forall c = 2, r \in R_c, \notin \overline{ANC}_{c,r}(1), t \in \overline{\hat{T}}_{c,r} \quad (4.128)$$

Eqs. 4.129-4.130 compute the probabilities of the scenarios that realize. To identify the scenarios that realize, Eqs. 4.129-4.130 use the variables $x^{CBM}_{t,s,c}$ since the production campaign might be active at the branching time but the maintenance activities might start before the realization of the uncertain parameter (e.g. at $\hat{t} = FT_{c,s} - 1$ and $\hat{t} > \hat{T}_{c,r}$).

$$p^{FT}_{s,c} \leq h_{s,c} * S_{s,c} + (1 - K + x^{CBM}_{t,s,c}) \quad \forall c \in C, s \in S, t \in FT_{c,s} - 1 \quad (4.129)$$

$$p^{FT}_{s,c} \geq h_{s,c} * S_{s,c} - (1 - K + x^{CBM}_{t,s,c}) \quad \forall c \in C, s \in S, t \in FT_{c,s} - 1 \quad (4.130)$$

Eqs. 4.131-4.132 compute the probabilities of the shifted breakdown scenarios according to the hazard and survival functions.

$$p^{FT}_{s,c} \leq h_{s,c} * S_{s,c} + (K + x^{CBM}_{t,s,c}) \quad \forall c = 2, s \in S, t \in \overline{FT}_{c,s} - 1 \quad (4.131)$$

$$p^{FT}_{s,c} \geq h_{s,c} * S_{s,c} - (K + x^{CBM}_{t,s,c}) \quad \forall c = 2, s \in S, t \in \overline{FT}_{c,s} - 1 \quad (4.132)$$

Eqs. 4.133-4.134 force to one the sum of the probabilities of the uncertain failures for each production campaign. For the second production campaign, the sum of the probabilities is enforced only if both the campaigns are active at their branching times. This condition is again enforced with the big-M term $(c - \sum_{c\prime \in \{1,\dots,c\}} x^{campaign}_{t,s\prime,c\prime})$.

$$\sum_{s \in ANC_{c,r}} p^{RUL}_{s,c} \geq 1 - (c - \sum_{c\prime \in \{1,\dots,c\}} x^{campaign}_{t,s\prime,c\prime}) \quad \forall c \in C, r \in R_c, t \in \hat{T}_{c,r}, s\prime \in ANC_{c,r}(1) \tag{4.133}$$

$$\sum_{s \in ANC_{c,r}} p^{RUL}_{s,c} \leq 1 + (c - \sum_{c\prime \in \{1,\dots,c\}} x^{campaign}_{t,s\prime,c\prime}) \quad \forall c \in C, r \in R_c, t \in \hat{T}_{c,r}, s\prime \in ANC_{c,r}(1) \tag{4.134}$$

Eqs. 4.135-4.136 force the sum of the probabilities of the uncertain failures that are shifted to be equal to one if the breakdown scenarios realize. This condition is implemented with the term $(1 - x^{campaign}_{t,s\prime,c} + K)$.

$$\sum_{s \in \overline{ANC}_{c,r}} p^{FT}_{s,c} \geq 1 - (1 - x^{campaign}_{t,s\prime,c} + K) \quad \forall c = 2, r \in R_c, t = \hat{\bar{T}}_{c,r}, s\prime \in \overline{ANC}_{c,r}(1) \tag{4.135}$$

$$\sum_{s \in \overline{ANC}_{c,r}} p^{FT}_{s,c} \leq 1 + (1 - x^{campaign}_{t,s\prime,c} + K) \quad \forall c = 2, r \in R_c, t = \hat{\bar{T}}_{c,r}, s\prime \in \overline{ANC}_{c,r}(1) \tag{4.136}$$

The scenarios that do not realize are associated to probabilities that are equal to zero. As described later by Eqs. 4.143-4.144, the conditional probability of a path of the multi-stage tree is the product of the probabilities of the branches of the tree along the path. Therefore, to avoid a conditional probability equal to zero, if all the scenarios of the first production campaign do not realize their probabilities cannot be all set to zero. In this case, Eq. 4.137-4.138 force to one the probability of the first uncertain breakdown scenario or in other words of the first failure ($s \in ANC_{c,r}(1)$) and to zero the remaining ones ($s \in ANC_{c,r}, s \notin ANC_{c,r}(1)$).

$$p^{FT}_{s,c} \geq 1 - x^{campaign}_{t,s,c} \quad \forall c = 1, r \in R_c, s \in ANC_{c,r}(1), t \in FT_{c,s} - 1 \tag{4.137}$$

$$p^{FT}_{s,c} \leq x^{campaign}_{t,s,c} \quad \forall c = 1, r \in R_c, s \in ANC_{c,r}, s \notin ANC_{c,r}(1), t \in FT_{c,s} - 1 \tag{4.138}$$

Similarly, for the second campaign Eqs. 4.139-4.142 force to one the probability of the earliest failure and to zero the remaining ones if all the scenarios of the campaign do not realize. In particular, Eqs. 4.139-4.140 cover the case where the scenarios of the first campaign realize ($K = 1$) and Eqs. 4.141-4.142 consider the shifted set of failure times ($\overline{FT}_{c,s}$) in case the first campaign is not active at the branching time of

the scenario-tree ($K = 0$).

$$p^{FT}_{s,c} \geq 1 - x^{campaign}_{t,s,c} - (1-K) \quad \forall c = 2, r \in R_c, s \in ANC(1), t \in FT_{c,s} - 1 \tag{4.139}$$

$$p^{FT}_{s,c} \leq x^{campaign}_{t,s,c} + (1-K) \quad \forall c = 2, r \in R_c, s \in ANC, s \notin ANC(1), t \in FT_{c,s} - 1 \tag{4.140}$$

$$p^{FT}_{s,c} \geq 1 - x^{campaign}_{t,s,c} - K \quad \forall c = 2, r \in R_c, s \in ANC(1), t \in \overline{FT}_{c,s} - 1 \tag{4.141}$$

$$p^{FT}_{s,c} \leq x^{campaign}_{t,s,c} + K \quad \forall c = 2, r \in R_c, s \in ANC, s \notin ANC(1), t \in \overline{FT}_{c,s} - 1 \tag{4.142}$$

Eqs. 4.143-4.146 compute the conditional probabilities of the multi-stage scenario-tree by multiplying the probabilities of the nodes along the path of the scenario tree. The computation of the conditional probabilities is influenced by the structure of the scenario-tree and, therefore, by the variable K. If the first production campaign is not active at the branching time of the scenario-tree ($K = 0$), the conditional probability of the multi-stage tree considers only the first scenario of the first production campaign ($s\prime \in ANS_{c,r}(1)$) since it is associated to a probability equal to one (Eqs. 4.145-4.146).

$$p^{MSSP}_{s} \leq \prod_{c \in C} p^{FT}_{s,c} + (1-K) \quad \forall s \in S \tag{4.143}$$

$$p^{MSSP}_{s} \geq \prod_{c \in C} p^{FT}_{s,c} - (1-K) \quad \forall s \in S \tag{4.144}$$

$$p^{MSSP}_{s} \leq p^{FT}_{s\prime,c} * p^{FT}_{s,c+1} + K \quad \forall c = 1, r \in R_c, s \in S, s\prime \in ANS_{c,r}(1) \tag{4.145}$$

$$p^{MSSP}_{s} \geq p^{FT}_{s\prime,c} * p^{FT}_{s,c+1} - K \quad \forall c = 1, r \in R_c, s \in S, s\prime \in ANS_{c,r}(1) \tag{4.146}$$

4.2.5 Extension to multiple production campaigns

The extension of the proposed formulations to several production campaigns is a necessary step to apply a moving horizon strategy that can enable the solution of large-scale industrial problems. As discussed later in Chapter 5, we foresee a minimum of three production campaigns for the application of the moving horizon strategy in order to take into account the effect of the decisions of the current campaign on the following one without the influence of the terminal costs. The extension of both formulations to multiple production campaigns is straightforward and does not require major modifications of the mathematical models that have been presented.

For the superstructure tree formulation, Figure 4.18 depicts the scenario-tree with three production campaigns and two uncertain failures per campaign. We highlight once again that the white nodes that in Figure 4.13 represent the preventive maintenance actions are not included in the scenario-tree in Figure 4.18 since they are modelled by the decisions variables x^{CBM}. The adjustment of the sets and parameters (S, R_c, $ANC_{c,r}$, $\hat{T}_{c,r}$, $FT_{c,s}$) that are described in Section 4.2.4 to the new scenario-tree is the only modification needed to apply the proposed mathematical formulation to several production campaigns.

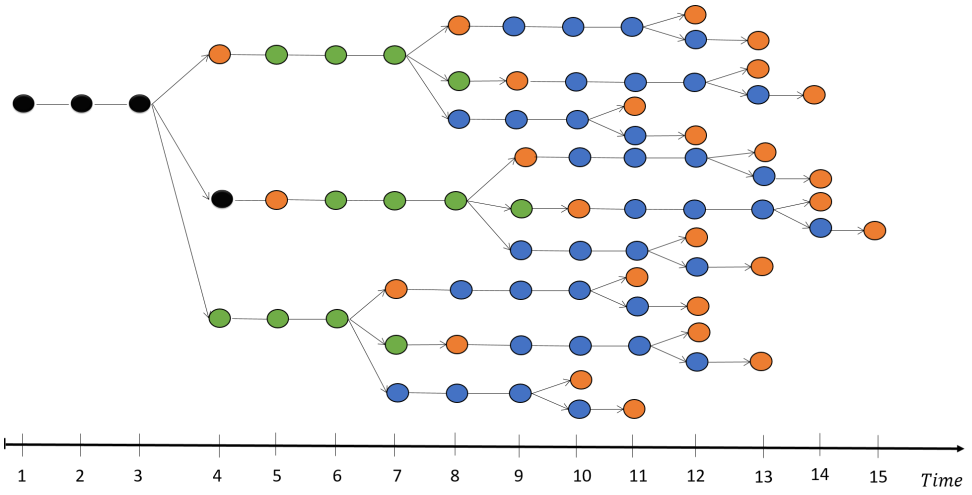

FIGURE 4.18: Full scenario-tree for three production campaigns (black, green and blue nodes) and for each campaign two uncertain failure scenarios (orange nodes) for the superstructure tree formulation. Source: (Leo and Engell, 2023)

For the formulation that is based on the conditional NACs, Figure 4.19 depicts the scenario-tree with three production campaigns and two uncertain failures per campaign. As for the superstructure tree formulation, the sets and parameters S, R_c, $ANC_{c,r}$, $\hat{T}_{c,r}$, $FT_{c,s}$ must be adjusted to the depicted scenario-tree. Additionally, for this formulation the extension to multiple production campaigns requires the identification of the variables that activate the conditional NACs for each production campaign except for the last one. In the proposed formulation with two production campaigns, this was enforced by Eq. 4.109. Therefore, for each production campaign c (except for the last one) the variable K_c must be defined to identify if the campaign c is active when the tree branches and, therefore, if the conditional NACs must be activated.

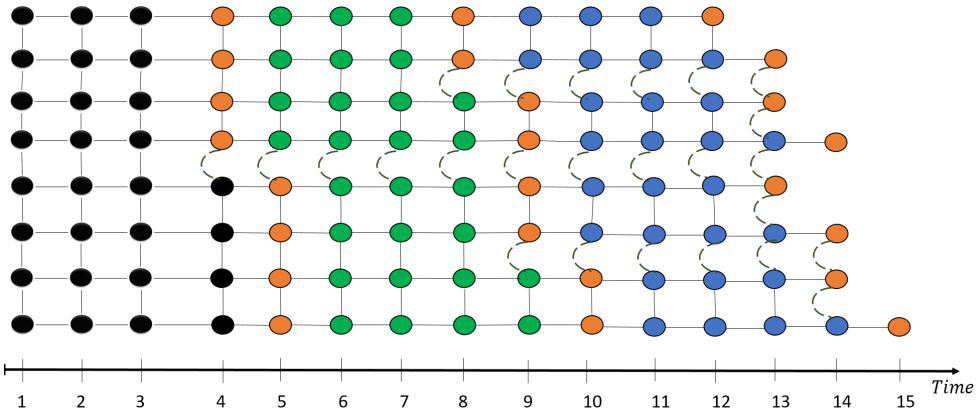

FIGURE 4.19: Full scenario-tree for three production campaigns (black, green and blue nodes) and for each campaign two uncertain failure scenarios (orange nodes) for the formulation that is based on the conditional NACs. Source: (Leo and Engell, 2023)

4.2.6 Solution method

The proposed formulations were solved by generating the MINLP deterministic equivalent problem and using the global solver BARON (Kilinc and Sahinidis, 2018) that was enhanced with several custom branching priority strategies to speed up the solution phase. The idea behind the branching priority schemes is to assign high branching priorities to the complicating variables that when temporarily fixed render the resulting sub-problems much easier to solve. Different branching priority strategies were tested considering as complicating variables:

- the bilinear terms of the objective function p_s^{MSSP} and $cost_s$ (*branching 1*)
- the degradation variables $d_{s,t,c}$ to decouple the probabilities of the scenarios and the Cox model (*branching 2*)
- the stage probabilities $p_{s,c}^{RUL}$ (*branching 3*).

All the formulations were implemented within the algebraic modelling language Julia/JuMP and the MINLP models were solved using the solver BARON version 18.12.26 on an Intel Core i7-2600 machine at 3.40 GHz with 8 processors and 8 GB RAM running Windows 7 Professional.

4.2.7 Results

We present here the results of the two proposed modelling approaches in terms of computational effort and quality of the solution in comparison with a deterministic optimization.

Computational results

To analyse the computational results of the two formulations, Figures 4.20-4.21 show the upper and lower bounds of the global optimum over the solution time.
All the computational results, including the ones that are obtained without a branching priority strategy, are summarized in Tables 4.5-4.6 in terms of the optimal objective function value z^*, upper and lower bounds of the solution UB/LB, optimality gap, and solution time $CPU[s]$.

The case where no branching priority strategy is applied shows that both the formulations are able to reach the global optimum ($UB = LB = 1172$). The superstructure scenario-tree formulation outperforms the conditional NACs formulation in terms of computational time solving the MINLP problem in 3.7 hours against the approximately 7 hours that are needed by the conditional NACs approach.

The branching priority strategies yield different results for the two formulations. As shown in Figure 4.20, the implementation of any branching priorities for the superstructure scenario-tree formulation increases the computational time needed to solve the MINLP problem to the point that the solver is not able to close the optimality gap within the given time limit (15 hours). It is worth to notice though that the upper bound reaches the global optimum solution.

On the other side, Figure 4.21 shows that the implementation of the branching priority strategies drastically reduces the computational time of the the conditional

NACs formulation. The lowest computational effort is obtained by prioritizing the bi-linear terms of the objective function (*branching 1*). This renders the conditional NACs formulation (that is solved in approximately 2.8 hours) more efficient than the superstructure tree formulation (that is solved in approximately 3.7 hours).

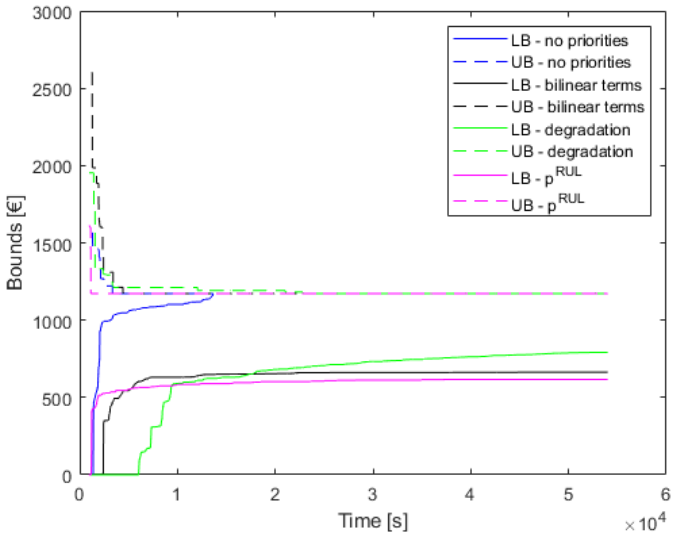

FIGURE 4.20: Upper and lower bounds of the global optimum for the superstructure scenario-tree formulation with different branching priority strategies. Source: (Leo and Engell, 2023)

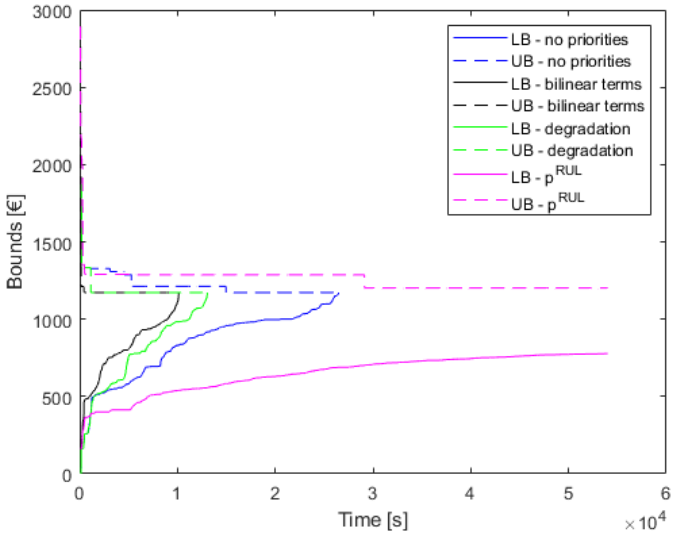

FIGURE 4.21: Upper and lower bounds of the global optimum for the conditional NACs formulation with different branching priority strategies. Source: (Leo and Engell, 2023)

TABLE 4.5: Computational results for the formulation that is based on the conditional NACs. Source: (Leo and Engell, 2023)

	z^*	LB	Gap	CPU [s]
branching 1	1172	1172	0 %	10200
branching 2	1172	1172	0 %	13050
branching 3	1202	777.2	33.6 %	$>$ 54000
no priority	1172	1172	0 %	26470

TABLE 4.6: Computational results for the formulation that is based on the superstructure tree. Source: (Leo and Engell, 2023)

	z^*	LB	Gap	CPU [s]
branching 1	1172	663.5	43.3 %	$>$ 54000
branching 2	1172	791.4	32.4 %	$>$ 54000
branching 3	1172	616.5	47.3 %	$>$ 54000
no priority	1172	1172	0 %	13650

Optimal production and maintenance strategies

The goal of this section is to analyze the differences between the production and maintenance strategies that are obtained by solving the deterministic and stochastic formulations. The solution of the deterministic problem is shown in Figure 4.22 in terms of the degradation trajectories (with the corresponding timing of the maintenance activities) and production profiles. We refer here to the deterministic optimization as a deterministic condition-based model where a perfectly known degradation model is embedded into the optimization problem to define the RUL according to the operating conditions of the plant, as proposed in many works on CBM optimization (Jain and Grossmann, 1998; Xenos et al., 2015; Leo and Engell, 2017). As already described in Section 4.1.3, it is worth to highlight that we consider a deterministic CBM optimization instead of a standard Expected Value Problem (where the uncertain parameters are replaced by their mean values) since it generates more realistic and less conservative results. In fact, a standard Expected Value Problem would define a fixed duration of the production campaigns loosing the degrees of freedom that are provided by the relation between operating conditions and RUL of the plant.

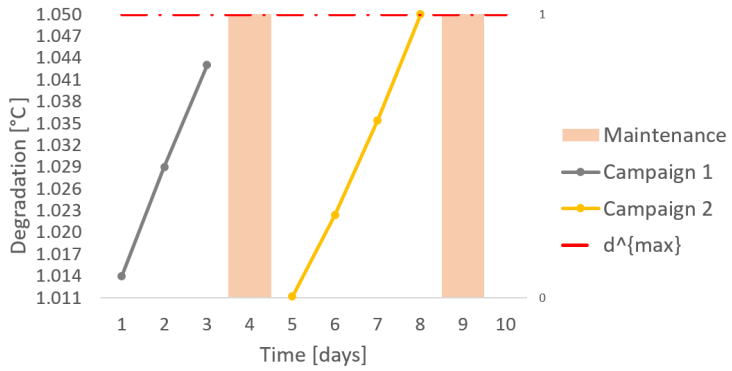

(a)

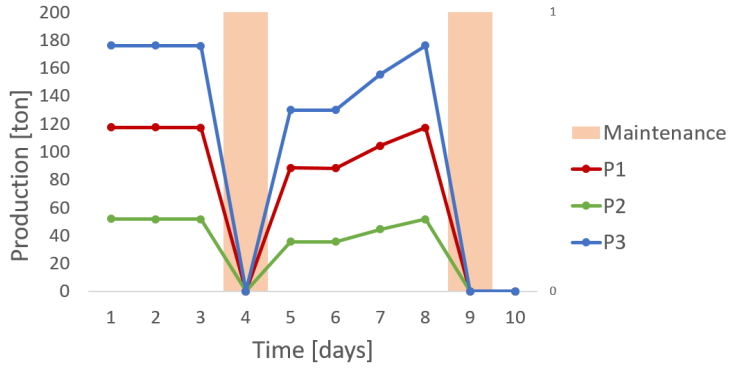

(b)

FIGURE 4.22: Results of the deterministic CBM optimization: (a) degradation trajectories and timing of the maintenance activities, (b) production profiles. Source: (Leo and Engell, 2023)

The results of the stochastic approach represent the global optimum of the conditional NACs formulation and are shown for a high (0.004) and a low value (0.001) of the parameter β of the Cox model. The parameter β influences the hazard function of the plant for a given degradation level $d_{t,c,s}$: higher values of the parameter β increase the probability of realization of the earlier failure times. Low values render more likely the later uncertain failure times of the plant.

Figure 4.23 shows the resulting scenario tree when the high value of β is considered. Figure 4.24 shows the trajectory of the degradation, the timing of the maintenance activities, the production profiles and the optimal probabilities of the scenarios.

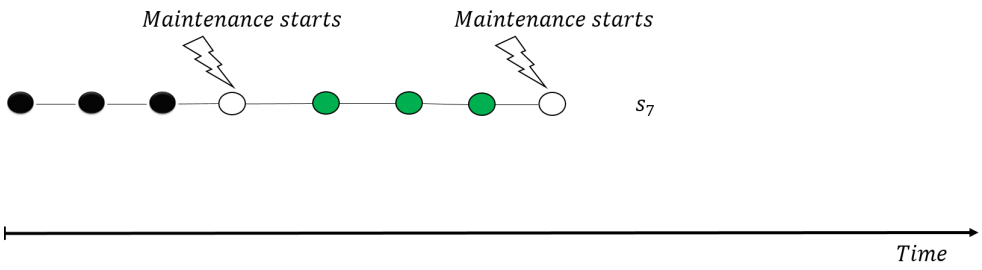

FIGURE 4.23: Optimal scenario tree for a high value of β. Source: (Leo and Engell, 2023)

Compared to the results of the deterministic CBM optimization, the stochastic model anticipates the timing of the maintenance activities by increasing the production levels and, consequently, the degradation rates. The optimal scenario-tree that is depicted in Figure 4.23 represents a deterministic tree since only one scenario for each campaign realizes. In fact, for both the production campaigns the maintenance activities are performed at the time of the earliest realization of the uncertain failure and, therefore, only the first scenario realizes with a probability equal to one.

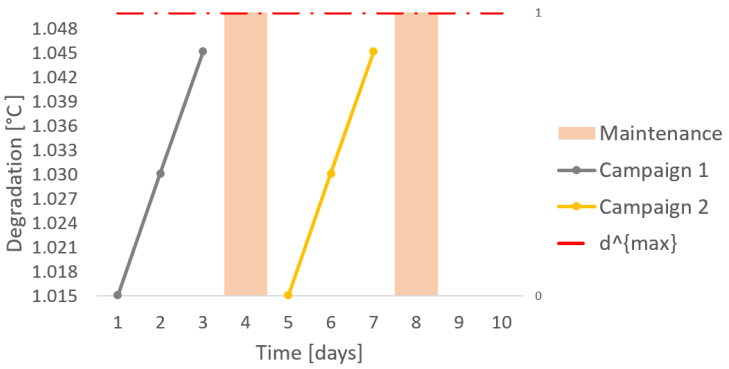

(a)

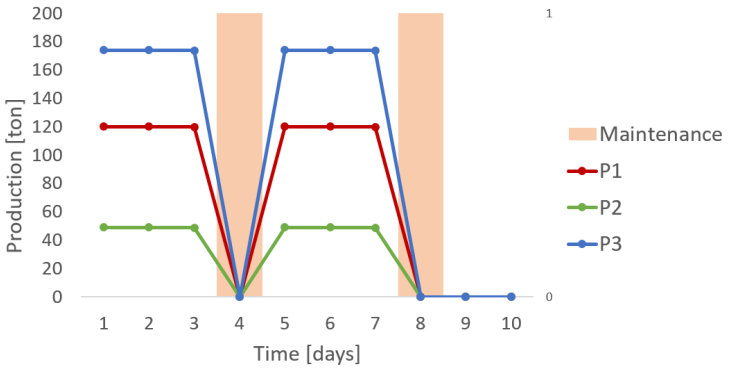

(b)

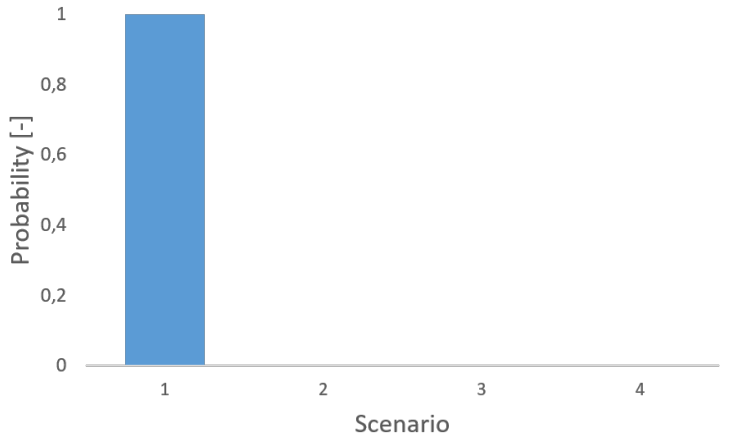

(c)

FIGURE 4.24: Results of the stochastic problem for $\beta = 0.004$: (a) timing of the maintenance activities and degradation trajectory, (b) production profiles, (c) probabilities of the scenarios. Source: (Leo and Engell, 2023)

Figure 4.25 shows the resulting scenario-tree when a low value of the parameter β is considered: the timings of the maintenance activities let all the uncertain failure times realize and therefore the optimal scenario tree represents a multi-stage tree.

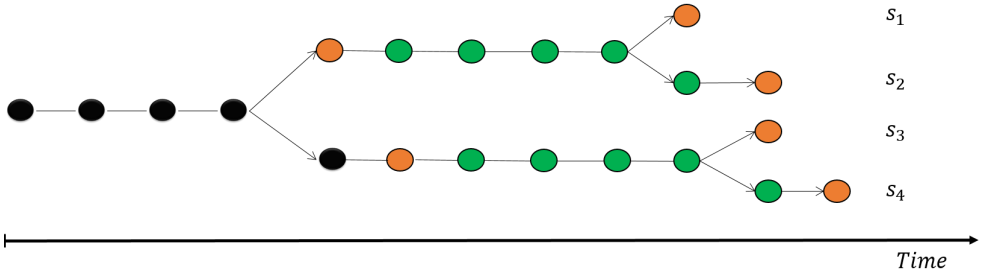

FIGURE 4.25: Optimal scenario tree for low value of β. Source: (Leo and Engell, 2023)

As already described, a low value of β reduces for a given degradation level the hazard (and in this case also the probability) of the earlier failure. Consequently, the optimization results increase the probabilities of the later failures since they are associated to higher production volumes (due to the longer production time available), and therefore lower costs, by postponing the timing of the maintenance activities. The results for a low value of the parameter β are shown in Figures 4.26-4.28 in terms of the degradation trajectories, the timing of the maintenance activities, the optimal probabilities of the scenarios and the production profiles.

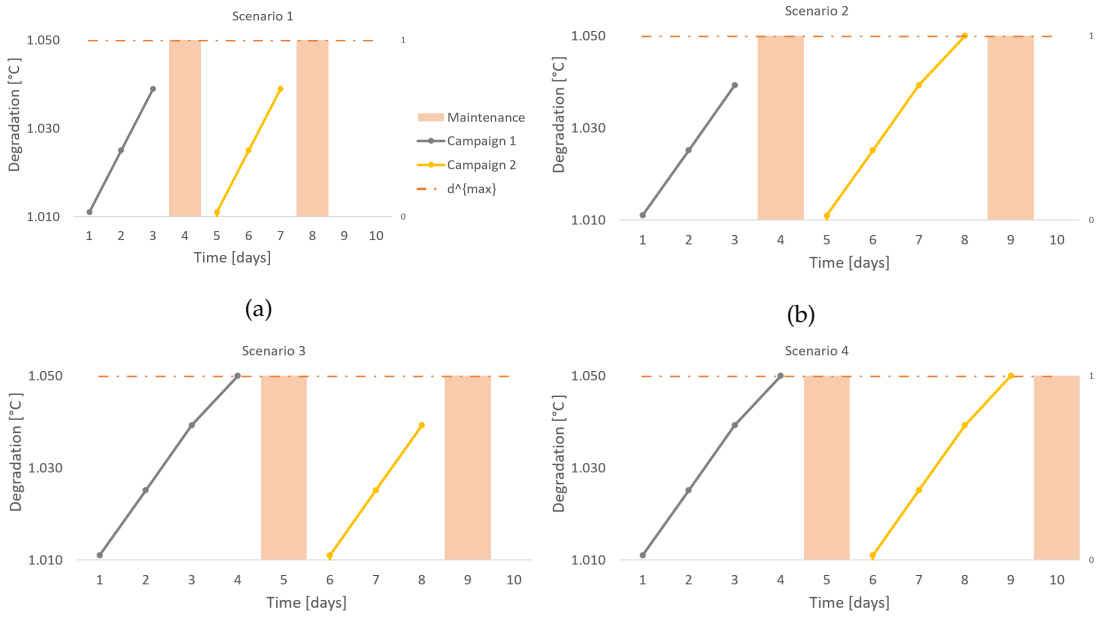

FIGURE 4.26: Results of the stochastic problem for $\beta = 0.001$: (a) degradation profiles for scenario (a) s1, (b) s2, (c) s3, (d) s4. Source: (Leo and Engell, 2023)

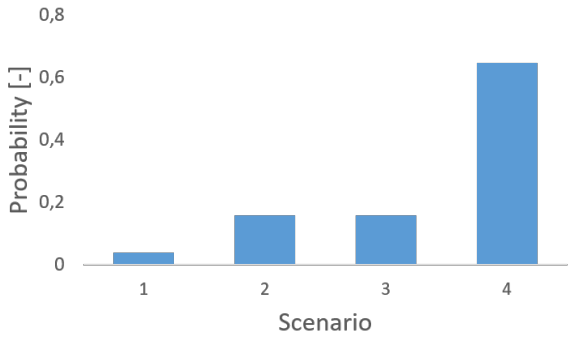

FIGURE 4.27: Probabilities of the scenarios. Source: (Leo and Engell, 2023)

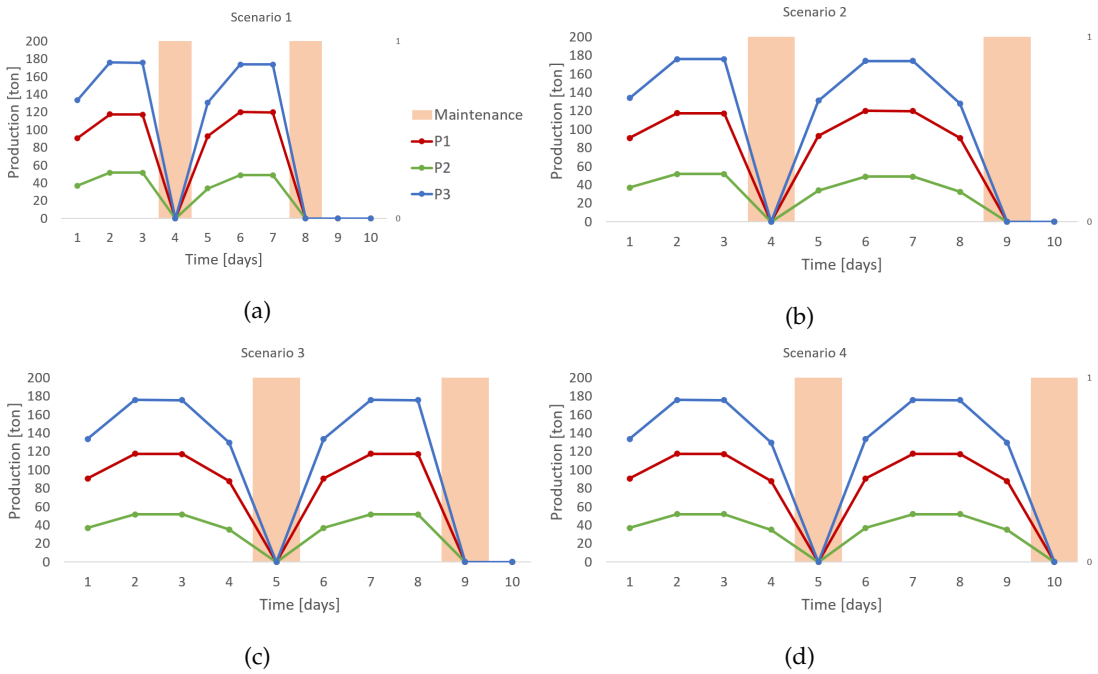

FIGURE 4.28: Results of the stochastic problem for $\beta = 0.001$: production profiles for scenario (a) s1, (b) s2, (c) s3, (d) s4. Source: (Leo and Engell, 2023)

Part IV

Final remarks

Chapter 5

Summary, Conclusions and Discussion

The development and solution of stochastic programming formulations to exploit the concept of Enterprise-wide optimization was discussed in the thesis. Planning and scheduling problems with uncertain information were the focus of this work paying particular attention to the integration of layers of the decision process. The applications considered in this thesis dealt with the integration of production scheduling with energy management and of production planning with predictive maintenance optimization.

In the context of industrial Demand-Side Management, a two-stage stochastic program has been proposed to simultaneously define the production schedule and the day-ahead electricity procurement that is performed via a bidding process. Accounting for the inherit uncertainty of the day-ahead bidding, where the electricity price becomes known only after the electricity commitment is communicated to the electricity provider, revealed to be crucial to reduce the electricity cost and to adjust the production schedule to the time-varying price signal. To reduce the electricity that is purchased during the uncertain price peaks, which are associated to high electricity costs, the introduction of a risk measure is necessary. We showed the advantages of a risk-averse optimization in terms of energy cost reduction when the optimization problem is solved to optimality. However, as often happens, the benefits come at the price of an increased solution complexity that renders the formulation not solvable with an off-the-shelf tool. When the proposed approach was applied to a real-world industrial case study, the progressive hedging algorithm was used to find good-quality near-optimal solutions of the large-scale MILP formulation.
The same trade-off between formulation benefits and complexity appeared for the stochastic multi-stage mixed integer optimization problem that is proposed in this work to optimize the amount of electricity that is purchased from the TOU power contracts and from the day-ahead market and the amount of electricity that is generated with a real-world industrial combined heat and power plant over a medium-term time horizon. The complexity of the multi-stage formulation that considers an uncertain day-ahead price rises because of the decisions regarding the power contracts that must be made at a point in time before the beginning of the considered time horizon (first-stage) and because of the daily revelation of the uncertain day-ahead price. The large-scale deterministic equivalent formulation was solved by approximating the multi-stage optimization in a series of two-stage stochastic programs within a shrinking horizon procedure. Additionally, to handle the multi-scale nature of the

problem (i.e. the contract decisions cover a time horizon of one week while the process decisions only one hour) a detailed model for the short-term future and an aggregate one for the impact on the long-term horizon were integrated.

The exploitation of the financial incentives that are set up by the grid operator is unanimously recognized by large electricity consumers as a profitable way to reduce the electricity cost. Realistic formulations able to capture the significant features of the electricity purchasing options are still missing. A promising extension of the proposed work is the integration of the intraday electricity purchasing option to strategically bid on different spot markets. Intraday power trading refers to the continuous purchasing and selling of electricity that takes place during the same day as the power delivery. The intraday trading allows the consumer to adjust the day-ahead electricity procurement to unforeseen plant conditions (breakdowns, delays,...) by selling or buying electrical power with short lead times (up to five minutes). However, since multiple markets have different pricing mechanisms and, therefore, different revelations of their uncertain prices (e.g. the intraday prices are assessed in continuous trading based on each transaction that is completed), a multi-stage mixed-integer formulation would have to be developed. Since a multi-stage formulation is notoriously hard to solve, the need of realistic formulations comes with the need of efficient solution algorithms. In particular, large-scale stochastic integer formulations with integer recourses are still an open challenge due to the non-convexity that is introduced by the integer variables.

Similar considerations can be made on the computational challenge rising from the solution of non-convex (stochastic and deterministic) MINLP problems as shown with the novel stochastic program with endogenous uncertainty that is proposed in this thesis to integrate production planning, prognosis and condition-based maintenance. In fact, the novel approach proposes a decision-dependent formulation that models the probabilities of the scenarios as decision variables giving rise to bi-linear non-convex terms. Since a global solver enhanced with different branching priority schemes was not able to solve the resulting non-convex MINLP deterministic equivalent problem, two primal decomposition algorithms (a local and global one) were applied to improve the computational time and the quality of the solution. The high complexity of the novel formulation is, nonetheless, justified by the advantages that are obtained respect to the corresponding deterministic counterpart. The advantages come not only from the awareness of the model about the uncertain parameters, the Remaining Useful Life of the plant in this case, but also from the additional degrees of freedom given to the decision maker by defining the probabilities of the scenarios as decision variables that depend on the plant operations. In particular, the endogenous uncertainty formulation made possible the integration of a prognosis model, the Cox model, into an optimization problem to make more profitable maintenance and production planning decisions.

A further step towards the deployment of the proposed formulation would be the integration with a monitoring system. In fact, an online application of the proposed formulation must be able to collect measurements of the degradation process to update the parameters of the degradation model. A more accurate degradation model would improve the estimation of the probabilities of the scenarios and gradually resolve the uncertainty. In fact, according to the collected measurements some of the scenarios that are considered at the beginning of the horizon might become not realizable with the additional side effect of reducing the problem size and consequently

the computational effort required by the optimizer.

The class of stochastic programs with decision-dependent probabilities is a relative novel class of optimization problems with several open questions from both the modelling and the solution perspectives. The integration of a risk measure for this class of problems has not received much attention in the scientific literature. A deviation-based risk measure, e.g. the Expected Excess, could be integrated without altering the proposed problem decomposition and solution algorithms that are proposed in this thesis, the Generalized Benders and the Global Optimization decompositions. Moreover, with a non-convex MINLP problem emerges also the need of solution algorithms able to find the global optimum in a reasonable amount of time.

We further extended the proposed approach to a medium-term planning horizon by modelling a stochastic program with decision-dependent probabilities and a decision dependent structure of the scenario tree. In particular, the scenario-tree representing the stochastic optimization problem is characterized not only by the probabilities of the scenarios that are modelled as decision variables but also by the timing of the revelation of the uncertainty (and therefore the structure of the scenario tree) that is influenced by the decision variables (i.e. the timing of the maintenance activities in the proposed work). This is the first time that such a formulation has been proposed in the scientific literature. We focused on the formulation perspective by proposing two modelling approaches (the superstructure scenario-tree and the conditional NACs approach) to systematically construct an optimization program with both types of endogenous uncertainties. We compared the two resulting (equivalent) models in terms of the computational time that is needed to solve the problem to global optimality. From a computational perspective, we analysed the influence of different branching priority strategies on the lower and upper bounds of the global solution over the iterations of the solution algorithm. It can be concluded that the conditional NACs formulation is a more compact and efficient model that can gain advantage from a suitable branching priority strategy.

The number of open questions and potential future works for this challenging class of optimization are clearly very large and plentiful. From a modelling perspective, a continuous-time formulation and, in particular, the application of the disjunctive programming technique (Grossmann and Ruiz, 2012) (along with the different reformulations) may provide suitable alternatives to systematically build up such optimization models and, at the same time, to reduce the required computational effort. Moreover, the integration of a risk measure and its impact on the production strategy and on the computational effort should be analysed. From an algorithmic perspective, the application of decomposition techniques can enable the solution of larger problems with an increased number of scenarios.
Furthermore, given the generality of the proposed approach, several industrial case studies (from continuous and batch production) could be analysed to integrate production planning and predictive maintenance. The application to industrial size problems would pose the computational challenge of finding good quality solutions in a reasonable amount of time. An efficient approach to handle this challenge is the adoption of the rolling horizon strategy that defines a moving time window to solve repetitively the optimization problem. Since this is the first formulation of a stochastic problem with Type-I and Type-II endogenous uncertainties, the rolling horizon approach has not been applied to this class of problems. However, we can foresee that a crucial parameter for the application of this strategy is the number

of production campaigns (or in other words the length of time horizon of the optimization problem) that are optimized. The number of production campaigns to be optimized should be chosen such that the effect of the decisions of the near future can be seen within the horizon of the optimization problem. We suggest that a minimum number of three campaigns should be considered if the rolling horizon strategy is applied. By considering three production campaigns for each iteration of the rolling horizon strategy, the effect of the decisions on the current campaign is taken into account in the following one leading to a reduced impact of cut-off effects of the terminal costs but still manageable computation times.

Part V

Appendix

.1 Data of the illustrative example for stochastic DSM

TABLE 1: Minimum stay time.

$\theta_{mm\prime}[h]$	off	startup	on
	8	2	6

TABLE 2: Uncertain day-ahead prices.

	1	2	3	4	5	6	7	8	9	10	11	12	13	14	15	16	17	18	19	20	21	22	23	24	p_s
s1	54	58	60	62	60	66	71	76	81	83	77	69	60	46	45	47	57	66	80	70	62	57	65	76	0.01
s2	57	54	51	54	58	67	77	82	91	99	96	93	83	74	69	67	68	70	58	50	47	48	52	52	0.05
s3	55	50	55	58	67	69	80	76	71	69	67	62	63	65	65	64	61	53	53	58	50	52	52	47	0.01
s4	57	57	64	64	77	85	86	84	80	68	62	48	47	43	45	45	45	43	44	46	56	55	56	55	0.1
s5	52	51	47	48	51	50	52	55	59	62	62	48	56	61	68	70	68	66	60	56	57	61	62	59	0.13
s6	53	59	66	68	63	63	58	50	52	53	53	43	42	48	52	55	57	58	60	63	74	77	77	72	0.05
s7	53	57	65	66	69	79	89	88	86	80	75	68	63	65	61	50	50	41	34	26	32	34	39	46	0.31
s8	49	50	53	63	60	59	57	54	54	53	55	52	48	51	51	53	52	44	46	55	59	64	62	60	0.09
s9	60	55	62	64	63	60	55	55	52	46	51	50	49	36	32	37	44	53	58	55	49	48	43	40	0.1
s10	53	48	52	68	75	73	82	77	71	64	63	61	59	54	57	57	66	64	54	49	38	33	35	36	0.15

TABLE 3: Load deviation prices for over-consumption (p^+_{st}). The prices for under-consumption are defined as $p^-_{st} = p^+_{st} - 10$

	1	2	3	4	5	6	7	8	9	10	11	12	13	14	15	16	17	18	19	20	21	22	23	24
s1	133.3	137.1	139.1	141	139.6	145	150.7	155.3	160.3	162.3	156.8	148.0	139.7	125.6	124.3	126.3	136.6	145.3	159.9	149.1	141.0	136.3	144.4	155.3
s2	149.5	146.0	143	146.4	150	159	169	174.7	183.9	191	188	185	175	166	161	159	160	162	150	142.4	139.9	140.7	144.9	144
s3	130.1	125	130	133	142	144.4	155	151	146	144	142	137	138.0	140	140	139	136.3	128	128	76.9	127	127	122	
s4	135.5	135	142	142	155.9	163	164	162	158.6	146	140	126	125.9	121	123.4	123	123.4	121	122	124	134	133	134	133
s5	120.2	119	115	116	119.6	118	120	123	127.6	130	130	116	124.6	129.3	136.8	138.4	136.6	134	128	124	125	129	130	127
s6	127.2	133	140.6	142	137	137	132	124	126	127	127	117	116	122	126	129	131.6	132	134	137	148	151	151.9	146
s7	138.6	142	150	151	154.6	164	174	173	171	165	160	153	148	150.4	146	135	135	126	119.2	111	117	119	124	131
s8	113.9	114.9	117.9	127.6	124.5	123.1	121.1	118	118	117	119	116	112	115	115.4	117.1	116	108	110.3	119	123	128	126.6	124
s9	114.3	109	116	118.6	117	114.1	109	109	106.1	100	105	104.2	103	90	86	91	98.4	107	112	109	103	102	97	94
s10	131.9	126.4	130.6	146.3	153.6	151.1	160.9	155.9	149.7	142.2	141	139	137	132.6	135	135.3	144	142.6	132	127.9	116.6	111	113.2	114

TABLE 4: Vertices of the mode operating region.

Mode	Vertex	$P1$ [kg]	$P2$ [kg]
Off	1	0	0
Startup	1	5	5
On	1	10	10
On	2	50	10
On	3	30	40
On	4	70	40

TABLE 5: Coefficients to compute the electricity consumption

Mode	δ_m [kWh]	γ_{P1} [kWh/kg]	γ_{P2} [kWh/kg]
Off	0	0	0
Startup	500	0	0
On	800	20	30

TABLE 6: Upper and lower bounds of the amount of inventory.

	IV_{min}/IV_{max} [kg]	IV_{init}/IV_{fin} [kg]	D_t
P1	600/6000	1000/1000	65
P2	300/3000	500/500	35

.2 Data of the industrial case study for stochastic DSM

TABLE 7: Steel Heat/Group mapping

group g1	group g2	group g3	group g4	group g5	group g6
$H_1 - H_4$	$H_5 - H_8$	$H_9 - H_{12}$	$H_{13} - H_{17}$	$H_{18} - H_{20}$	$H_{21} - H_{24}$

TABLE 8: Power Consumption [MW]

EAF_1	EAF_2	AOD_1	AOD_2	LF_1	LF_2	CC_1	CC_2
85	85	2	2	2	2	7	7

TABLE 9: Maximum waiting time [min]

EAF	AOD	LF	CC_1	CC_2
0	0	90	60	60

TABLE 10: Processing times [min]

	EAF	AOD	LF	CC_1	CC_2
$H_1 - H_4$	80	75	35	30	30
H_5	80	80	45	30	30
H_6	85	80	45	30	30
$H_7 - H_8$	85	80	20	30	30
$H_9 - H_{12}$	90	95	45	30	30
$H_{13} - H_{16}$	85	85	25	60	60
$H_{17} - H_{18}$	80	85	25	45	45
$H_{19} - H_{20}$	80	95	45	45	45
H_{21}	80	95	30	60	60
$H_{22} - H_{24}$	80	80	30	60	60

.3 Data for the stochastic formulations with endogenous uncertainties

TABLE 11: Feed parameters.

$Type$	IC_f [-]	$price_f^{feed}$ [e]	UB_f^{feed} [ton]
1	1	100	3600
2	0.9	200	3600
3	0.8	300	3600
4	0.7	400	3600
5	0.6	500	3600
6	0.5	600	3600
7	0.4	700	3600
8	0.3	800	3600
9	0.2	900	3600
10	0.1	1000	3600

TABLE 12: Degradation model parameters.

α_i^1	α_i^2	$d0$	d^{max}	d^{CBM}	d^{min}	p_s^0	β
150	0	1000	1280	2	1220	0.1	0.04

TABLE 13: Process model parameters.

$\gamma_{P1,1}$	$\gamma^{P1,1}$	$\gamma_{P2,1}$	$\gamma_{P2,1}$	$\gamma_{P3,1}$	$\gamma^{P3,1}$	r_{P1}	r_{P2}	r_{P3}

TABLE 14: Product demand D_p and maximum production capacity $UB^y_{p,s}$.

P_1 [ton]	P_2 [ton]	P_3 [ton]
3600	1600	5600
4800	2680	7360

TABLE 15: Average production cost in the following campaign or products purchasing price.

P_1 [€/kg]	P_2 [€/kg]	P_3 [€/kg]
35	30	15

TABLE 16: Cost parameters.

steam price [€/ton]	fuel price [€/ton]	c^{CBM}
28	214	1000

TABLE 17: Lower and upper bound plant inputs.

feed flow [ton/day]	severity [-]	steam 105 bar [ton/day]	steam 30 bar [ton/day]
340/450	0.7 / 0.95	40 /120	0/50

.4 Generation of the optimality cuts for the Benders decomposition

$$-\hat{\lambda}_{1,p,s} * (-D_p + \sum_{t \in T^{1stage}} y_{p,t} + \hat{PP}_{p,s} + \sum_{t \in T^s} \hat{y}_{p,t,s}) \quad \forall s \in S, p \in P \tag{1}$$

$$-\hat{\lambda}_{2,i,t,s} * (\hat{u}_{i,t,s} - UB^{input}_{i,t,s} * (1 - x^{CBM}_t) \quad \forall s \in S, i \in I, t \in T^s \tag{2}$$

$$-\hat{\lambda}_{3,i,t,s} * (-\hat{u}_{i,t,s} + LB^{input}_{i,t,s} * (1 - x^{CBM}_t) \quad \forall s \in S, i \in I, t \in T^s \tag{3}$$

$$-\hat{\lambda}_{4,t,s} * (\hat{d}_{t,s} - d^{max}_s * (1 - x^{CBM}_t)) \quad \forall s \in S, i \in I, t \in T^s \tag{4}$$

$$-\hat{\lambda}_{5,p,t,s} * (\hat{y}_{p,t,s} - UB^y_{p,t,s} * (1 - x^{CBM}_t)) \quad \forall s \in S, i \in I, t \in T^s \tag{5}$$

$$-\hat{\lambda}_{6,t,s} * (-\hat{d}_{t,s} + d_{t-1,s} + \sum_{i \in I} \alpha^i * \hat{u}_{i,t} + \sum_{f \in F} IC_f * y_{f,t}^{feed} - M * x_t^{CBM}) \quad \forall s \in S, t = T_1^s \tag{6}$$

$$-\hat{\lambda}_{7,t,s} * (\hat{d}_{t,s} - d_{t-1,s} - \sum_{i \in I} \alpha^i * \hat{u}_{i,t} - \sum_{f \in F} IC_f * y_{f,t}^{feed} - M * x_t^{CBM}) \quad \forall s \in S, t = T_2^s \tag{7}$$

$$-\hat{\lambda}_{8,t,s} * (-\hat{d}_{t,s} + \hat{d}_{t-1,s} + \sum_{i \in I} \alpha^i * \hat{u}_{i,t} + \sum_{f \in F} IC_f * y_{f,t}^{feed} - M * x_t^{CBM}) \quad \forall s \in S, t \in \{T_2^s, \ldots, |T^s|\} \tag{8}$$

$$-\hat{\lambda}_{9,t,s} * (\hat{d}_{t,s} - \hat{d}_{t-1,s} - \sum_{i \in I} \alpha^i * \hat{u}_{i,t} - \sum_{f \in F} IC_f * y_{f,t}^{feed} - M * x_t^{CBM}) \quad \forall s \in S, t \in \{T_2^s, \ldots, |T^s|\} \tag{9}$$

$$-\hat{\lambda}_{10,s} * (\hat{d}_{t,s} - d^{min} + \epsilon - (M + \epsilon) * x_s^{scenario}) \quad \forall s \in S, \in T^s \tag{10}$$

Bibliography

Aggarwal, S, L Saini, and A Kumar (2009). "Electricity price forecasting in deregulated markets: A review and evaluation." In: *International Journal of Electrical Power & Energy Systems* 31.1, pp. 13–22.

Alsyouf, I (2007). "The role of maintenance in improving companies' productivity and profitability." In: *International Journal of Production Economics* 105, pp. 70–78.

Apap, RM and IE Grossmann (2017). "Models and computational strategies for multistage stochastic program- ming under endogenous and exogenous uncertainties." In: *Comput Chem Eng* 103, pp. 233–274.

Balas, E, S Ceria, and G Cornuéjols (1993). "A lift-and-project cutting plane algorithm for mixed 0-1 programs." In: *Mathematical Programming* 58.1-3, pp. 295–324.

Balasubramanian, J and IE Grossmann (2004). "Approximation to Multistage Stochastic Optimization in Multiperiod Batch Plant Scheduling under Demand Uncertainty". In: *Ind. Eng. Chem. Res.* 43.14, 3695–3713.

Basciftc, B et al. (2018). "Stochastic Optimization of Maintenance and Operations Schedules under Unexpected Failures". In: *IEEE Transactions on Power Systems* 33 (6), pp. 6755–6765.

Basciftci, B, S Ahmed, and N Gebraeel (2019). "Data-driven maintenance and operations scheduling in power systems under decision-dependent uncertainty". In: *IISE Transactions*, pp. 1–14.

Benders, JF (1962). "Partitioning procedures for solving mixed-variables programming problems." In: *Numer Math* 4 (1), pp. 238–252.

Beraldi, P et al. (2011). "Short-term electricity procurement: a rolling horizon stochastic programming approach." In: *Appl Math Model* 35.8, pp. 3980–90.

Biondi, M, G Sand, and I Harjunkoski (2017). "Optimization of multipurpose process plant operations: A multi-time-scale maintenance and production scheduling approach." In: *Comput. Chem. Eng.* 99, pp. 325–339.

Birge, JR and F Louveaux (1997). "Multistage Stochastic Programs". In: *Introduction to Stochastic Programming*, pp. 233–252.

Birge, JR and F. Louveaux (2011). "Introduction to stochastic programming". In: *2nd ed Springer Science+Business Media*.

Birge, JR and FV Louveaux (1998). "A multicut algorithm for two-stage stochastic linear programs". In: *European Journal of Operational Research* 34 (3), pp. 384–392.

Boland, N, I Dumitrescu, and G Froyland (2008). "A multistage stochastic programming approach to open pit mine production scheduling with uncertain geology". In: *7th joint Australia-NewZealandMathematics Convention*. Ed. by ANZMC2008. Christchurch, New Zealand.

British Standards Institute, London (1993). *BS 3811-Glossary of Maintenance Management Terms in Terotechnology*. Ed. by BSI. Vol. 3811.

Carøe, C and J Tind (1998). "L-Shaped decomposition of two-stage stochastic programs with integer recourse." In: *Mathematical Programming* 83(1-3), pp. 451–464.

Carøe, CC and R R Schultz (1999). "Dual decomposition in stochastic integer programming". In: *Operations Research Letters* 24.1, pp. 37–45.

Carøe, CC and J Tind (1997). "A cutting-plane approach to mixed 0-1 stochastic integer programs." In: *European Journal of Operational Research* 101.2, pp. 306–316.

Carrión, M et al. (2007). "A stochastic programming approach to electric energy procurement for large consumers." In: *IEEE Trans Power Syst* 22.2, pp. 744–54.

Castro, PM, L Sun, and I Harjunkoski (2013). "Resource Task Network Formulations for Industrial Demand Side Management of a Steel Plant". In: *Industrial and Engineering Chemistry Research* 52(36), pp. 13046–13058.

Colvin, M and CT Maravelias (2008). "A stochastic programming approach for clinical trial planning in new drug development." In: *Comput Chem Eng* 32 (11), pp. 2626–42.

Colvin, M and CT Maravelias (2009). "Scheduling of testing tasks and resource planning in new product development using stochastic programming." In: *Comput Chem Eng* 33 (5), pp. 964–976.

Colvin, M and CT Maravelias (2010). "Modeling methods and a branch and cut algorithm for pharmaceutical clinical trial planning using stochastic programming." In: *Eur J OperRes* 203 (1), pp. 205–15.

Compare, M, P Baraldi, and E Zio (2020). "Challenges to IoT-enabled Predictive Maintenance for Industry 4.0". In: *IISE Transactions* 7 (5), pp. 4585–4597.

Conejo, AJ et al. (2006). *Decomposition Techniques in Mathematical Programming*. Ed. by Springer. Vol. 1.

Cox, DR (1972). "Regression Models and Life-Tables". In: *Journal of the Royal Statistical Society, Series B* 34, pp. 187–220.

Cui, J and S. Engell (2010). "Medium-term planning of a multiproduct batch plant under evolving multi-period multi-uncertainty by means of a moving horizon strategy". In: *Comput. Chem. Eng.* 5.10, 598–619.

Dalle Ave, G, I Harjunkoski, and S Engell (2018). "Industrial Demand Side Management Formulation for Simultaneous Electricity Load Commitment and Future Load Prediction". In: *International Symposium on Process Systems Engineering - PSE 2018*. San Diego, California, USA.

De Jonge, B and P Scarf (2020). "A review on maintenance optimization." In: *European Journal of Operational Research* 285, pp. 805–824.

Dedopoulos, IT and N Shah (1995). "Preventive maintenance policy optimisation for multipurpose plant equipment." In: *Comput. Chem. Eng.* 19, S693–S698.

Dupačová, J, N Gröwe-Kuska, and W Römisch (2003). "Scenario reduction in stochastic programming: An approach using probability metrics". In: *Math. Program.* Ser.A.95, pp. 493–511.

Engell, S (2009). "Uncertainty, decomposition and feedback in batch production scheduling". In: *19th European Symposium on Computer Aided Process Engineering – ESCAPE19*, pp. 43–62.

Escudero, LF et al. (2007). "The value of the stochastic solution in multistage problems". In: *TOP* 15, pp. 48–64.

Escudero, LF et al. (2018). "On preparedness resource allocation planning for natural disaster relief under endogenous uncertainty with time-consistent risk-averse management". In: *Comput Oper Res* 32(4), pp. 84–102.

Fleten, SE and TK Kristoffersen (2007). "Stochastic programming for optimizing bidding strategies of a Nordic hydropower producer". In: *European Journal of Operational Research* 181, pp. 916–928.

Floudas, CA and V Visweswaran (1990). "A global optimization algorithm (GOP) for certain classes of nonconvex NLPs: I. Theory". In: *Computers and Chemical Engineering* 14(12), pp. 1397–1417.

Geoffrion, A (1972). "Generalized benders decomposition." In: *J Optim Theory Appl* 10 (4), 237–260.

Gestore Mercati Energetici (2019). "https://www.mercatoelettrico.org/it/Mercati/MercatoElettrico/MPE.aspx".

Goel, V and IE Grossmann (2004). "A stochastic programming approach to planning of offshore gas field developments under uncertainty in reserves." In: *Comput Chem Eng* 28(8), pp. 1409–1429.

Goel, V and IE Grossmann (2006). "A class of stochastic programs with decision dependent uncertainty." In: *Math Program* 108(2), pp. 355–394.

Grossmann, IE (2005). "Enterprise–wide optimization: a new frontier in process systems engineering". In: *AIChE J* 51, pp. 1846–57.

Grossmann, IE and JP Ruiz (2012). *Generalized Disjunctive Programming: A Framework for Formulation and Alternative Algorithms for MINLP Optimization*. Ed. by Leyffer S (eds) Mixed Integer Nonlinear Programming. The IMA Volumes in Mathematics In: Lee J and New York NY. its Applications Springer. Vol. 154.

Hadera, H et al. (2015). "Optimization of steel production scheduling with complex time–sensitive electricity cost". In: *Computers and Chemical Engineering* 76, pp. 117–136.

Hadera, H et al. (2019). "Integration of production scheduling and energy-cost optimization using Mean Value Cross Decomposition". In: *Computers and Chemical Engineering* 129.

Heitsch, H and W Römisch (2001). "Scenario reduction algorithms in stochastic programming". In: *Institut für Mathematik, Humboldt-Universität zu Berlin* 95, 01–08.

Hellemo, L, PI Barton, and A Tomasgard (2018). "Decision-dependent probabilities in stochastic programs with recourse". In: *Comput Manag Sci* 15, pp. 369–395.

Jain, V and IE Grossmann (1998). "Cyclic scheduling of continuous parallel-process units with decaying performance." In: *AIChE J.* 44, pp. 1623–1636.

Jalal Kazempour, S, AJ Conejo, and C Ruiz (2015). "Strategic Bidding for a Large Consumer". In: *IEEE transactions on power systems* 30, NO. 2.

Jonsbraten, TW, RJ Wets, and DL Woodruff (1998). "A Class of Stochastic Programs with Decision Dependent Random Elements." In: *Annals of Operations Research* 82, pp. 83–106.

Kilinc, M and NV Sahinidis (2018). "Exploiting integrality in the global optimization of mixed-integer nonlinear programming problems in BARON". In: *Optimization Methods and Software* 33, pp. 540–562.

Kim, K and VM Zavala (2015). "Algorithmic innovations and software for the dual decomposition method applied to stochastic mixed-integer programs". In: *Optimization Online*.

Laporte, G and FV Louveaux (1993b). "The integer l-shaped method for stochastic integer programs with complete recourse". In: *Operations Research Letters* 13.3, pp. 133–142.

Laporte, G and FV Louveaux (1993a). "The integer L-shaped method for stochastic integer programs with complete recourse." In: *Operations Research Letters* 13(3), 133–142.

Lawless, JF (2002). *Statistical Models and Methods for Lifetime Data, Hoboken, NJ: Wiley-Interscience*.

Leo, E and S Engell (2017). "Condition-based operational optimization of industrial combined heat and power plants under time-sensitive electricity prices". In: *Proceedings of the 27th European Symposium on Computer Aided Process Engineering, October 1st-5th,Barcelona, Spain* 40, pp. 1261–1266.

Leo, E and S Engell (2018). "Multi-stage integrated electricity procurement and production scheduling". In: *International Symposium on Process Systems Engineering - PSE 2018*. San Diego, California, USA.

Leo, E and S Engell (2019a). "Applying Stochastic Optimization to Demand-Side Management of a Combined Heat and Power Plant". In: *The 12th European Congress of Chemical Engineering (ECCE12)*. Florence.

Leo, E and S Engell (2019b). "Integrated day-ahead energy procurement and production scheduling." In: *Automatisierungstechnik* 66 (11), pp. 950–963.

Leo, E and S Engell (2020). "A novel multi-stage stochastic formulation with decision-dependent probabilities for condition-based maintenance optimization". In: *Proceedings of the 30th European Symposium on Computer Aided Process Engineering, May 24-27, Milano, Italy* 48, pp. 1795–1800.

Leo, E and S Engell (2021). "Condition-based maintenance optimization via stochastic programming with endogenous uncertainty". In: *Computers and Chemical Engineering*, pp. 00–00.

Leo, E and S Engell (2023). "Handling Type-I and Type-II endogenous uncertainties in simultaneous production planning and condition-based maintenance optimization in continuous production". In: *Computers & Chemical Engineering* 174, p. 108227.

Leo, E et al. (2021). "Stochastic short-term integrated electricity procurement and production scheduling for a large consumer". In: *Computers and Chemical Engineering* 145, p. 107191.

Li, C and I Grossmann (2019). "A finite ϵ-convergence algorithm for two-stage convex 0-1 mixed-integer nonlinear stochastic programs with mixed-integer first and second stage variables". In: *Journal of Global Optimization* 75, 921–947.

Li, P, H Garcia, and W Gunter (2008). "Chance constrained programming approach to process optimization under uncertainty". In: *Computer Aided Chemical Engineering* 32.1, pp. 1245–1250.

Louveaux, F and JR Birge (2008). "L-shaped Method for Two-stage Stochastic Programs with Recourse". In: *In: Floudas C., Pardalos P. (eds) Encyclopedia of Optimization* Springer, Boston, MA.

Maravelias, CT and C Sung (2009). "Integration of production planning and scheduling: Overview, challenges and opportunities". In: *Computers and Chemical Engineering* 33.12, pp. 1919 –1930.

Mello, T Homem-de and BK Pagnoncelli (2016). "Risk aversion in multistage stochastic programming: A modeling and algorithmic perspective". In: *European Journal of Operational Research* 249.1, pp. 188 –199.

Merkert, L et al. (2014). "Scheduling and energy - Industrial challenges and opportunities". In: *Comput. Chem. Eng.* 72, pp. 183–98.

Meyer, C and C Floudas (2006). "Global optimization of a combinatorially complex generalized pooling problem." In: *AIChE journal* 52, 1027–1037.

Mitra, S et al. (2013). "Optimal scheduling of industrial combined heat and power plants under time-sensitive electricity prices". In: *Energy* 54, pp. 194–211.

Mitsos, A, B Chachuat, and P Barton (2009). "McCormick-based relaxations of algorithms". In: *SIAM J Optim* 20, 573–601.

Nikulin, M and H Wu (2016). *The Cox Model and Its Applications, Springer Berlin, Heidelberg*.

Nogales, FJ et al. (2002). "Forecasting next-day electricity prices by time series models". In: *IEE* 17(2).1–12, pp. 342–348.

Nolde, K and M Morari (2010). "Electrical load tracking scheduling of a steel plant". In: *Comput. Chem. Eng.* 34 (11), pp. 1899–1903.

Pantelides, CC (1994). "Unified Frameworks for the Optimal Process Planning and Scheduling". In: *In Proceedings of the Second Conference on Foundations of Computer Aided Operations* 52(36), p. 253.

Paulus, M and F Borggrefe (2011). "The potential of demand–side management in energy–intensive industries for electricity markets in Germany". In: *Appl. Energy* 88, p. 432.

Peeta, S et al. (2010). "Pre-disaster investment decisions for strengthening a highway network". In: *Comput Oper Res* 37, pp. 1708–1719.

Pflug, G (1996). *Optimization of stochastic models: the interface between simulation and optimization*. Kluwer Academic, Boston.

Pflug, G and A Pichler (2016). "Time-Consistent Decisions and Temporal Decomposition of Coherent Risk Functionals". In: *Mathematics of Operations Research* 41.2, pp. 682–699.

Rahimi-Adli, K et al. (2021). "Optimization of the operation of an industrial power plant under steam demand uncertainty". In: *Energies* 21, p. 7213.

Rahmani, R et al. (2017). "The Benders decomposition algorithm: A literature review". In: *European Journal of Operational Research* 259.3, pp. 801 –817.

Rajagopalan, S et al. (2017). "Risk analysis of turnaround reschedule planning in integrated chemical sites". In: *Computers and Chemical Engineering*, pp. 381–394.

Ramin, D, S Spinelli, and A Brusaferri (2018). "Demand-side management via optimal production scheduling in power-intensive industries: The case of metal casting process." In: *Applied Energy* 225, pp. 622–636.

Rockafellar, RT (2015). "Coherent Approaches to Risk in Optimization Under Uncertainty". In: *INFORMS Tutorials in Operations Research*, pp. 38–61.

Rockafellar, RT and S Uryasev (2000). "Optimization of conditional value-at-risk". In: *J Risk* 2.95, pp. 21–42.

Rockafellar, RT and RJ Wets (2006). "Scenarios and policy aggregation in optimization under uncertainty". In: *Mathematics of Operations Research* 16.1, pp. 203–223.

Ruszczyński, A (1997). "Decomposition methods in stochastic programming". In: *Mathematical Programming* 79, pp. 333–353.

Sahinidis, NV and IE Grossmann (1991). "Convergence properties of generalized Benders decomposition". In: *Comput Chem Eng* 15(7), pp. 481–491.

Sand, G et al. (2000). "Approximation of an ideal online scheduler for a multiproduct batch plant". In: *Comput. Chem. Eng.* 24.361, 361–367.

Sanmarti, E, A Espuna, and L Puigjaner (1997). "Batch production and preventive maintenance scheduling under equipment failure uncertainty." In: *Comput. Chem. Eng.* 21, 1157–1168.

Schultz, R and S Tiedemann (2006). "Conditional Value-at-Risk in Stochastic Programs with Mixed-Integer Recourse." In: *Math. Program.* 105, pp. 365–386.

Sen, S and HD Sherali (2006). "Decomposition with branch-and-cut approaches for two-stage stochastic mixed-integer programming." In: *Mathematical Programming* 106(2), 203–223.

Shapiro, JF (2001). *Modeling the Supply Chain*. Ed. by Pacific Grove Duxbury. Vol. 1.

Sherali, HD and BM Fraticelli (2002). "A modification of Benders' decomposition algorithm for discrete subproblems: An approach for stochastic programs with integer recourse." In: *Journal of Global Optimization* 22, 319–342.

Siano, P (2014). "Demand response and smart grids - A survey". In: *Renewable and Sustainable Energy Reviews* 30, pp. 461–478.

Solak, S et al. (2010b). "Optimization of R&D project portfolios under endogenous uncertainty." In: *European Journal of Operational Research* 207, pp. 420–433.

Solak, S et al. (2010a). "Optimization of R&D project portfolios under endogenous uncertainty". In: *Eur J Oper Res* 207(1), pp. 420–433.

Statistics and Machine Learning Toolbox (2006). The MathWorks, Natick, MA, USA.

Tan, JS and MA Kramer (1997). "A general framework for preventive maintenance optimization in chemical process operations". In: *Computers and Chemical Engineering*, pp. 1451–1469.

Uryasev, S (2000). "Conditional Value-at-Risk: Optimization Algorithms and Applications". In: *Financial Engineering news* 14.

Uryasev, S (2017). "Value-at-Risk vs. Conditional Value-at-Risk in Risk Management and Optimization". In: *INFORMS Tutorials in Operations Research*.

Watson, JP and DL Woodru (2011). "Progressive hedging innovations for a class of stochastic mixed-integer resource allocation problems". In: *Computational Management Science*, pp. 355–370.

Wenzel, S et al. (2019). "An optimization model for site-wide scheduling of coupled production plants with an application to the ammonia network of a petrochemical site". In: *Optim Eng* 19, pp. 1–31.

Wiebe, J, I Cecilio, and R Misener (2018). "Data-Driven Optimization of Processes with Degrading Equipment". In: *Ind. Eng. Chem. Res* 57,50, 17177–17191.

Willans, PW (1888). "Economy trials of a non-condensing steam-engine: simple, compound and triple. (Including tables and Plate at back of Volume)". In: *Minutes of the Proceedings*, pp. 128–188.

Xenos, DP et al. (2015). "Operational optimization of networks of compressors considering condition-based maintenance." In: *Comput. Chem. Eng.* 6, pp. 325–339.

Zhan, Y et al. (2016). "Generation Expansion Planning With Large Amounts of Wind Power via Decision-Dependent Stochastic Programming". In: *IEEE Transactions on power systems* 32(4), pp. 3015–3026.

Zhang, Q and IE Grossmann (2015). "Planning and scheduling for industrial demand side management: advances and challenges". In: *Alternative energy sources and technologies: process design and operation*. Ed. by M Martin.

Zhang, Q et al. (2016). "Risk-based integrated production scheduling and electricity procurement for continuous power-intensive processes". In: *Computers and Chemical Engineering* 86.1–12, pp. 90–105.